GEORGIA INSTITUTE OF TECHNOLOGY
OFFICE OF CONTRACT ADMINISTRATION
SPONSORED PROJECT INITIATION

Date: 8/14/78

Project Title: Air Defense Studies for Nuclear Facility Protection

Project No: A-2176

Project Director: Mr. E. F. Greneker

Sponsor: Sandia Laboratories; Albuquerque, N.M. 87115

Agreement Period: From 6/26/78 Until 9/30/78 (R&D Performance)

Type Agreement: Subcontract No. 13-0854 (Under U.S. Dept. of Energy Prime)

Amount: $51,012

Reports Required: Monthly Progress Letters; Monthly Cost Status Reports; Final Report

Sponsor Contact Person (s):

Technical Matters

Mr. A. M. Fine, Org. 1758
Sandia Laboratories
Kirtland AFB, (East)
Albuquerque, N.M. 87185

Contractual Matters
(thru OCA)

Mr. G. T. Kupper
Sandia Laboratories
Purchasing Organization 3721
P. O. Box 5800
Albuquerque, N.M. 87185
Phone (505) 264-1936

Defense Priority Rating: DO-E2 under DMS Reg. 1.

Assigned to: RAIL (School/Laboratory)

COPIES TO:

- Project Director
- Division Chief (EES)
- School/Laboratory Director
- Dean/Director—EES
- Accounting Office
- Procurement Office
- Security Coordinator (OCA)
- Reports Coordinator (OCA) ✓
- Library, Technical Reports Section
- EES Information Office
- EES Reports & Procedures
- Project File (OCA)
- Project Code (GTRI)
- Other

OCA-2 (3/76)

Posted
EW

OHK

GEORGIA INSTITUTE OF TECHNOLOGY
OFFICE OF CONTRACT ADMINISTRATION

SPONSORED PROJECT TERMINATION

Date: March 27, 1979

Project Title: Air Defense Studies for Nuclear Facility Protection

Project No: A-2176

Project Director: Mr. E. F. Greneker

Sponsor: Sandia Laboratories

Effective Termination Date: 2/28/79 (Subcontract expiration)

Clearance of Accounting Charges: by 2/28/79

Grant/Contract Closeout Actions Remaining:

X Final Invoice and Closing Documents
_ Final Fiscal Report
_ Final Report of Inventions
X Govt. Property Inventory & Related Certificate ← Cert. to Sandia on 3 April '79 OHK
_ Classified Material Certificate
_ Other _____

Assigned to: Radar Instrumentation Laboratory (School/Laboratory)

COPIES TO:

Project Director
Division Chief (EES)
School/Laboratory Director
Dean/Director—EES
Accounting Office
Procurement Office
Security Coordinator (OCA) ✓
Reports Coordinator (OCA)

Library, Technical Reports Section
EES Information Office
Project File (OCA)
Project Code (GTRI)
Other _____

CA—4 (1/79)

Sandia Laboratories
PURCHASING ORGANIZATION

ALBUQUERQUE, NEW MEXICO 87185
LIVERMORE, CALIFORNIA 94550

MONTHLY COST STATUS REPORT

CONTRACT NO. 13-0854

PERIOD ENDING (1) July 31, 1978

TOTAL FUNDS AUTHORIZED		$ 51,012
ACTUAL COST INCURRED TO DATE (2)		$5,065
ESTIMATED COST TO COMPLETE: (3)		
1ST MONTH FOLLOWING (1)	$16,500 August	
2ND MONTH	$14,500 Sept.	
3RD MONTH	$14,500 Oct.*	
4TH MONTH	$447 Nov-Jan.	
5TH MONTH		
6TH MONTH		
BALANCE OF FISCAL YEAR (4)	$36,065	
SUBSEQUENT FISCAL YEARS	$14,947	
TOTAL ESTIMATE TO COMPLETE		$51,012
TOTAL ESTIMATED COST AT COMPLETION		$ 51,012

NOTES:

(1) LAST FULL MONTH FOR WHICH ACTUAL COSTS ARE AVAILABLE.

(2) COST INCLUDES APPLICABLE FEE.

(3) ESTIMATES FOR COSTS TO BE INCURRED (DO NOT INCLUDE COMMITMENTS), INCLUDING APPLICABLE FEE.

(4) FISCAL YEAR IS 10/1 THRU 9/30. BALANCE OF FISCAL YEAR MEANS ALL MONTHS IN A FISCAL YEAR FOLLOWING THE 6TH MONTH SHOWN ON THE LINE ABOVE.

*No cost extension on technical work will be requested for period Oct 1, 1978-Oct. 31, 1978.

SF 6432-CS (5-78)

H-2116

ENGINEERING EXPERIMENT STATION
GEORGIA INSTITUTE OF TECHNOLOGY • ATLANTA, GEORGIA 30332

August 3, 1978

Sandia Laboratories
Kirtland Air Force Base (East)
Albuquerque, NM 27185

Attention: Mr. A. M. Fine, org. 1758
Project Monitor

Subject: Research and Development Status Report No. 1,
"Air Defense Studies for Nuclear Facilities Protection,"
Status Report covering the period June 26 through July 31, 1978.

Gentlemen:

This status report describes activities for the months of June and July. The June and July reports are being combined due to the short 6-day performance period from 26 June to 30 June. Those activities conducted under the subject contract for the period referenced are summarized in this research and development status report no. 1.

I. Ga. Tech/Sandia Contract Kick-off Meeting at Sandia

Georgia Tech personnel J. L. Eaves, Associate Director of the Radar and Instrumentation Laboratory, E. F. Greneker, Project Director, and T. P. Morton, Project Physicist, met with Dr. C. E. Olson and Mr. A. M. Fine of Sandia at Sandia Albuquerque on 27 and 28 June 1978. A technical approach to the study of generic systems that will detect aircraft (helicopters) approaching a nuclear facility was discussed during this meeting. In addition, an effort was made to define what airborne vehicles constitute the airborne threat, what a typical nuclear facility might look like (physically), and other factors that require definition.

II. Acoustic Sensor Assessment

The utility of acoustic sensors used for aircraft detection was studied during July. The basic principles of acoustic aircraft detection, the various acoustic systems used in the past and present work in acoustic detection systems were defined during July. This data base will be used during August to develop the chapter for the final engineering technical report on acoustic aircraft detection sensors.

III. Radar Studies

The technical approach that will be used during the radar detection system study phase was developed during July. The present plans include

A-2176

ENGINEERING EXPERIMENT STATION
GEORGIA INSTITUTE OF TECHNOLOGY • ATLANTA, GEORGIA 30332

9 September 1978

Sandia Laboratories
Kirtland Air Force Base (East)
Albuquerque, New Mexico 27185

Attention: Mr. A. M. Fine, Org. 1758
Project Monitor

Subject: Research and Development Status Report No. 2,
"Air Defense Studies for Nuclear Facilities Protection",
Status Report Covering the Period August 1 through August 31, 1978.

Gentlemen:

This status report describes activities for the month of August. Those activities conducted under the subject contract for the period referenced are summarized in this research and development status report no. 2.

I. Bi-Static Radar Analysis

Analysis on the role of bi-static radar was begun during the reporting period. The role that the bi-static radar will play has not be determined on an absolute basis; however, threat analysis indicates that the bi-static system should be employed as a "fence" type detection system. The main utility of this approach is that the bi-static configuration allows a relatively simple system to be used for initial acquisition and early warning purposes.

II. Acoustic Sensor Analysis

During August the information gathered during July and August was used as a basis for the final technical report on acoustic detection and classification of overflying aircraft. The basic physics and theory of sound propagation together with meteorological effects have been broadly delineated. The acoustical characteristics of various types of aircraft have been documented with special emphasis on helicopter acoustical spectra.

Considerations of optimal deployment of acoustic sensors for the considered application are currently being treated with views toward establishing proper grouping of sensors for phased direction determination and estimating signal-to-noise ratio requirements. The technology of microprocessing of acoustical data and electronic fast fourier transforms have also been brought under study for the final technical report. Some assessment of prototype acoustic detection systems already in existence will be rendered pending receipt of field performance tests.

III. No-Cost Project Extension

A no-cost project extension will be requested through contracting channels.

The no-cost 30 day extension will be requested to allow project staff members to receive and evaluate data that has been ordered but not yet received. These missing data consist of technical reports, radar site informaion and other information that will enhance the quality and depth of technical data presented in the final engineering report.

Respectfully submitted,

Gene Greneker
Project Director

Approved:

Jim D. Echard, Head
Radar Applications Division

saw

cc: C. E. Olson, Org. 1700

A-2176

ENGINEERING EXPERIMENT STATION
GEORGIA INSTITUTE OF TECHNOLOGY • ATLANTA, GEORGIA 30332

12 October 1978

Sandia Laboratories
Kirtland Air Force Base (East)
Albuquerque, New Mexico 27185

Attention: Mr. A. M. Fine, Org. 1758
Project Monitor

Subject: Research and Development Status Report No. 3
"Air Defense Studies for Nuclear Facilities Protection
Status Report Covering the Period September 1 Through
September 30, 1978, Subcontract 13-0854 (A2176)

Gentlemen:

This status report describes activities for the months of September and October. Those activities conducted under the subject contract for the period referenced are summarized in this research and development status report no. 3. This report serves as the combined September and October report because the final draft engineering technical report will be issued at the end of October in leiu of the 4th monthly status report.

I. Conclusion of the Sensor Analysis Effort

The analysis stage was concluded on the radar, acoustic and optical sensor systems during the reporting period. The resulting data is presently being assembled for presentation in the final draft engineering technical report. Given these findings it is postulated that radar will serve the role as a primary sensor; acoustic detectors will serve as fence sensors; and optics will serve in the role of a terminal phase acquisition sensor in the airborne detection system.

II. Briefing on Preliminary Findings

A briefing was held at Sandia Labs on October 4th and 5th. The briefing conducted by Gene Greneker, Tom Morton, and Rodger Johnson of Georgia Tech, highlighted the project findings to date.

III. FAA/NORAD Resources Study

Mark Samuels of Georgia Tech visited Washington FAA Headquarters on 4 October to determine which FAA facilities may be useful to detect the

air threat at specified DOE facilities. The data developed from this inquiry will be presented in the draft version of the final engineering technical report to be issued at the end of October.

IV. Study to Determine Controlled Airspace Considerations

An effort was undertaken during September to determine the effect on Airborne Penetration Detection System cost as a function of controlling or not controlling airspace over a DOE facility. This question was addressed at the request of Messrs. C. Olson and A. Fine of Sandia. The results of this study effort were presented at the 4 October briefing. These findings will also be highlighted in the draft version of the final technical report to be issued at the end of October.

Respectfully Submitted,

E. F. Greneker
Project Director

EFG/vcy

Approved:

J. D. Echard
Chief, Radar Applications Division
Radar and Instrumentation Laboratory

cc: C. Olson, J. Stigler - Organization 1758
G. Kupper - Organization 3721
E. K. Reedy
J. L. Eaves

Sandia Laboratories
PURCHASING ORGANIZATION

ALBUQUERQUE, NEW MEXICO 87185
LIVERMORE, CALIFORNIA 94550

MONTHLY COST STATUS REPORT

CONTRACT NO. 13-0854
Georgia Tech project no. A-2176

PERIOD ENDING (1) Aug. 31, 1978

TOTAL FUNDS AUTHORIZED			$ 51,012
ACTUAL COST INCURRED TO DATE (2)			19,159
ESTIMATED COST TO COMPLETE: (3)			
1ST MONTH FOLLOWING (1)	$15,500	Sept.	
2ND MONTH	14,500	Oct.	
3RD MONTH	1,853	Nov.-Dec.	
4TH MONTH			
5TH MONTH			
6TH MONTH			
BALANCE OF FISCAL YEAR (4)	$34,659		
SUBSEQUENT FISCAL YEARS	$16,353		
TOTAL ESTIMATE TO COMPLETE			51,012
TOTAL ESTIMATED COST AT COMPLETION			$ 51,012

NOTES:

(1) LAST FULL MONTH FOR WHICH ACTUAL COSTS ARE AVAILABLE.

(2) COST INCLUDES APPLICABLE FEE.

(3) ESTIMATES FOR COSTS TO BE INCURRED (DO NOT INCLUDE COMMITMENTS), INCLUDING APPLICABLE FEE.

(4) FISCAL YEAR IS 10/1 THRU 9/30. BALANCE OF FISCAL YEAR MEANS ALL MONTHS IN A FISCAL YEAR FOLLOWING THE 6TH MONTH SHOWN ON THE LINE ABOVE.

SF 6432-CS (5-78)

A-2176

Sandia Laboratories
PURCHASING ORGANIZATION

ALBUQUERQUE, NEW MEXICO 87185
LIVERMORE, CALIFORNIA 94550

MONTHLY COST STATUS REPORT

CONTRACT NO. 13-0854
Georgia Tech project no. A-2176

PERIOD ENDING (1) 30 September, 1978

TOTAL FUNDS AUTHORIZED		$ 51,012
ACTUAL COST INCURRED TO DATE(2)		32,504
ESTIMATED COST TO COMPLETE:(3)		
1ST MONTH FOLLOWING (1)	October 11,500	
2ND MONTH	November-December 7,348	
3RD MONTH		
4TH MONTH		
5TH MONTH		
6TH MONTH		
BALANCE OF FISCAL YEAR(4)	0	
SUBSEQUENT FISCAL YEARS	$18,508	
TOTAL ESTIMATE TO COMPLETE		51,012
TOTAL ESTIMATED COST AT COMPLETION		$ 51,012

NOTES:

(1) LAST FULL MONTH FOR WHICH ACTUAL COSTS ARE AVAILABLE.

(2) COST INCLUDES APPLICABLE FEE.

(3) ESTIMATES FOR COSTS TO BE INCURRED (DO NOT INCLUDE COMMITMENTS), INCLUDING APPLICABLE FEE.

(4) FISCAL YEAR IS 10/1 THRU 9/30. BALANCE OF FISCAL YEAR MEANS ALL MONTHS IN A FISCAL YEAR FOLLOWING THE 6TH MONTH SHOWN ON THE LINE ABOVE.

SF 6432-CS (5-78)

A-2176

Sandia Laboratories
PURCHASING ORGANIZATION

ALBUQUERQUE, NEW MEXICO 87185
LIVERMORE, CALIFORNIA 94550

MONTHLY COST STATUS REPORT

CONTRACT NO. 13-0854
Georgia Tech project no. A-2176

PERIOD ENDING (1) Oct. 31, 1978

TOTAL FUNDS AUTHORIZED		$ 51,012
ACTUAL COST INCURRED TO DATE (2)		$ 43,542
ESTIMATED COST TO COMPLETE: (3)		
1ST MONTH FOLLOWING (1)	Nov.-Dec. $6,701	
2ND MONTH		
3RD MONTH		
4TH MONTH		
5TH MONTH		
6TH MONTH		
BALANCE OF FISCAL YEAR (4)	0	
SUBSEQUENT FISCAL YEARS	$6,701	
TOTAL ESTIMATE TO COMPLETE		51,012
TOTAL ESTIMATED COST AT COMPLETION		$ 51,012

NOTES:

(1) LAST FULL MONTH FOR WHICH ACTUAL COSTS ARE AVAILABLE.

(2) COST INCLUDES APPLICABLE FEE.

(3) ESTIMATES FOR COSTS TO BE INCURRED (DO NOT INCLUDE COMMITMENTS), INCLUDING APPLICABLE FEE.

(4) FISCAL YEAR IS 10/1 THRU 9/30. BALANCE OF FISCAL YEAR MEANS ALL MONTHS IN A FISCAL YEAR FOLLOWING THE 6TH MONTH SHOWN ON THE LINE ABOVE.

SF 6432-CS (5-78)

H - 2176

Sandia Laboratories
PURCHASING ORGANIZATION

ALBUQUERQUE, NEW MEXICO 87185
LIVERMORE, CALIFORNIA 94550

MONTHLY COST STATUS REPORT

CONTRACT NO. 13-00854
Georgia Tech Project No. A-2176

PERIOD ENDING (1) Nov. 30, 1978

TOTAL FUNDS AUTHORIZED		$ 51,012
ACTUAL COST INCURRED TO DATE (2)		48,502
ESTIMATED COST TO COMPLETE: (3)		
1ST MONTH FOLLOWING (1)	December - $2,000	
2ND MONTH	510	
3RD MONTH		
4TH MONTH		
5TH MONTH		
6TH MONTH		
BALANCE OF FISCAL YEAR (4)		
SUBSEQUENT FISCAL YEARS		
TOTAL ESTIMATE TO COMPLETE		51,012
TOTAL ESTIMATED COST AT COMPLETION		$ 51,012

NOTES:

(1) LAST FULL MONTH FOR WHICH ACTUAL COSTS ARE AVAILABLE.

(2) COST INCLUDES APPLICABLE FEE.

(3) ESTIMATES FOR COSTS TO BE INCURRED (DO NOT INCLUDE COMMITMENTS), INCLUDING APPLICABLE FEE.

(4) FISCAL YEAR IS 10/1 THRU 9/30. BALANCE OF FISCAL YEAR MEANS ALL MONTHS IN A FISCAL YEAR FOLLOWING THE 6TH MONTH SHOWN ON THE LINE ABOVE.

SF 6432-CS (5-78)

Sandia Laboratories
PURCHASING ORGANIZATION

ALBUQUERQUE, NEW MEXICO 87185
LIVERMORE, CALIFORNIA 94550

MONTHLY COST STATUS REPORT

CONTRACT NO. 13-00854
Georgia Tech Project A-2176
PERIOD ENDING (1) Dec. 30, 1978

OTAL FUNDS AUTHORIZED	$ 51,012.00
CTUAL COST INCURRED TO DATE (2)	$ 48,554.00
STIMATED COST TO COMPLETE: (3)	
1ST MONTH FOLLOWING (1)	Jan. - $2,458.42*
2ND MONTH	
3RD MONTH	
4TH MONTH	
5TH MONTH	
6TH MONTH	
BALANCE OF FISCAL YEAR (4)	
SUBSEQUENT FISCAL YEARS	
TOTAL ESTIMATE TO COMPLETE	$51,012.00
OTAL ESTIMATED COST AT COMPLETION	$ 51,012.00

OTES:

1) LAST FULL MONTH FOR WHICH ACTUAL COSTS ARE AVAILABLE.

2) COST INCLUDES APPLICABLE FEE.

3) ESTIMATES FOR COSTS TO BE INCURRED (DO NOT INCLUDE COMMITMENTS), INCLUDING APPLICABLE FEE.

4) FISCAL YEAR IS 10/1 THRU 9/30. BALANCE OF FISCAL YEAR MEANS ALL MONTHS IN A FISCAL YEAR FOLLOWING THE 6TH MONTH SHOWN ON THE LINE ABOVE.

All major charges have been made to this project. The remaining $2,458.42 is budgeted toward the layout and printing of the Final Technical Report (presently in progress). As there is no standard time for the receipt of printing bills, please consider that this sum will be expended in January.

FINAL REPORT

AIR PENETRATION DETECTION STUDIES FOR NUCLEAR FACILITY PROTECTION

By

E. F. Greneker
D. R. Johnson
T. P. Morton

Technical Contributions by

M. A. Samuels

Prepared for

Sandia Laboratories
Safeguards Evaluation Division (1758)
Albuquerque, New Mexico

Under

Contract No. 13–0854

October 31, 1978

GEORGIA INSTITUTE OF TECHNOLOGY

Engineering Experiment Station
Atlanta, Georgia 30332

GT EES

1978

AIR PENETRATION DETECTION STUDIES FOR NUCLEAR FACILITY PROTECTION

Final Engineering Technical Report

By:
E. F. Greneker
D. R. Johnson
T. P. Morton
Technical Contributions by
M. A. Samuels

Prepared For

Sandia Laboratories
Safeguards Evaluation Division (1758)
Albuquerque, New Mexico
Contract No. 13-0854

October 31, 1978

Prepared By

Radar Applications Division
Radar and Instrumentation Laboratory

(This Page Intentionally Blank)

FOREWORD

The research on this program was conducted within the Radar Applications Division, Radar and Instrumentation Laboratory, Engineering Experiment Station, Georgia Institute of Technology, with Mr. E. F. Greneker serving as Project Director. This program is designated as Georgia Tech Project A-2176 and was sponsored by Sandia Laboratories, Albuquerque, New Mexico under contract to the U. S. Department of Energy.

This final technical report was designed to survey generic sensors that could be used to develop a security system to detect the airborne penetration of nuclear site perimeter areas.

This report covers technical analysis done between the dates of June 26, 1978 and October 31, 1978. The data contained in this final engineering technical report was developed within the four month project performance period and does not represent an exhaustive discourse on the subject of nuclear site defense against the airborne penetrator.

Approved:

J. D. Echard
Radar Applications Division Chief

Respectfully submitted

E. F. Greneker
Project Director

(This Page Intentionally Blank)

ACKNOWLEDGEMENTS

We would like to thank Mr. A. M. Fine, Project Monitor, and Mr. C. E. Olson and Mr. J. E. Stiegler of Sandia Laboratories, for their assistance and guidance during this study.

We would like to acknowledge the technical contribution made by Mr. M. A. Samuels, Co-Op Student Project Member, also Co-Op Students M. A. Corbin, R. V. Folea and R. G. Futrell for their assistance in the preparation of illustrative materials for this report.

We would like to thank the Federal Aviation Administration Personnel who contributed their time; also selected personnel in the various military and scientific organizations consulted during the collection of material for this report.

We would like to thank Report Typist Ms. D. E. Weaver for her untiring efforts toward the completion of this report and Ms. Washington, Technical Area Secretary, for her assistance with the preparation of dictated transcriptions.

(This Page Intentionally Blank)

TABLE OF CONTENTS

Topic	Page
I. Introduction	1
A. Site Security; An Historical Perspective	1
B. The Air Threat	3
C. Report Organization	4
II. Radar Fundamentals of Airborne Intrusion Detection	7
A. Basic Principles	7
1. Monostatic	7
2. Bistatic	10
B. Detection Limits	15
1. Range	15
a. Monostatic	15
b. Bistatic	16
2. Angle	18
a. Monostatic	18
b. Bistatic	18
C. Radar Range Equation	18
1. Monostatic	18
2. Bistatic	20
D. Special Radar Information Considerations	21
1. Discrimination of Target Type	21
2. Detection of Object Separating from Aircraft	22
E. Performance Considerations	28
1. Natural Effects	28
2. Man-Made Effects	34
References (Section II)	36
III. Fundamentals of Acoustic Detection of Airborne Intrusion	37
A. Review of Airborne Threats Considered Detectable by Acoustic Means	37
1. Helicopter	37
2. Fixed-Wing Reciprocating Engine Aircraft	38
3. Jet or Turboprop Aircraft	38
4. Autogyro	38
B. Review of Airborne Threats Considered Nondetectable by Acoustic Means	38
1. Hang Gliders	38
2. Hot Air Balloons	38
3. Parachutist	39
4. Backmounted Rocket	39

TABLE OF CONTENTS

(Continued)

Topic	Page
C. Sources of Aircraft Acoustic Energy	39
1. Piston Engine Exhausts	39
2. Propeller and Rotor Blades	41
3. Gearboxes	41
4. Jet Turbines	41
5. Turbojet and Turbofan Engines	44
6. Aerodynamic Disturbances	44
D. Factors Determing the Power Received from an Airborne Acoustic Source as a Function of Range	44
1. Introduction to Acoustic Measurements	44
2. Propagation and Attenuation of Sound in the Atmosphere	50
3. Overflight Geometry, Kinematics and Doppler Effect	59
E. Acoustical Detection Range	67
F. Acoustic Sensor Arrays	71
G. Concepts of Acoustic Data Handling	71
References (Section III)	75
IV. Optical Sensors	77
V. Evaluation and Rating of Generic Sensors	79
A. Tabular Rating and Evaluation Matrix	79
B. Detailed Expansion of Elements in Matrix	79
VI. Introduction to Existing Air Surveillance Facilities	91
A. The U. S. Air Traffic System	91
B. The Aircraft Detection Network in the U. S.	93
C. FAA Resources Considered for Airborne Penetration Surveillance	93
D. Information Flow within the Long Range Air Surveillance and Terminal System	95
E. The ASR System	103
F. Data Pick-Off Points within the FAA System	106
G. Study of FAA Facilities with Possible Application to DoE Needs	107
H. Considerations Relating to National Airspace Restriction over Nuclear Sites	112
VII. Conclusions	115
VIII. Recommendations	117

LIST OF FIGURES

	Figure	Page
II- 1.	Geometry for Monostatic Radar	8
II- 2.	Example Configuration for Bistatic Radar	11
II- 3.	Geometry for Bistatic Radar	13
II- 4.	Relationship of Range to Optical Horizon and Radar Height	17
II- 5.	Comparison for Example Doppler Frequency Characteristics for Helicopter and Small Airplane	23
II- 6.	Angular Resolution Requirements for Detection of Separating Objects	25
II- 7.	Impact of Beamwidth Requirement on Phased Array Diameter and Coverage	27
II- 8.	Atmospheric Absorption by the 1.35-cm Line of Water Vapor and 0.5-cm Line of Oxygen	30
II- 9	Theoretical Rain Attenuation vs. Rainfall Rate	30
II-10.	Geometry of Multipath Reflection	32
II-11.	Illustration Showing the Effects on a Free Space Antenna Pattern of Interference Resulting from Ground Reflections	33
III- 1.	Piston Engine Aircraft Spectral Lines	40
III- 2.	UH-1A External Noise Spectrum at Distance of 200 Feet	42
III- 3.	Two Hz Bandwidth Analysis of UH-1B Noise Spectrum	43
III- 4.	Atmospheric Temperature vs. Altitude	46
III- 5.	Speed of Sound vs. Altitude	47
III- 6.	Limits of Audibility	49
III- 7.	Inversion Layer	51
III- 8.	Upward Refraction of Sound	53

LIST OF FIGURES

(Continued)

	Figure	Page
III- 9.	Acoustical Skip Zone	55
III-10.	Bending of Sound Rays by Wind Gradients	55
III-11.	Overflight Geometry	60
III-12.	Overflight Kinematics	63
III-13.	Doppler Shifted Frequency	65
III-14.	Doppler Kinematics	66
III-15.	Acoustic Range Equation	69
III-16.	Perimeter Array Segment	72
III-17.	Subarray Elements	73
VI- 1.	Diagram Showing the Long Range Air Route Surveillance Network in the Southwest Region of the United States	96
VI-2.	Detection and Processing Equipment Associated with an FAA Long Range Radar Site	97
VI-3.	Major Data Flow Points within the ARTCC	101
VI-4.	Detection and Processing Equipment Associated with the ASR Terminal Radar Installation	105

LIST OF TABLES

	Table	Page
Table III-I	Classical Attenuation Formulas	58
Table V-I	Tabular Rating and Evaluation Matrix	80
Table VI-I	Correlation of DoE Facility Location and Nearest FAA Radar Facility	108-109

(This Page Intentionally Blank)

SECTION I

INTRODUCTION

The Nuclear Facilities Protection Program is currently administered in part by Sandia Laboratories for the U. S. Department of Energy (DoE). Sandia has developed a broad class of ground intrusion sensors to fill the DoE ground based security mission. To date, very little research has been done toward the development of an aircraft penetration, detection and warning system; possibly because from an historical perspective the airborne threat has not been considered as serious a problem. However, the availability of helicopters, fixed-wing aircraft (conventional and short take-off and landing), hot air balloons, hang gliders and other airborne recreational equipment to the general public has increased over the past decade. Given this wide spread availability of various airborne vehicles the Radar Applications Division of the Radar and Instrumentation Laboratory, Engineering Experiment Station, Georgia Institute of Technology was tasked by Sandia in June 1978 to examine certain ramifications of the airborne threat detection problem. This report represents the Phase I findings of the Georgia Tech study which represents a broad review of the relevent subject matter consistent with the performance period given for study completion.

A. Site Security; An Historical Perspective

The methods used to protect and defend high value resources, such as a nuclear facility have been traditionally developed to allow defense of these sites against the ground intruder. Historically, the methodology developed to achieve site security against ground intrusion consists of four basic elements: 1) early

warning of a ground intruder's presence outside of a perimeter area, 2) barriers to delay the intruder's advancement from the perimeter to more sensitive areas, 3) an armed security force to physically repell the "intruder" and 4) a secondary enclosure or confinement system around the nuclear device or material being protected. Each of these elements in the ground intrusion security system plays an important role in the development of the coordinated response by site security forces against an "intruder".

The present mix of ground intrusion/detection systems utilized at a facility gives site security forces an early warning that an adversary is attempting to penetrate the perimeter. The perimeter barrier confines the extent of the restricted area and serves to delay the penetration effort. If the perimeter barrier is breached, the intrusion/detection system supplies security forces with information concerning the penetrator's movements within the inner perimeter of the site. Following a breach in the barrier system, the undamaged sections of the barrier serve to concentrate the penetrator force during their entry (i.e., a funneling effect on the penetration force is created). Thus given the initial warning and the effects of barrier system delays, the security forces can more effectively block the penetrator from reaching sensitive areas.

The lack of the early warning to an intruder's presence or lack of barrier system delay could compromise certain aspects of site security. Given enough time before detection, a penetrator force might establish a position that could hold the security force to a small area within the complex. While it would be difficult for an intruder to compromise the present ground security system, an airborne assault could be a possible method to achieve successful penetration force

placement within sensitive areas through surprise and circumvention of the many elements of the barrier system.

B. The Air Threat

Any method that would allow undetected penetration of a sensitive area inside the security perimeter of the facility should be considered in the conduct of threat studies. Numerous methods of airborne transportation could be available for attempting this type of hostile forces mission objective. The various threat scenarios could include the use of helicopters, parachutes, hang gliders, light aircraft, or other airborne assault modes. The helicopter assault is probably the most credible of all airborne threats. And for report purposes will represent the primary threat to be considered.

As a threat vehicle, the helicopter can serve a multiple purpose role as: 1) weapons platform, 2) assault forces transport vehicle, 3) area command post and 4) a stolen nuclear materials transport system. Thus, a helicopter is useful for a low level undetected approach to the facility and a landing of hostile forces inside the perimeter boundaries. The element of surprise may compromise the reaction time of a security force that depends on being allowed a minimum reaction time after a penetrator has been detected. If a helicopter assault force is to be adequately countered, detection must occur sufficiently prior to the helicopter reaching the facility boundary, especially if it is necessary that facility security forces be given adequate time to secure sensitive areas of the facility.

C. Report Organization

This report is organized into eight major sections. Section II is entitled "Radar Fundamentals of Airborne Intrusion Detection" and is presented as a tutorial discussion on the principles of both bistatic and monostatic radar detection of airborne targets. This section also serves to highlight some of the problems and considerations that will be encountered in the conduct of airborne penetration analysis as it relates to the radar detection problem. Section III entitled "Fundamentals of Acoustic Detection of Airborne Intrusion" presents a tutorial discussion of basic acoustics and discusses the applications of acoustic detection to the problem of low level aircraft detection. Typical ranges at which targets may be detected for both the radar and acoustic cases are presented for typical situations. Section IV is entitled "Optical Sensors". This section was developed to discuss the general capabilities and limitations of optical sensors as a primary aircraft detection system and to define the role that an optical sensor should play given these capabilities and limitations.

The primary output of this report is contained in Section V which is entitled "The Valuation and Rating of Generic Sensors". A tabular rating and evaluation matrix is presented that allows the reader to determine the performance of a sensor as a function of various operational considerations and parameters. A detailed expansion of elements in the rating matrix is also presented in Section V. The detailed expansion further amplifies the basic concepts presented in key word form in the matrix. It is in Section V that the potential application of the sensor systems are presented. These applications include both deployment concepts and system design considerations.

Section VI entitled "Introduction to Existing Air Surveillance Facilities" discusses the role that the existing FAA enroute air traffic system radars might play in the design of an airborne intrusion detection and warning system at one of 17 selected Department of Energy nuclear facilities. An overview of the FAA long range radar system operational concepts and site location data is presented along with a first cut analysis of which long range radars or terminal radar systems might be of interest as a primary sensor to be included as an element in an airborne penetration/detection and warning system for selected DoE sites.

Section VII presents the conclusions developed from the analysis in the preceeding sections. These conclusions were developed on the basis of the data that were presented and from Georgia Tech's experience in the field of air defense studies. Section VIII is devoted to recommendations that should be addressed in future phases following this initial study. These recommendations represent a course of proposed action toward addressing the Department of Energy's concerns for airborne penetration detection and warning system developmental problems.

(This Page Intentionally Blank)

SECTION II

RADAR FUNDAMENTALS OF AIRBORNE INTRUSION DETECTION

A. Basic Principles

The value of radar to the airborne intrusion detection problem can be simply stated. In general, radar can be utilized to detect an airborne target at significant distances and to determine its position and velocity with relatively high accuracy. Two basic generic radar types will be discussed in the following sections. The first type of system that will be discussed is the monostatic radar; the second is the bistatic case.

1. Monostatic Radar. The term monostatic radar refers to the case where the transmitted signal is received at the same point as its origination after being reflected from a target. Usually a single antenna is used for both transmission and reception. The example diagram in Figure II-1 presents the monostatic operational principle.

Referring to Figure II-1, the electromagnetic energy is transmitted, via the antenna beam, in the direction of the target of interest. A portion of the transmitted energy is reflected directly back along the same path to the radar from the target. If the time of transmission (t_o) of a pulse of energy is recorded and the time of reception of the reflected energy (t_1) is also recorded, then the range to the target can be computed given the speed of light (c):

$$\text{Range} = R = \frac{c\,(t_1 - t_o)}{2} \qquad (1)$$

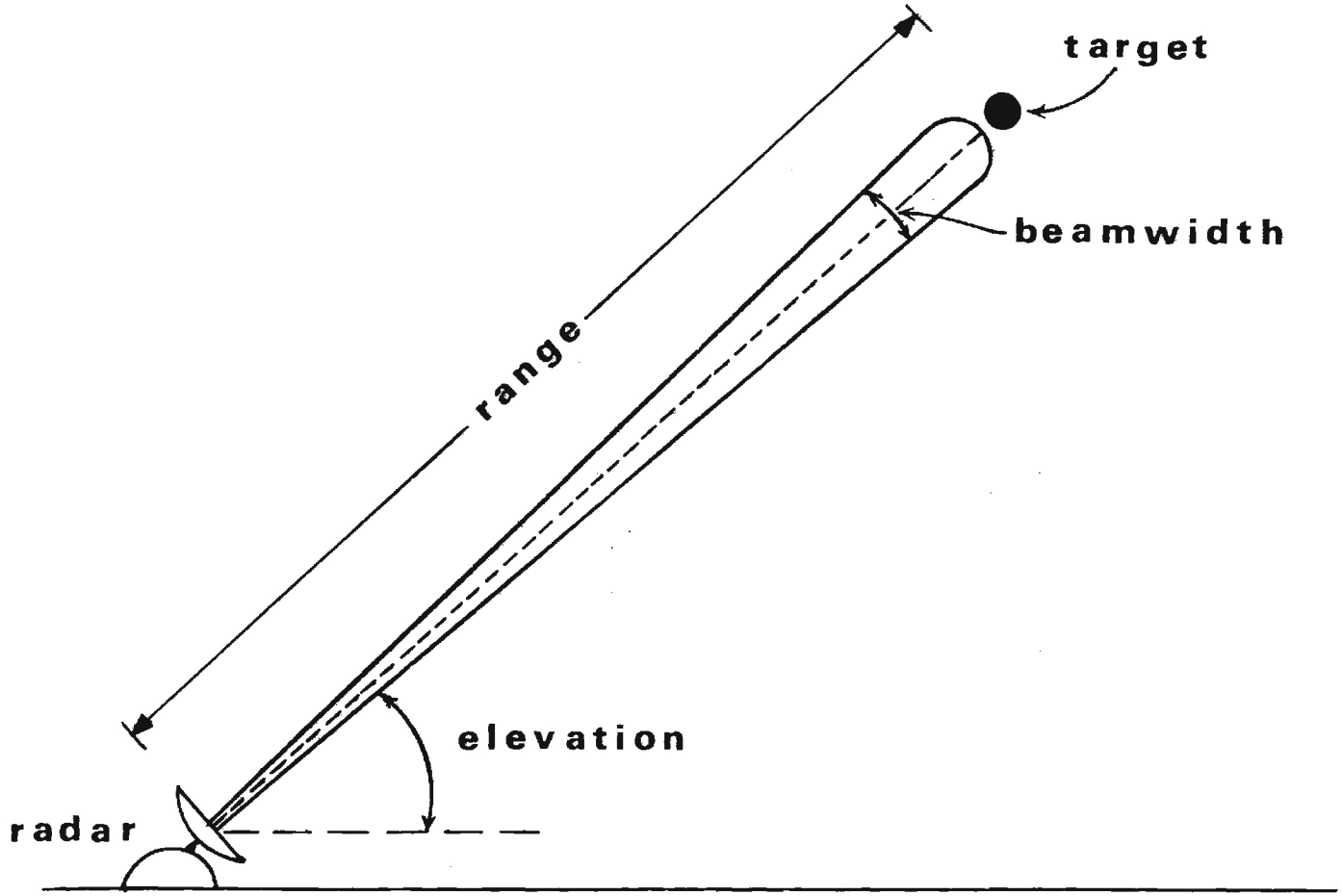

Figure II-1. Geometry for Monostatic Radar.

The 2 appears in the denominator because the total path length is doubled for any given range when a signal must travel to the target and return via the same path. The 2-way path is common to the monostatic radar configuration.

Angular information is available on the elevation and azimuth of the target. The accuracy of the elevation or azimuthal data is dependent on the nature and shape of the antenna beam. If the beamwidth is very narrow (i.e. the radiation from the antenna is concentrated around an axis representing beam center) then highly accurate knowledge of the angular position of the target may be obtained by recording the elevation and azimuthal angle at the time of the range measurement of the received signal. The antenna beamwidth is most frequently referred to in terms of the half-power or 3 dB points.[1] Thus two identical targets are said to be resolved in angle if they are separated by an angular distance θ_{BW} where θ_{BW} is the 3 dB beamwidth. For example, if $\theta_{BW} = 1^{o}$, then the position of a target of interest can be determined separate from other targets to within 1°. (i.e., 0.5 degrees each side of antenna boresite center axis.)

Information about the target velocity is also available from a radar signal due to the Doppler effect. Reflection of a signal by a moving target modifies the return frequency by an amount called the Doppler shift (f_d):

$$f_d = \frac{2Vfo}{c} \qquad (2)$$

Where: V is the velocity of the target relative to the radar.

c is the velocity of light.

f_o is the transmitted frequency.

Given the above relationship, the frequency returned to the receiver will be (f_o+f_d). Measurement of the frequency shift, f_d, by the receiver allows estimation of V as

$$V = \frac{cf_d}{2f_o} \tag{3}$$

In the diagram of Figure II-1, if the target is moving parallel to the ground and in the plane of the antenna beam with velocity V_o, then the relative velocity would be $V = V_o \cos$ (elevation angle). Thus the Doppler shift would be determined by the relationship:

$$f_d = \frac{2V_o \cos(EL)\, f_o}{c} \tag{4}$$

The real world accuracies which will be experienced with a given radar will depend on both the detailed design of that radar and the conditions under which it will operate. These will be discussed in more detail in the following sections.

2. Bistatic Concept. A bistatic radar is distinguished from monostatic by the fact that the receiver site is separate from the transmitter site. Detection of a target is still dependent on the reflection of electromagnetic energy. However, the signal of interest is that which reflects from a target in the direction of the receive antenna rather than in the direction of the original path of transmission as in the monostatic case.

An example configuration of a bistatic radar is given in Figure II-2. In this case rather broad transmit and receive antenna beams are fixed in space such

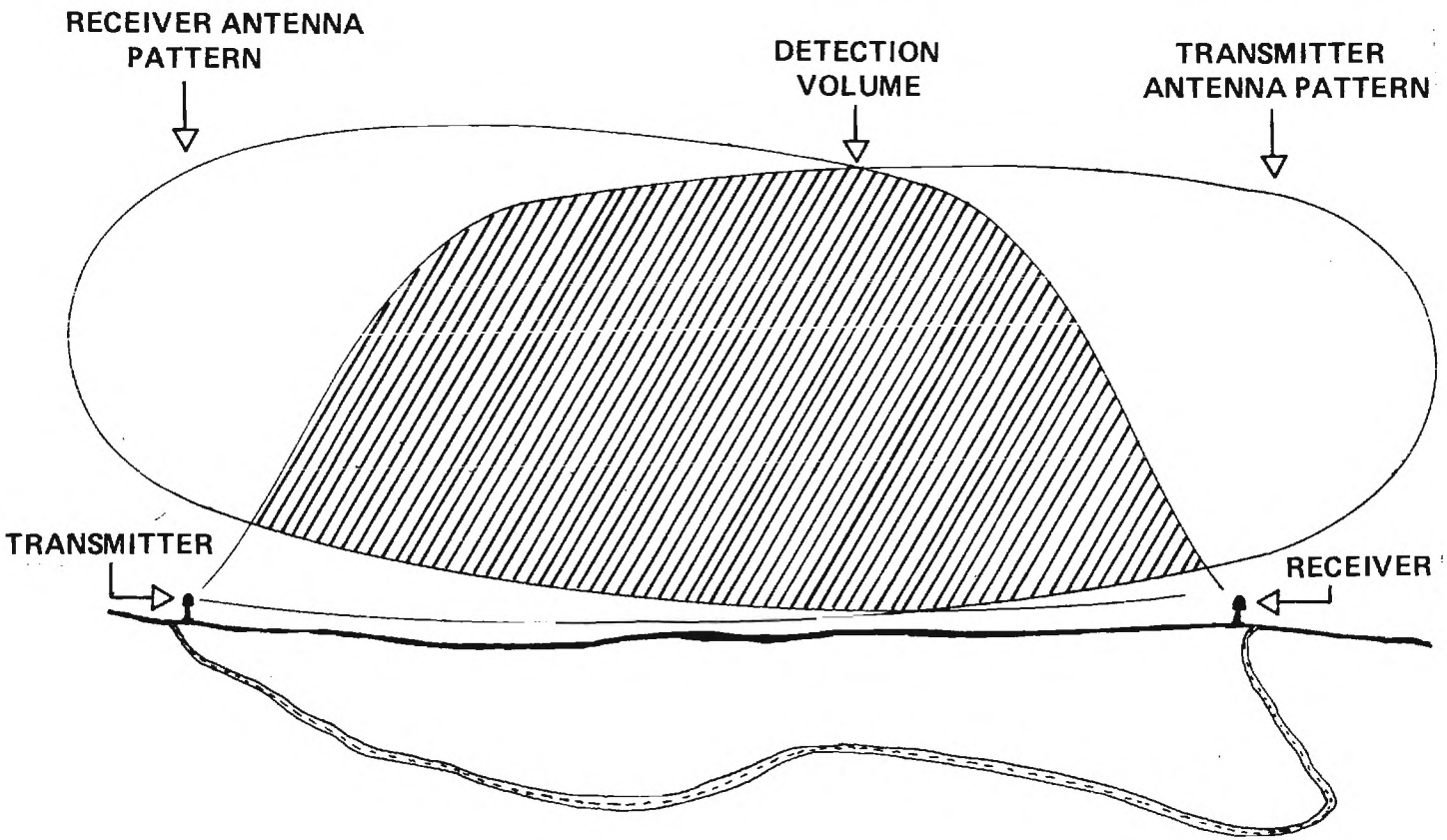

Figure II-2. Example Configuration for Bistatic Radar.

that an overlap region (given by cross-hatch in the figure) defines the space where detection is possible. By having the beams fixed in this manner, a "fence" configuration is formed. Any object entering the common coverage region will produce a corresponding Doppler output.

In a bistatic radar, some form of knowledge is maintained by the receiver as to when a transmission has been sent. This may be done either via a communication link (represented by the link shown at the bottom of Figure II-2), via syncronized clocks at both the transmitter and the receiver, or by direct propagation of the transmitted signal to the receiver.

Figure II-3 displays a typical geometry for a bistatic radar detection of an aircraft. The symbols are defined as follows:

D_b - distance from transmitter to receiver

D_t - distance from transmitter to target

D_r - distance from target to receiver

V_r - target velocity

h - target altitude

ϕ - crossing angle of velocity vector

r - location of target along crossing vector

b - distance from transmitter to crossing point.

It can be seen that measurement of the time difference between transmit and receive for a bistatic radar, (t_1-t_o), gives the total distance, S, that the signal has traveled. Thus,

$$S = D_t + D_r \tag{5}$$

and

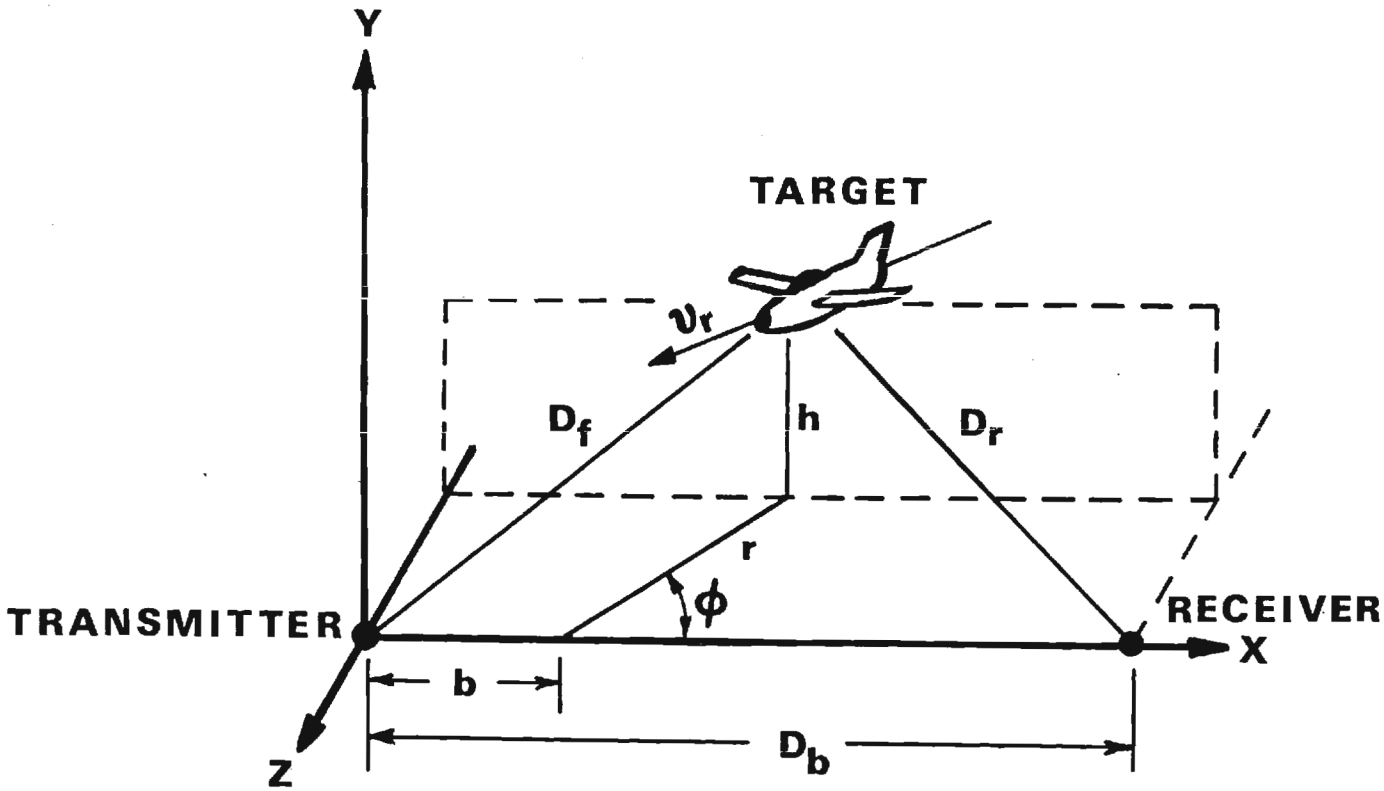

Figure II-3. Geometry for Bistatic Radar.

$$S = D_t + D_r = c\,(t_1 - t_o) \tag{6}$$

Generally, given a configuration such as Figure II-2 measurement of S does not facilitate a determination of D_t and D_r. This is acceptable if the desire is to create a simple means for detection of an intrusion through a specified space.

Likewise, angle information obtainable from a bistatic radar may be minimal. The amount of angular resolution depends on the characteristics of the beams utilized. If they are designed to be broad in elevation coverage, then it is not possible to resolve elevation of the forward scatter from the target in the way that this information is obtained in narrow beamwidth systems. However, gross angular data coupled with Doppler information may facilitate an estimation of the total target position and velocity.

For the bistatic radar, the Doppler frequency can be shown from Figure II-3 to be expressed as[2]

$$f_d = \frac{V_r f_o}{c} \left[\frac{r + b\cos\phi}{(b^2 + r^2 + h^2 + 2br\cos\phi)^{1/2}} + \frac{r - (D_b - b)\cos\phi}{(D_b - b)^2 + r^2 + h^2 - 2(D_b - b)\,r\cos\phi)^{1/2}} \right] \tag{7}$$

Measurement of f_d a minimum of five times in succession has been shown to allow estimation of the unknown quantities in the above relationship[2]. This however, requires that target altitude (h), velocity (V_r), and crossing angle (ϕ) remain constant over the time of measurement. It also requires that complex real-time processing be utilized.

As with the monostatic radar, the actual performance capabilities of a bistatic radar will depend on the specific design and the environment under which that radar will operate.

B. Detection Limits.

It is useful, in considering the application of radar to airborne intrusion detection, to discuss the general detection limits possible, given specific system parameters. Of course, the actual limits which would be experienced in a specific deployment are the results of the complex interactions of various factors. These factors will be addressed in subsequent sections. This section is intended to give a basic understanding of radar detection limits for general comparison to other candidate sensors.

1. Range

a. Monostatic. Monostatic radars have been designed for acquisition and tracking of objects at extremely long distances.[1] However, for the problem under consideration specific range and elevation limits can be defined. As stated, the primary threat considered in this study is the helicopter. Since they are capable of operation at near zero altitudes, the monostatic radar is forced to operate at extremely low angles in order to cover an entire detection volume from the ground up.

This requirement then defines the farthest point along the earth's surface which will be visible to observation will be the optical horizon. The optical horizon is simply the point on the earth's surface beyond which objects may exist hidden to the observer by the earth's curvature itself. Assuming a smooth

surfaced earth the range to the horizon can be seen to be a function of the height of the radar as shown in Figure II-4.

Thus

$$R = \sqrt{(R_e + h)^2 - R_e} \tag{8}$$

with the terms defined in the figure. Using R_e = 6356.9 kilometers, the range to the horizon can be approximated as

$$R = 3.56 \sqrt{h} \tag{9}$$

This would give R 19.5 kilometers for a radar deployed on a 30 meter tower.

It should, of course, be remembered that this is an approximation since local terrain and atmospheric refraction (bending of the propagating waves) will enter the problem along with the actual radar design parameters. However, the optical horizon does provide a useful measure of the detection range at which a monostatic radar can acquire low flying targets of interest to the airborne intrusion problem.

b. Bistatic. With respect to detection range, the bistatic radar should not be thought of in the same terms as the monostatic system. The receiver and transmitter of a bistatic system are seperated from each other to provide an electromagnetic fence for detection of targets crossing towards the defended area. Thus, detection distance from the sensor is dependent on numerous factors such as intervening terrain; transmitter and receiver height; target altitude, and antenna pattern (common volume coverage).

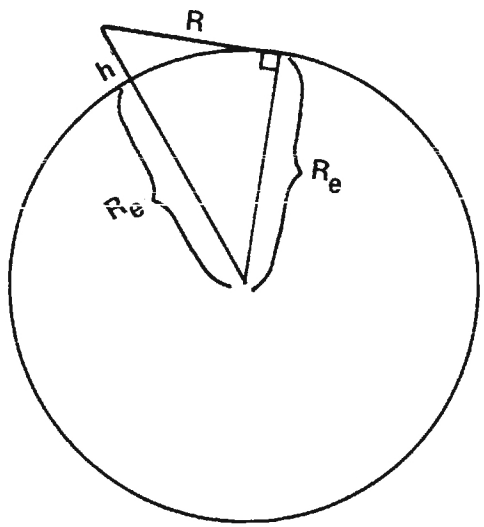

h – HEIGHT OF RADAR (METERS)

R – RANGE TO OPTICAL HORIZON (KILOMETERS)

R_e – EARTH'S RADIUS (KILOMETERS)

$$(R_e + h_r)^2 = R_e^2 + R^2$$

$$\therefore R = \sqrt{(R_e + h_r)^2 - R_e^2}$$

$$R \approx 3.56\sqrt{h} \text{ (KILOMETERS)}$$

Figure II-4. Relationship of Range to Optical Horizon and Radar Height.

2. Angle

a. Monostatic. The angular coverage obtainable by a monostatic radar is generally limited only by the scanning mechanism employed and the beam shape characteristics. Thus 360° coverage in azimuth and 90° coverage in elevation are commonly obtained. As was the case in the range discussion, the actual angular performance will be influenced by local terrain, etc.

b. Bistatic. The angular coverage limits of the bistatic radar will be a strong function of the beam shape employed. Assuming a fixed sector fence coverage, the beam shape will itself be the angular coverage.

C. Radar Range Equation

More precise evaluation of radar performance capabilities is obtained through use of the Radar Range Equation which provides a mechanism for studying and expressing the relationships between selected radar system parameters. A brief derivation and discussion of this equation for both the monostatic and bistatic radar concepts will be given in this section.

1. Monostatic. The Radar Range Equation for monostatic radar can be developed by following the signal from the transmitter to the target and back to the receiver.[1] Assuming the transmitted energy is radiated with power P_t uniformly in all directions, then the power per unit area at range R from the antenna is

$$\frac{P_t}{4\pi R^2} \tag{10}$$

Since actual antennae have directional characteristics represented by a gain factor[3], G_t, the power density at R from the antenna is

$$\frac{P_t G_t}{4 \pi R^2} \tag{11}$$

The radar cross-section, σ, of a target is represented in units of area and indicates the effect of the target in intercepting the transmitted energy and reradiating this energy isotropically (in all directions). Thus, the power density which will return to the antenna is

$$\left(\frac{P_t G_t}{4 \pi R^2} \right) \left(\frac{\sigma}{4 \pi R^2} \right) \tag{12}$$

The actual power which will be received by the radar depends on the effective capture area of the receiving antenna, A_e (often referred to as effective antenna aperture). This gives the received power, P_r, as

$$P_r = \left(\frac{P_t G_t}{4 \pi R^2} \right) \left(\frac{\sigma}{4 \pi R^2} \right) \left(A_e \right) \tag{13}$$

The effective aperture of a receiving antenna is related to the gain, G_r, by

$$A_e = \frac{G_r \lambda}{4\pi} \tag{14}$$

This gives the received power as

$$P_r = \left(\frac{P_r G_t}{4 \pi R^2} \right) \left(\frac{\sigma}{4 \pi R^2} \right) \left(\frac{G_r \lambda^2}{4 \pi} \right) \tag{15}$$

For a monostatic radar, the transmit and receive antennae are one and the same[3] so that $G_t = G_r = G$. This gives the simple form of the radar range equation as

$$P_r = \frac{P_t G^2 \lambda^2 \sigma}{(4 \pi)^3 R^4} \tag{16}$$

The radar range equation is the basis for analysis of the interactions and tradeoffs involved in design considerations of a radar. In actuality, many additional factors may be included to more thoroughly represent the complex environment and conditions under which a system will operate.

2. Bistatic. Development of the Radar Range Equation for the bistatic radar parallels that of the monostatic. The power density at a distance R from the antenna is again

$$\frac{P_t G_t}{4 \pi R^2} \tag{17}$$

Expressed in the terms of Figure II-3, this would be

$$\frac{P_t G_t}{4 \pi (D_t)^2} \tag{18}$$

Again, the power density which will be radiated to the receiver will be a function of D_r, the distance from the target to the receiver as

$$\left(\frac{P_t G_t}{4 \pi D_t^2} \right) \left(\frac{\sigma}{4 \pi D_r^2} \right) \tag{19}$$

The received power will then be determined by the expression

$$P_r = \left(\frac{P_t G_t}{4 \pi D_t^2} \right) \left(\frac{\sigma}{4 \pi D_r^2} \right) \left(\frac{G_r \lambda^2}{4 \pi} \right) \tag{20}$$

or

$$P_r = \frac{P_t G_t G_r \lambda^2 \sigma}{(4 \pi)^3 D_t^2 D_r^2} \tag{21}$$

Thus, the bistatic Radar Range Equation differs from the monostatic primarily in the need to account for the two antennae used and the individual path lengths from each antenna to the target.

D. Special Radar Information Considerations

1. Discrimination of Target Type. Of particular interest in the airborne intrusion problem is the capability of a radar system to have the capability to discriminate if a detected target is a helicopter. In the simplest situation, the target may display motion which after analysis of the track history would reveal whether the target is a helicopter or a small aircraft. However, it is very possible for these two aircraft types to exhibit nearly indentical motion, thus nullifying this simple discrimination technique.

A potential solution to this problem is to use Doppler processing to discriminate fixed wing aircraft from helicopters. As was discussed in Section A, a Doppler return is expected which corresponds to the relative velocity of the target. However, it has been observed that measurable additional doppler returns exist for helicopters. Figure II-5* shows a comparison of an example doppler return from a helicopter to that from a small airplane. Referring to Figure II-5, it can be shown that the spectrum of the fixed wing aircraft is very narrow around the frequency produced by the fuselage velocity. By comparison, the helicopter displays a significantly broader spectrum of discrete lines and harmonic relationships.

Various theories currently exist as to the mechanism that causes the spectrum for helicopters. It appears to be due to returns from the hub of the main rotor and possibly the blades themselves. This would be a result of the fact that the blade motion is such that it would appear to be moving relative to the radar and thus produce Doppler returns dependent on the rate of rotation of the blade and the relative motion of the helicopter itself. Given the difference in spectra between a helicopter and a fixed wing aircraft, radar systems using Doppler processing provide a basis not only for discrimination between aircraft types, but potentially for some distinction between individual helicopters with various blade rotation rates.

2. Detection of Object Separating from Aircraft. Some consideration has been given to the problem of detecting objects dropped from aircraft over an area

*For the purpose of this discussions, the data in the figure is displayed with a frequency of zero corresponding to the doppler return due to the relative velocity of the aircraft. Thus a strong component is present for both the helicopter and the airplane at zero.

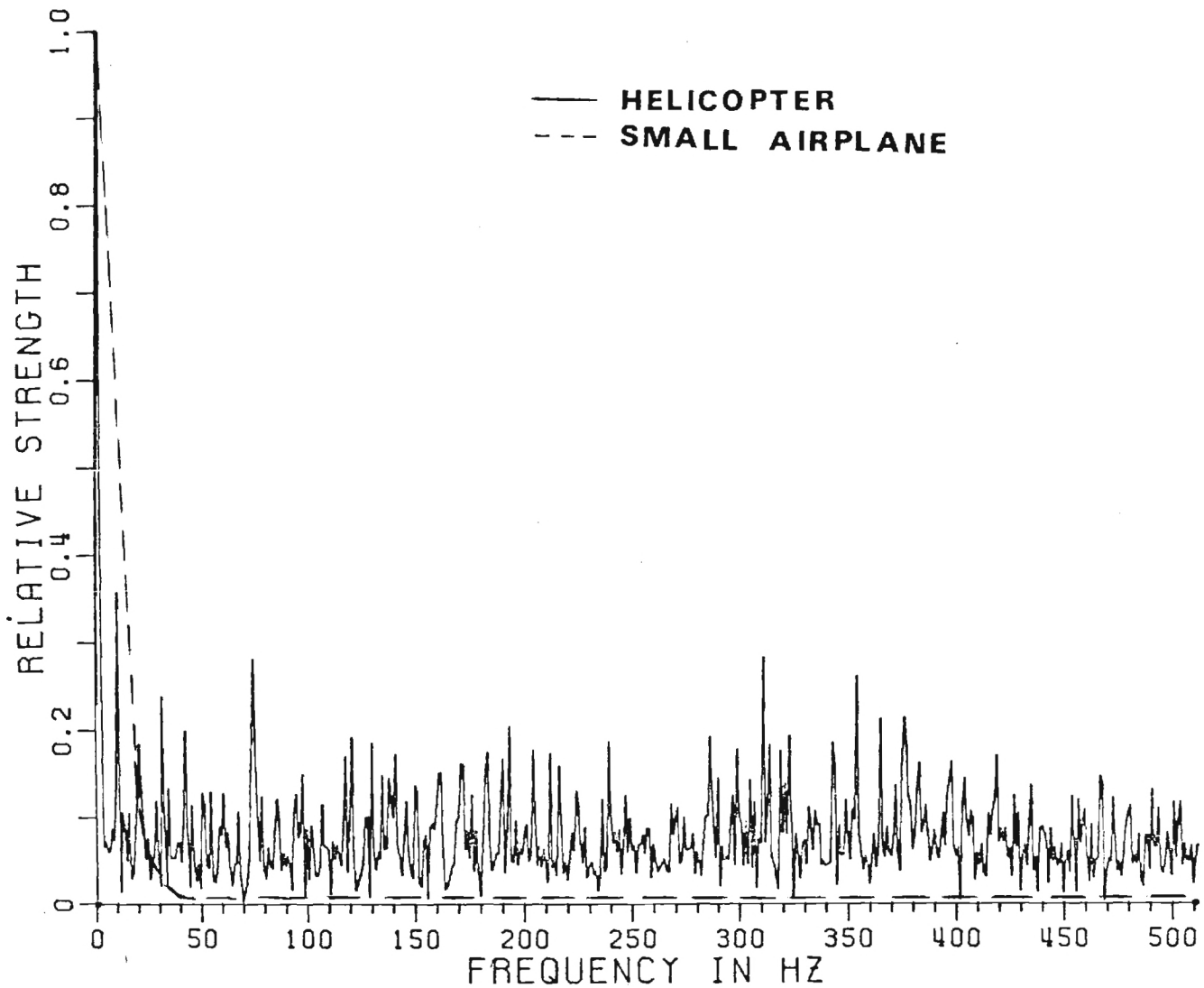

Figure II-5. Comparison of Example Doppler Frequency Characteristics for Helicopter and Small Airplane.

of interest. This problem is, of course, highly scenario dependent. However, in order to gain an appreciation for the impact on radar design, two examples have been chosen. In each example, the aircraft is assumed to be stationary in the sky at some point. These will be referred to as Case 1 and Case 2.

For Case 1, the aircraft is assumed to be at an altitude of 1000 meters and a ground range of 1000 meters. Case 2 assumes an altitude of 2000 meters and a ground range of 2000 meters. The problem then is to determine the angular resolution of the antenna beamwidth required to resolve the aircraft and the separating object. This analysis will show how the resolution requirements impact the radar design and performance.

In Section A, the 3 dB beamwidth was discussed as the function controlling the angular resolution of a radar. This means that if two objects are separated by an angular amount, θ, then a 3 dB beamwidth of θ will be required for a radar to observe each object as a seperate target. Thus, in Figure II-6, the angular separations (3 dB beamwidth) as a function of distance between aircraft and falling object are shown for the two cases. From Figure II-6, it can be seen that a radar with a 3 dB beamwidth of 0.5° would be capable of observing a falling object once it was ~17 meters from the aircraft in Case 1 and ~34 meters for Case 2. Likewise, a 1.5° beamwidth would resolve an object at ~50 meters in Case 1 and ~100 meters in Case 2. Thus it can be seen that in the two examples being examined the choice of antenna beamwidth has a significant impact on where an object would be detected as a seperate target from the "drop" aircraft.

Carrying the analysis a step further, it can be shown that the choice of beamwidth will impact a rapid scan phased array antenna design for the purpose of

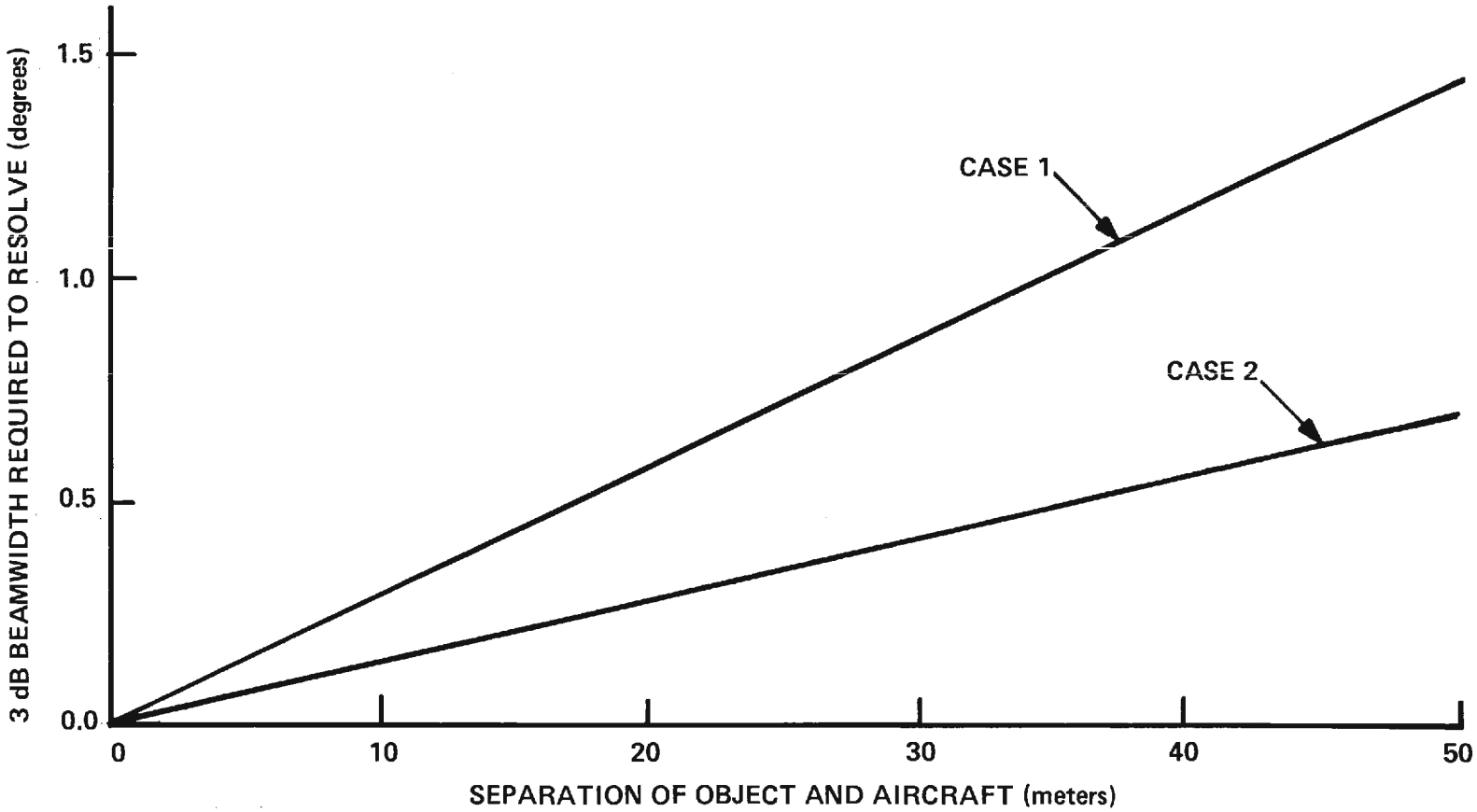

Figure II-6. Angular Resolution Requirements for Detection of Separating Objects.

falling object detection.* This can be accomplished using two basic relationships. The first relates the desired beamwidth to an array diameter by

$$D \simeq \frac{58\ \lambda}{\theta_{3dB}} \tag{22}$$

where D = array diameter

λ = wavelength of transmitted signal

θ_{3dB} = 3dB beamwidth

The second relates the choice of array diameter to the nearfield (Fresnel Zone) boundary by

$$R \simeq \frac{2D^2}{\lambda} \tag{23}$$

where R = boundary of nearfield.

The first relationship is fairly self-explanatory as it gives an idea of the size that an array would need to be. The second relates how a region of space near the antenna (the nearfield region) cannot be depended on for reliable measurements because of complex electromagnetic interactions which occur[3].

Figure II-7 shows both the array diameter and the nearfield boundary as a function of frequency for beamwidths of 0.5° and 1.5°. It can be seen that array diameters of from ~13 meters to ~1 meter may be required dependent on beam-

*A phased array antenna would be the most likely choice in this case due to the combined requirement for good angular resolution and the capacity to rapidly scan a volume surrounding the aircraft while maintaining track.

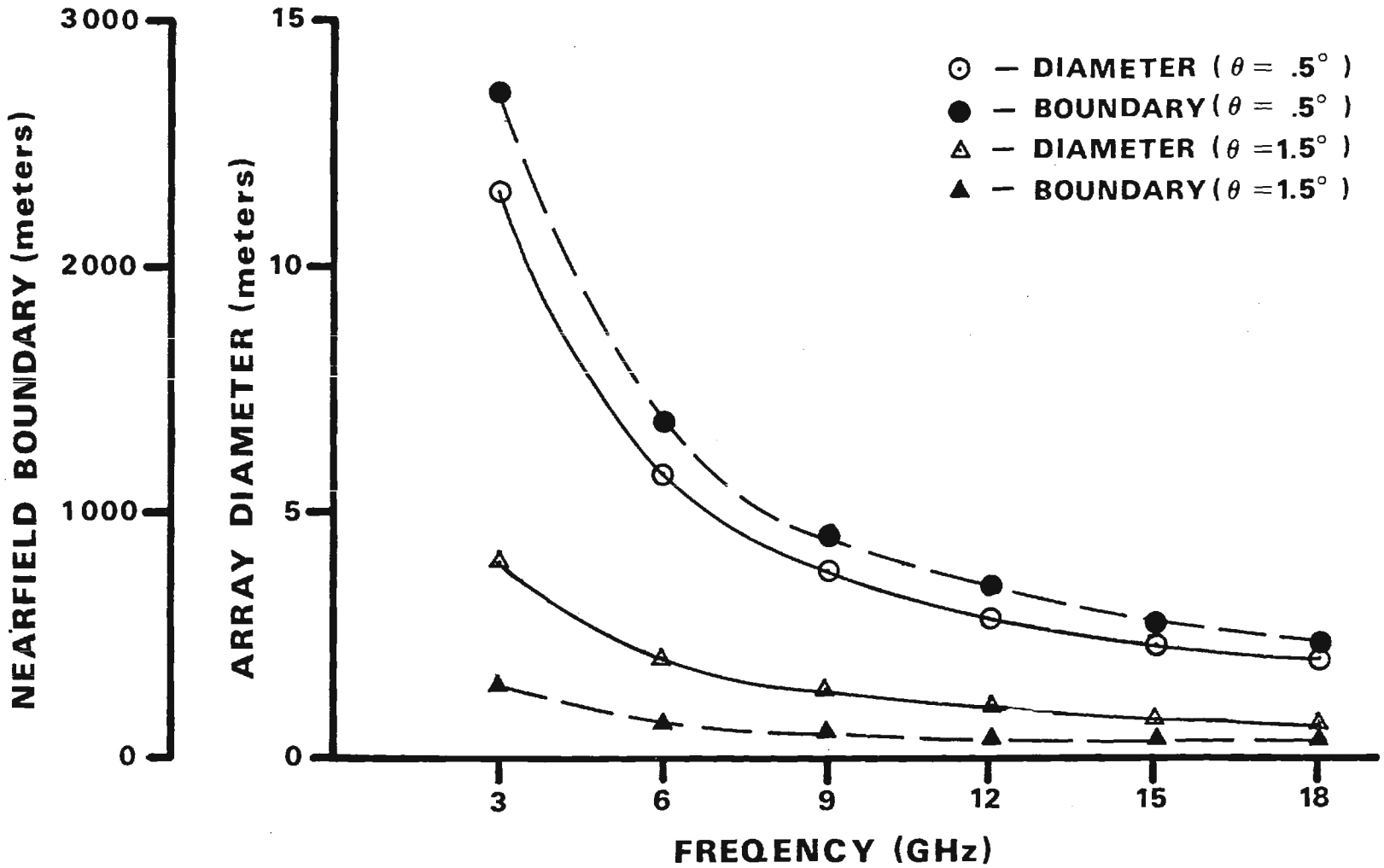

Figure II-7. Impact of Beamwidth Requirement on Phased Array Diameter and Coverage.

width alone. Also in some cases, significantly large areas of space around the radar would be unreliably covered. In some cases the nearfield boundary is as great as 2300 meters.

None of the previous discussion was guided by actual firm requirements to detect separating objects. It was included to show the impact that threat scenerio definition can have on the design of an airborne intrusion detection system.

E. Performance Considerations

All of the previous discussion pertaining to the application of radar to the airborne intrusion detection problem has been intended to give a basic understanding of the characteristics and performance which might occur in a general case. In actual deployment, radar, like all sensors, encounters many factors which influence performance. These include both natural and man-made effects.

It is the intention of this section to briefly list examples of how these effects relate to performance and to give some indication of their impact on a radar deployment. No one single radar will be influenced by all of the possible conditions. However, each effect must be considered in the analysis of the actual performance anticipated by a radar to ensure no unexpected degradation in performance once the system is put into operation.

1. Natural Effects. The primary natural effects which influence radar performance are weather, terrain, and vegetation. For weather, refraction of the radar beam by the atmosphere can create errors both in elevation angle and range measurements. A first order approximation of the geometric relationship that results from refraction is the 3/4 earth's model[1]

$$h_t = (0.1048)\, R^2 \cos^2 \theta + (1000)\, R \sin \theta + h_r \qquad (24)$$

where

h_t = target altitude (meters)

h_r = radar altitude (meters)

R = range to target (kilometers)

θ = elevation angle

More complex models exist but are most useful for radar applications over longer ranges than necessary for the airborne intrusion problem.

Attenuation due to atmospheric water vapor in various quantities and phases can be important in determining radar performance. Figure II-8 shows atmospheric absorption due to oxygen and water vapor.[1] Over a wide range of frequencies these effects are negligible. However, choice of frequencies around 22.22 GHz and 60GHz would result in severe attenuation of the signal.

Likewise, Figure II-9 shows theoretical rain attenuation (condensed water vapor) versus rainfall rate for several frequencies.[1] It can be seen that under particular conditions the attenuation experienced could have a major effect on the performance of a radar. Thus knowledge of the atmospheric conditions to be expected will dictate the careful selection of the radar operating parameters.

With respect to terrain, the primary radar performance considerations are blockages and multipath. Blockage simply refers to the condition where local terrain presents blockage between a radar and the target of interest. This may occur due to hills within the area of desired surveillance or local depressions in the topography. Thus, local site conditions must be thoroughly accounted for in determining the predicted performance for a radar site.

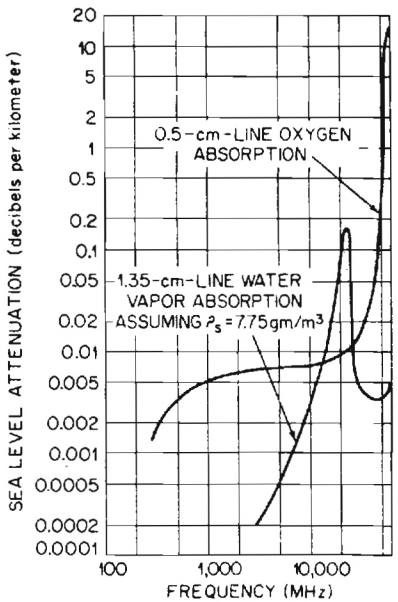

Figure II-8. Atmospheric Absorption by the 1.35-cm Line of Water Vapor and 0.5-cm Line of Oxygen. (from Reference 1)

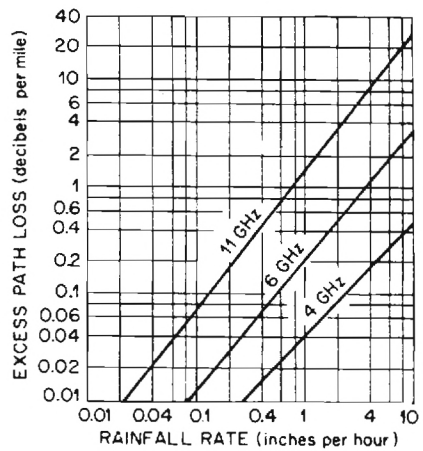

Figure II-9. Theoretical Rain Attenuation VS. Rainfall Rate. (from Reference 1)

Multipath presents problems to radar under conditions of operating at very low elevation angles.[4] Two types of multipath interference may occur. Figure II-10 displays the geometry involved and shows the condition that occurs when a reflection off of the target returns to the radar via ground reflection. An image target is created which is below the elevation of the actual target and appears to be at a range of $R_1 + R_2$, thus causing confusion as to which signal represents the actual target.

Also, multipath may be considered in terms of ray theory where two rays of energy arriving at a point in space appear to have originated from different locations. These rays recombine as a vector summation of the two original rays and either constructively reinforce or destructively interfere with each other. The result is a distortion of the original free space electromagnetic field. Antennas used to perform the search/surveillance functions may have what is generally described as a cosecant squared pattern. This shape for the antenna pattern is chosen because it provides good high elevation coverge and produces a signal return which is constant with a given separation in altitude. The distortion of the free space pattern due to multipath is illustrated in Figure II-11. The magnitudes of the interference nulls and lobes are dependent on the reflecting surface characteristics, antenna tilt, and free space beam shape. From Figure II-11, it is seen that targets flying in a null region may remain undetected for long periods of times, especially at long ranges where the elevation angle to the target is changing very slowly.

The existence and severity of multipath interference depends on several factors. These include the reflective characteristics of the target, the beamwidth of the antenna, the elevation of the target, and the reflective characteristics of

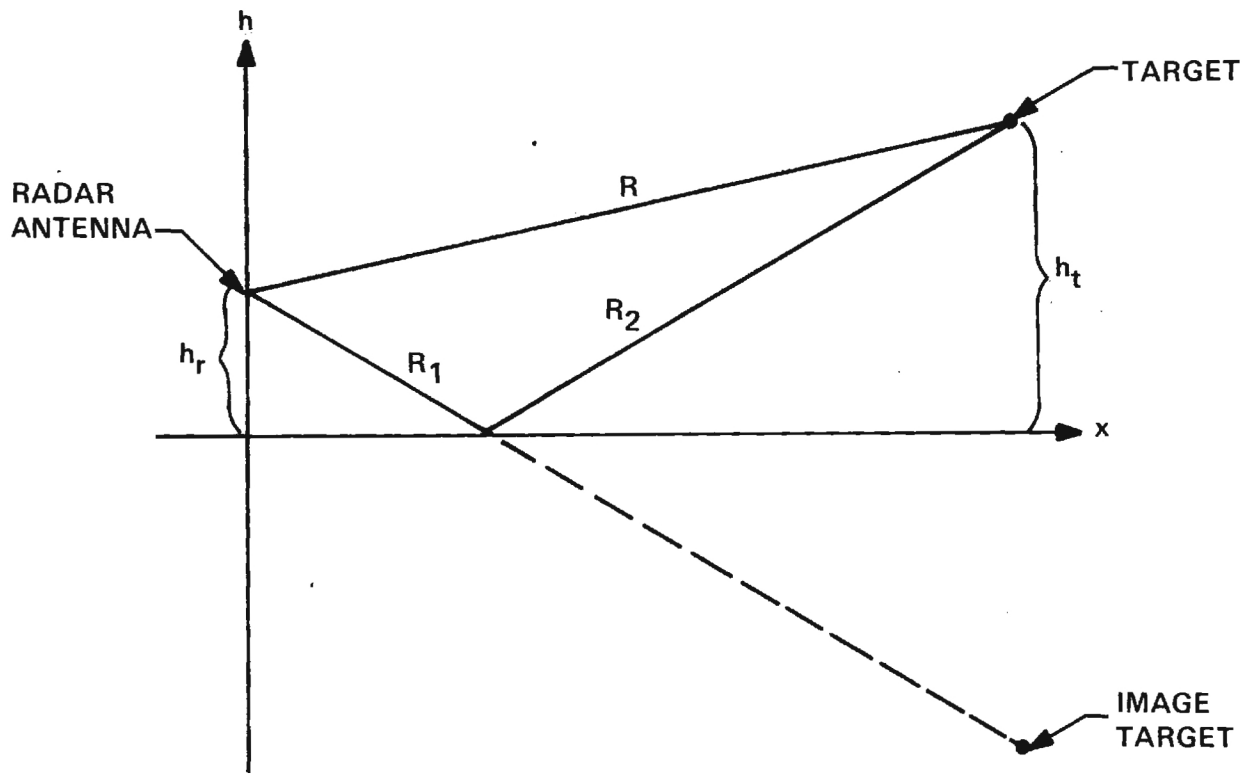

Figure II-10. Geometry of Multipath Reflection.

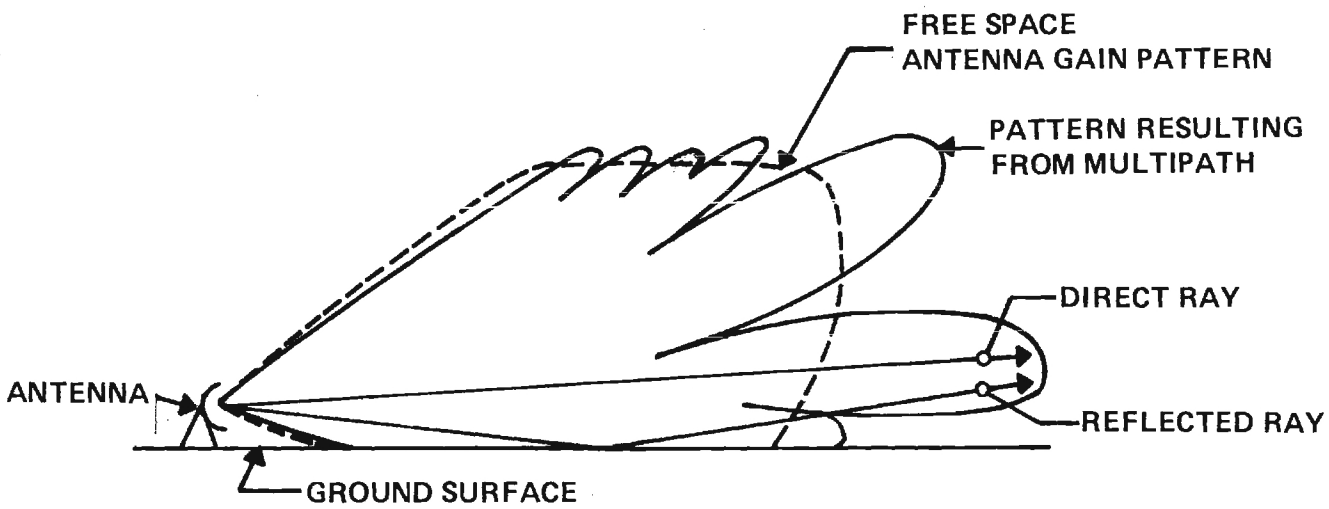

Figure II-11. Illustration Showing the Effects on a Free Space Antenna Pattern of Interference Resulting from Ground Reflections.

the ground. The errors which could result from this effect can be as great as several tenths of a beamwidth under particular conditions. Thus, proper modeling is essential to avoid catastrophic results in a radar deployment.

2. Man-Made Effects. Radar performance evaluation must also take into account effects that are man-made. These primarily include air and ground traffic in the vicinity of the radar, structures, and intentional electronic interference. The impact of air and ground traffic is to present non-threatening targets to the radar which must be sorted out and distinguished so as to avoid false alarm situations. This complicates the information processing requirements for the system and will be most severe if the radar is in the vicinity of an airfield or a highway.

Structures in the line of sight of a radar present the same difficulty as did the terrain discussed in Section E.1. Blockage may occur which premits an approaching target to remain undetected until it maneuvers from behind the obstacle. Thus these characterists of a specific site must be taken into account when conducting a radar site survey to determine the best location for an air penetration detection and warning system.

The final and most unpredictable man-made effect which requires some consideration is intentional electronic interference (i.e. jamming). Wide varieties of jamming techniques exist[1] all with the expressed purpose of minimizing the likelihood that a target will be properly detected and/or discriminated. Some methods attempt to increase the overall noise level being seen by the receiver so that detection is difficult. Others attempt to create false targets so as to cause uncertainty as to which, if any, returns are to be responded to by the system. The

exact character of the degradation that may be experienced depends on both the radar and the jamming technique.

SECTION II

REFERENCES

1. Skolnik, M. I., Radar Handbook, McGraw-Hill Book Company, New York, 1970.

2. Skolnik, M. I., "An Analysis of Bistatic Radar", IRE Transactions on Aerospace and Navigational Electronics, March 1961.

3. Kraus, J. D., Antennas, McGraw-Hill Book Company, New York, 1950.

4. Barton, D. K., "Low-Angle Radar Tracking", Preceedings of the IEEE, Vol. 62, No. 6, June 1974.

SECTION III

FUNDAMENTALS OF ACOUSTIC DETECTION OF AIRBORNE INTRUSION

Introduction

This section is intended to give the reader some heuristic insight into the field of acoustics from the perspectives of both the historical and scientific interests on one hand and the highly pragmatic applications of modern mensural acoustics to the purposes of aircraft detection, location and identification to be discussed. Most of the data presented in this section are intended for conveyance of qualitative information regarding the nature of the acoustic quantities commonly measured and their rough orders of magnitude rather than for the conveyance of quantitative information intended for direct application to system design. Since no particular system of units has ascended to near universal, exclusive usage in acoustic measurements, no attempt has been made at unit standardization in this section. It is felt that the information will be more illustrative of the developments and trends in acoustics if it is preserved in the form and units of original presentation by the reference sources.

A. Review of Airborne Threats Considered Detectable by Acoustic Means

1. Helicopter. The helicopter is the most credible vehicle to be used in an airborne attack on a nuclear facility. Helicopters are readily available commercially for sale or rent; can be piloted by novice aviators after several months of instruction; are able to land and take-off in small spaces; can carry stolen fissionable material or weapons; and are fast enough to escape to a safe distance within the expected effective pursuit response time at some sensitive installations.

2. Fixed-Wing Reciprocating Engine Aircraft. The abundance of fixed-wing piston engine aircraft makes such aircraft highly available for use in secure area intrusion. This form of aircraft includes fixed wing conventional aircraft and short take off and landing (STOL) aircraft.

3. Jet or Turboprop Aircraft. These would seem to be the least likely of the acoustically detectable aircraft to be used for the purpose herein considered. They are generally inferior in short field capabilities, however, they could be effectively employed to drop parachutists.

4. Autogyro. Although this intrusion mode may seem to be somewhat less likely than a helicopter, the autogyro does have the essential capabilities for intrusion; short take-off and landing, and escape speed. One-man autogyros can be purchased for approximately $3,000 and require less flight instruction than the minimum for private fixed-wing aircraft.

B. Review of Airborne Threats Considered Nondetectable by Acoustic Means

1. Hang Gliders. Although hang gliders are plentiful, inexpensive and quiet they require certain terrain and wind conditions for use and could probably offer no means of escape with stolen material. For these reasons they would seem to be an unlikely vehicle for secure area intrusion. Because of their low speeds, radar detection of hang glider intrusion threats would give a long lead time for defensive response. The hang glider would offer no detectable acoustic signature while airborne. However, powered hand gliders now exist with the capability of carrying over 200 pounds (including pilot).

2. Hot Air Balloons. The gas heaters used by hot air balloons do produce an audible roar; however, it is neither continuous nor spectral and for purposes of this

discussion will be considered inaudible. Radar detection would almost certainly give some advance warning of hot air balloon intrusion. In addition, the need for favorable winds would make a hot air balloon intrusion difficult to plan in advance.

3. Parachutist. After leaving the "drop" aircraft, a parachutist would have no detectable acoustic signature. The seismic signature of the parachutist landing could most likely be detectable by existing sensors.

4. Backmounted Rocket. A personal, backmounted H_2O_2 rocket pack could conceivably be used for secure area penetration from short ranges. It would most likely have a wide band acoustic output.

C. Sources of Aircraft Acoustic Energy

1. Piston Engine Exhausts. The exhaust blasts of piston engines occur at the firing rate, which is one half of the crankshaft rotation rate times the number of cylinders. For a directly driven two bladed prop powered by a six cylinder, two cycle engine at 1800 rpm, the propeller blade passing rate is: 2 blades/revolution x 30 revolution/sec., i.e. 60 Hz. The exhaust pulse rate is: 3 firings per revolution x 30 revolutions/sec., i.e. 90 Hz. The ratio of exhaust pulse rate to propeller blade rate is a constant 3/2. Because of the pulse like (pulsatile) nature of the exhaust bursts many harmonics are generated. Consequently the exhaust noise spectrum is highly spectral in character with a fundamental frequency equal to the cylinder firing rate (90 Hz in the example described above) and prominent harmonics at 2, 3, 4...n times the fundamental frequency where n may be as high as 20 or 30.[1] (See Figure III-1)

Multiple engine aircraft may have between engine distances on the order of wavelengths of the exhaust fundamental (wavelength equals about 12 feet for 90

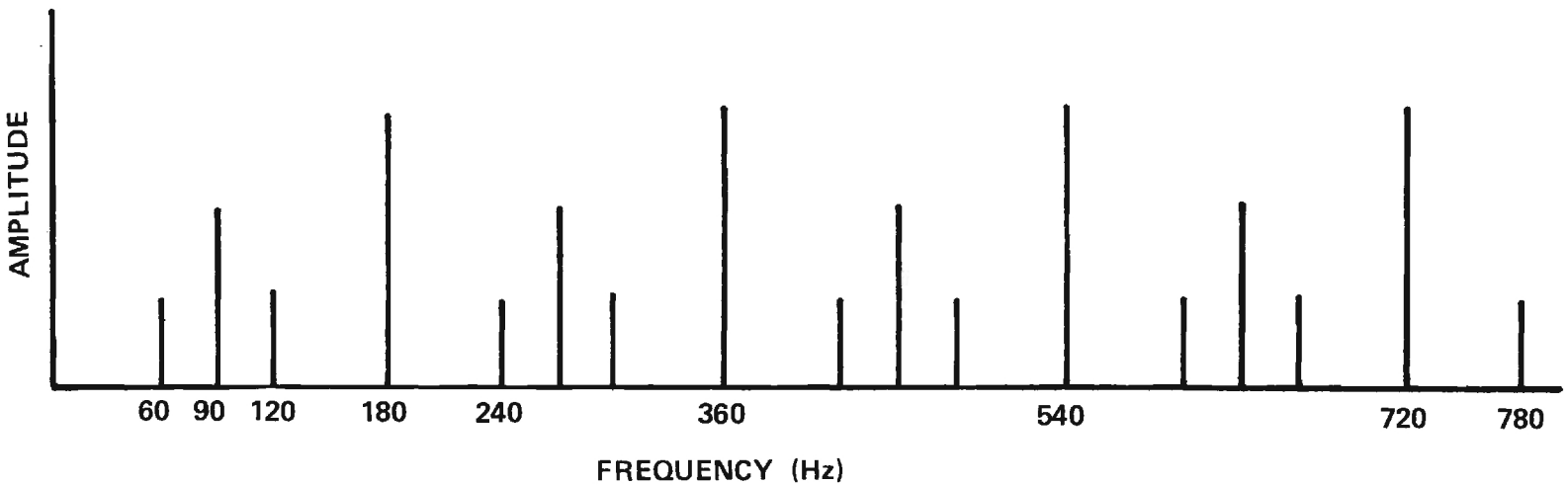

Figure III-1. Acoustic spectral lines produced by six cylinder piston engine aircraft with two blade direct prop turning at 1800 rpm. Exhaust fundamental at 60 Hz. Prop and exhaust spectra add at 180, 360, 540, 720, ---n 180 Hz.

Hz) and the engines may be nearly, but not quite, synchronous. Thus the exhaust pulses of the different engines may add constructively or destructively depending on the orientation of the aircraft and also on time. This effect will impart an amplitude modulation effect to the aircraft's acoustic signal.

2. Propeller and Rotor Blades. Propellers and helicopter rotors produce pulsatile acoustic signals with fundamental frequencies equal to the blade passing rate (i.e. the rate of drive shaft rotation times the number of blades) which, as a consequence of their pulsatile nature, have many associated harmonic frequencies.[2] (See Figures III-2 and III-3)

The mechanisms of helicopter rotor noise include: blade slap[3] (which results from interaction of a rotor blade with another rotor blade's tip vortex; occurring only under certain conditions), a tail rotor rotational noise, main rotor vortex noise and main rotor rotation noise.

3. Gearboxes. The tooth mesh in rotor gearboxes produces fundamentals at the mesh rate. Since the rotor rates are held approximately constant through all flight conditions the gearbox noise has approximately constant fundamentals. A UH-1A has 90° and 42° tail rotor gearboxes which give peak amplitudes around 1200 and 1800 Hz respectively. These higher frequencies (which typify helicopter gearbox noise) are attenuated by the atmosphere much more rapidly than are the lower frequencies. (see Figure III-2)

4. Jet Turbines. The acoustic output from turbine engines is basically white and in the frequency range from 1,000 to 10,000 Hz. Some very low intensity spectra of high fundamental frequencies are generated by the compressor and turbine blades, most noticably in front of the engine air intake. Turbine exhaust noise is relatively insignificant. About 90% of the power produced is coverted to

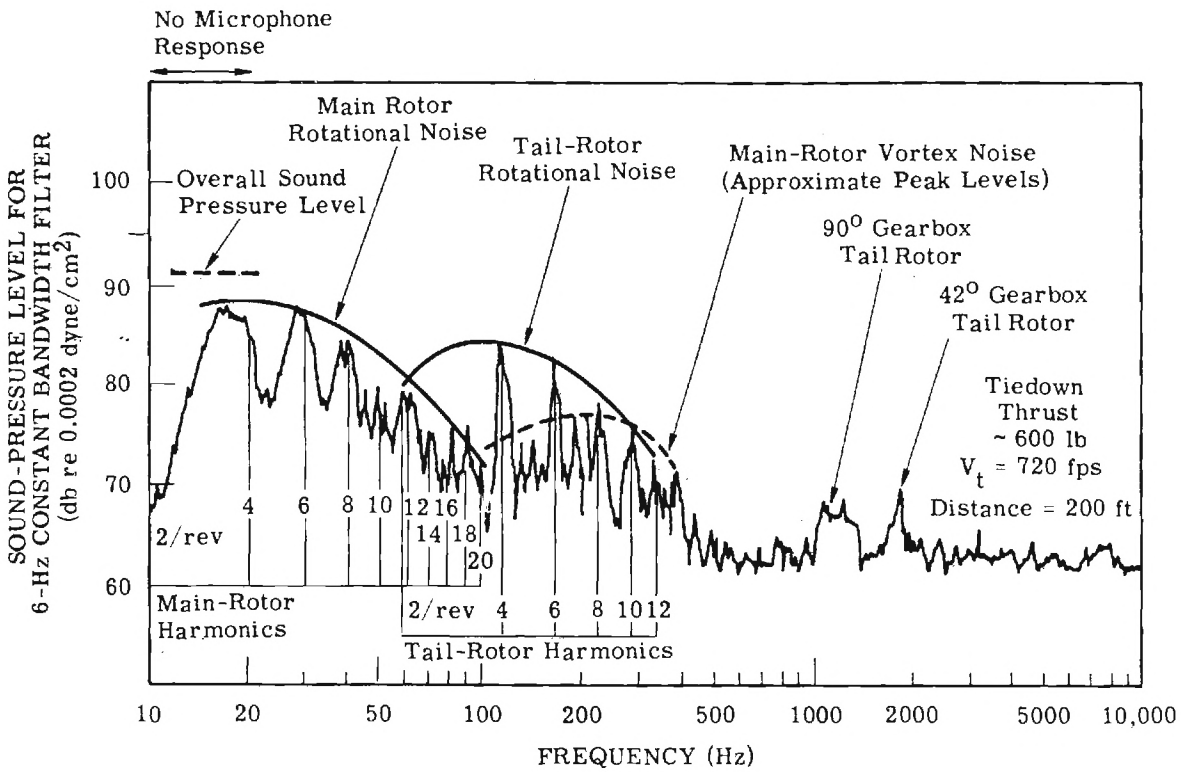

Figure III-2. UH-1A external noise spectrum at distance of 200 feet.

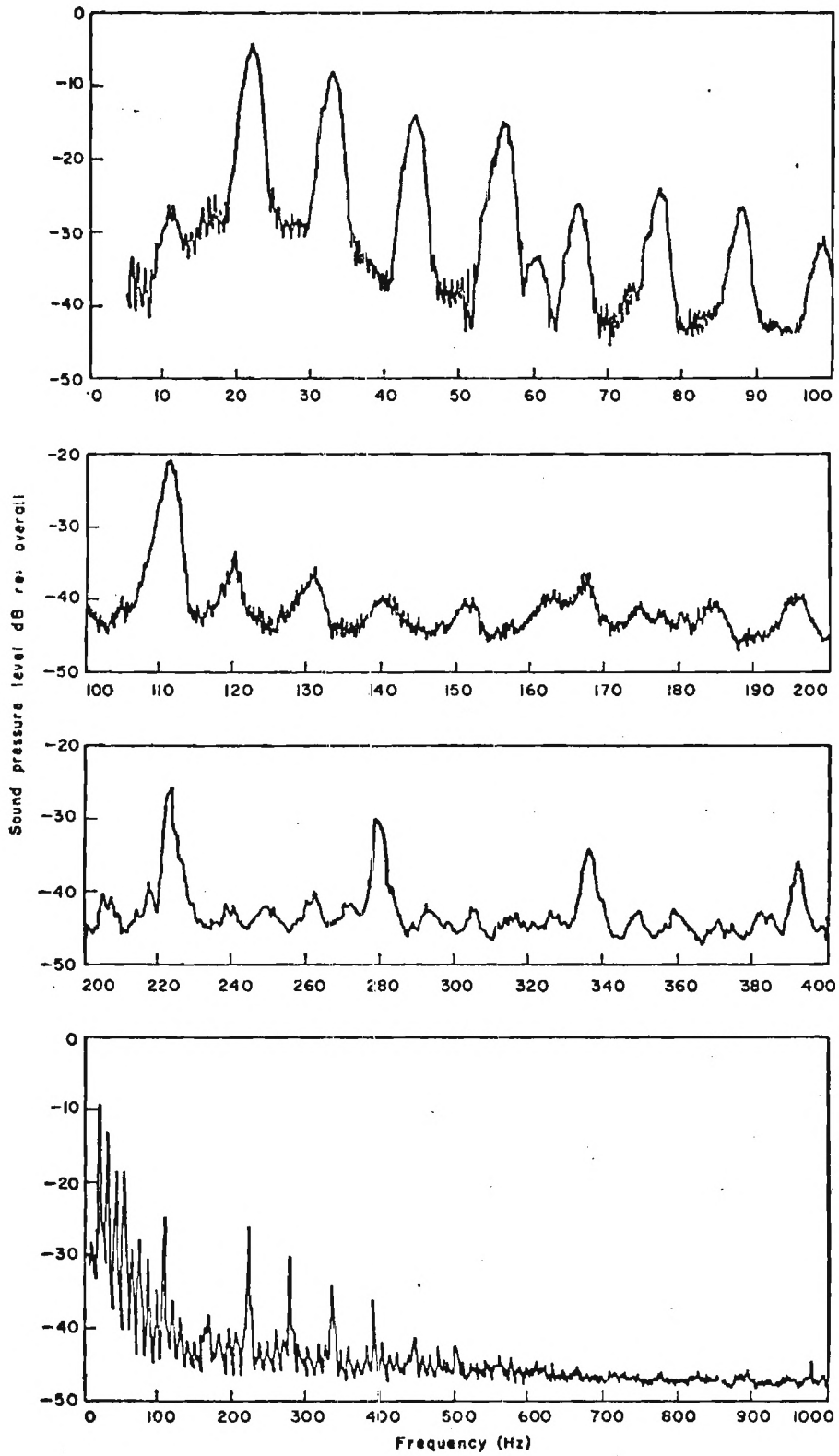

Figure III-3. Two Hz bandwidth analysis of UH-1B noise spectrum. Microphone approximately 100 ft. forward of rotor hub. Aircraft on ground, about to take off.

rotating shaft power. Generally, the rotor related noise of a helicopter strongly overrides the turbine noise.

5. Turbojet and Turbofan Engines. When operating at high power levels jet engines generate a broad, white noise with highest intensity in the exhaust direction. At low power levels the acoustic output acquires some high frequency narrow band spectra generated by the fan and compressor blades with the greatest sound intensity being in front of the engine inlet. Generally, the greater the engine thrust the lower will be the frequency of maximum acoustic power. The low power narrow band noise occurs between 1200 and 2400 Hz for a J57 turbojet and between 2400 and 4800 Hz for a TF33 turbofan.[1] At high power levels neither turbojets nor turbofans produce noticable noise spectra. The turbofan's bypass air mixing in the exhaust stream reduces its noise generation at high thrust to 10 dB or more below a comparable power turbojet.

6. Aerodynamic Disturbance. Aerodynamic friction noise covers a broad spectrum from about 150 to 10,000 Hz but has little power below about 600 Hz. Although it may be the principal source of foreward interior noise on many aircraft it contributes much less than propeller and engine to external noise.

D. Factors Determining the Power Received from an Airborne Acoustic Source as a Function of Range

1. Introduction to Acoustic Measurements. Sound is an oscillitory or wave phenomenon and as such its displacement amplitude is described by a function satisfying the general wave equation

$$\frac{1}{c^2} \frac{\partial^2 \psi}{\partial t^2} = \frac{\partial^2 \psi}{\partial x^2} + \frac{\partial^2 \psi}{\partial y^2} + \frac{\partial^2 \psi}{\partial z^2} \qquad (1)$$

where c is its phase velocity. For gases the value of c is given by $c = (\frac{E}{d}\gamma)^{1/2}$ where E is the bulk modulus of the gas, d is the density and γ is the ratio of specific heat at constant pressure to the specific heat at constant volume of the gas. For air and other diatomic gases $\gamma = 1.402$. The bulk modulus E is equal to the static pressure P_o which is about 1.013×10^6 dynes/cm^2 for air at standard pressure at sea level. The standard density of air is about .001293 gm/cm^3. These values lead to

$$c = \left(\frac{1.402 \times 1.013 \times 10^6 \text{ dynes/cm}^2}{.001293 \text{ gm/cm}^3}\right)^{1/2} \qquad (2)$$

c = 33,142 cm/sec. As the speed of sound in air (i.e., 1087.33 feet/sec).

From Charles' Law we have for one mole of gas PV = RT where R is the universal gas constant per mole equal to 8.31×10^7 erg/^{o}K. Then since one mole of air is 28.966 grams (dV = 28.966)

$$c = \left(\frac{P\gamma}{d}\right)^{1/2} = \left(\frac{RT\gamma}{dv}\right)^{1/2} = \left(\frac{1.402 \times 8.3 \times 10^7 T}{28.966}\right)^{1/2} \qquad (3)$$

$= 2005.5\ T^{1/2}$. Thus, the speed of sound in air is a function of temperature alone.

Since the speed of sound depends on temperature and temperature depends on altitude, the speed of sound is also a function of altitude as indicated in the graphs of Figures III-4 and III-5.[4]

The power density transmitted by a sound wave across a unit area perpendicular to its direction of travel is given by [5]

$$I = 2\pi^2 cf^2 dA^2 \qquad (4)$$

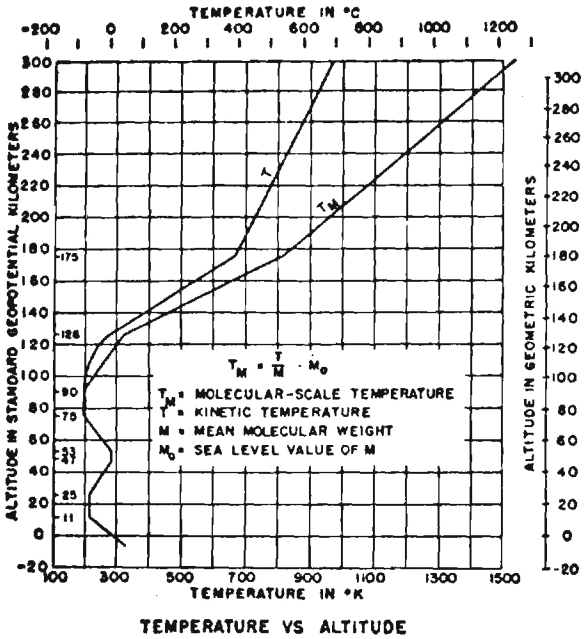

Figure III-4. Atmospheric temperature vs. altitude.

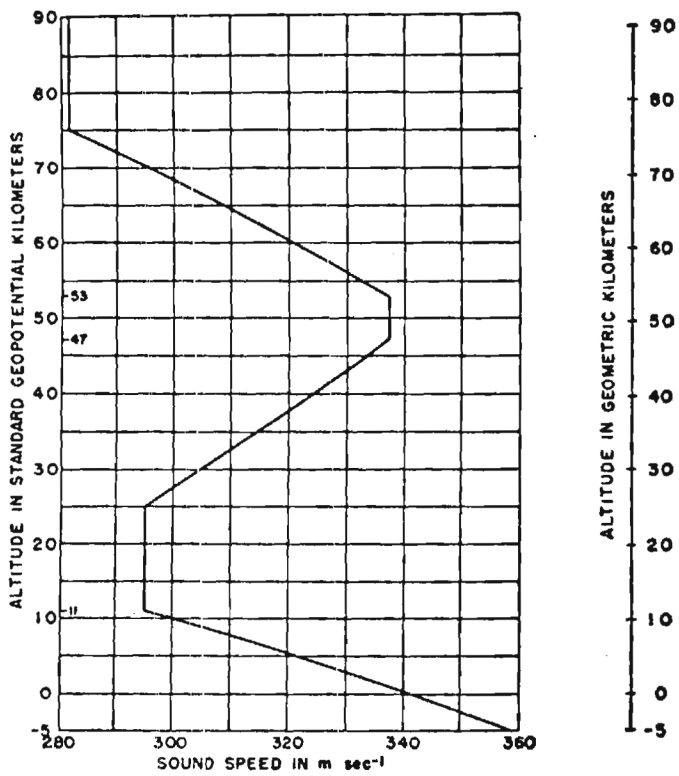

SPEED OF SOUND VS. ALTITUDE

Figure III-5. Speed of Sound Vs. Altitude.

where c is the wave speed, f is the frequency, d is the density of the medium and A is the amplitude of molecular displacement. It is known as the intensity of the wave and is given in erg/cm^2-sec. To exemplify the small displacements and slow oscillatory motions of sound medium molecules, consider the amplitude and particle speed ($2\pi fA$) of two 2000 Hz sound waves - one at the threshold of feeling (most intense sound perceived as sound) and the other at the threshold of hearing (the least intense sound perceptible; refer to Figure III-6),

MOST INTENSE SOUND AT f = 2000 Hz

$I = 10^{-4}$ watts/cm^2 = 10^3 erg/cm^2/sec= $2\pi^2 \times 33{,}142 \times 2000^2 \times .001293A^2$

amplitude $A = 5.44 \times 10^{-4}$cm

particle speed = $2\pi fA$ = 6.83 cm/sec.

LEAST INTENSE SOUND AT f = 2000 Hz, $I = 2\times10^{-17}$ watts/cm^2

$I = 2 \times 10^{-17}$w/cm^2 = 2×10^{-10}erg/cm^2/sec = $2\quad^2 \times 33{,}142 \times 2000^2 \times .001293A^2$

$A = 2.42 \times 10^{-10}$cm

particle speed = 9.6×10^{-6} cm/sec.

These examples illustrate not only the very small magnitudes of particle motion in a sound-transmitting medium but also the extreme dynamic range of the human ear - on the order of 10^{12} in power sensitivity.

Another way of writing the sound intensity I is

$$I = 2\pi^2 cf^2 dA^2 = \tfrac{1}{2} cd\,(2\pi fA)^2 = C\,\tfrac{1}{2}\,dv^2 \qquad (5)$$

where v is the maximum particle speed. This expression shows the kinetic nature of sound energy.

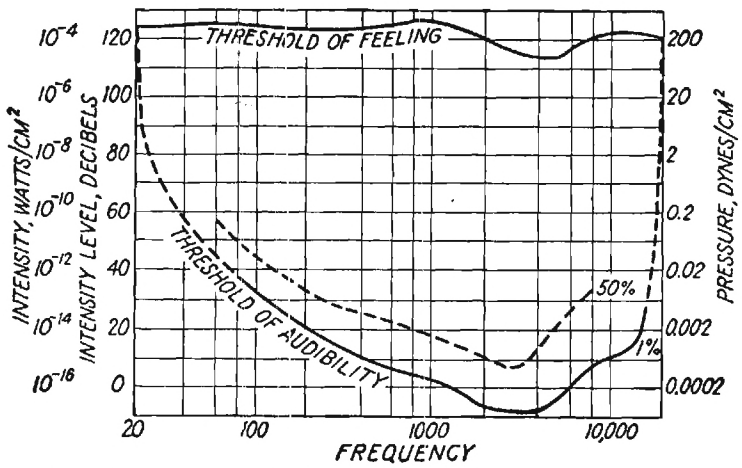

Limits of audibility. Only within the region of frequency and intensity enclosed by the curves is the sensation of sound excited.

Figure III-6. Limits of audibility. Only within the region of frequency and intensity enclosed by the curves is the sensation of sound excited.

The sound energy density time-averaged at a point over which an acoustic wave is passing is given by

$$E = \frac{I}{c} = 2\pi^2 f^2 dA^2 = \tfrac{1}{2} dv^2 \qquad (6)$$

Yet another expression for sound power intensity using rms sound pressure is: $I = \frac{P^2_{rms}}{dc}$ which in cgs units yeilds erg/cm^2-sec, or in mks units yields watts/m^2.

The concept of acoustic impedance is analogous to that of electrical impedance. By definition the specific acoustic impedance of a medium is the ratio (real or complex) of the sound pressure to particle velocity, $z = p/v$ (N/m^2-sec, a unit of specific acoustic impedance known as a "rayl" in mks units - p/v calculated in cgs units yields a unit of acoustic impedance, the acoustical ohm, 10 times larger than a rayl).[6]

Since $P = dc\, 2\pi fA$, and $v = 2\pi fA$, then

$$z = \frac{dc2\pi fA}{2\pi fA} = dc \qquad (7)$$

The cgs unit of z is acoustical ohm-cm^2.

The acoustic impedance of air at STP is $z = dc = 1.283 kg/m^3 \times 331.42 m/sec = 428.5$ rayls. For distilled water at 25° C, $d = .998 \times 10^3 \times 1498 = 1.495 \times 10^6$ rayls, and for sea water at 25° C, $z = 1.025 \times 10^3 \times 1531 = 1.569 \times 10^6$ rayls.

2. Propagation and Attenuation of Sound in the Atmosphere. Thermal gradient refraction and ducting can occur under thermal inversion conditions as illustrated in Figure III-7. An inversion layer may occur over land on clear calm

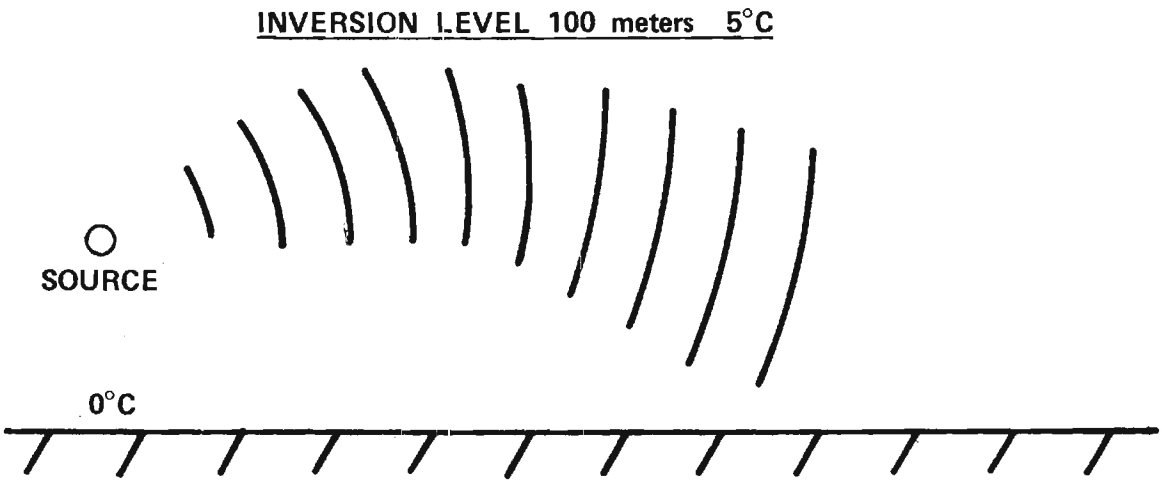

Figure III-7. Inversion layer causing acoustic ducting. Power intensity tends toward 1/R dependency.

nights as the Earth's surface radiatively cools and in so doing, cools the layer of air just above to a height of perhaps 50 to 100 meters. Inversions occur at higher altitudes, too. Level cloud layers almost always have overlying inversions.

If the inversion level is at 100 meters and the inversion temperature is 5° C above the surface temperature as in Figure III-7, sound waves generated at an acoustic source will be refracted toward the Earth's surface. A plane acoustic wave front moving horizontally will undergo wave vector refraction at a rate of about $.52^{\circ}$ per hundred meters in this thermal gradient inversion. Under these conditions, the wave front of a source located at a height of about 50 meters will be refracted downward from the inversion level at a range of about 1050 meters from the source. Acoustic waves thus refracted by the inversion layer will tend to be contained by and directed within the inversion layer out to larger radii and hence tend toward a 1/R dependency of power on horizontal distance R from the source. This ducting phenomenon accounts for the exceptional clarity of distant-source sounds on some clear, still evenings.

In contrast to the extended range afforded sound waves by inversion layers is the relatively short range associated with unstable, turbulent atmosphere as evidenced by the usual inaudibility of thunder beyond a range of about 10 km. The frequency spectrum of thunder is characterized by the dominance of infrasonic waves of about 5 Hz which are propagated over much greater distances than are the audible waves.

Under standard conditions, in the absence of an inversion layer, i.e., if the speed of sound decreases with increasing altitude, an acoustic wave front will be refracted upward as shown in Figure III-8 (with a radius of curvature of about 52 miles) to the stratosphere where the temperature will begin to increase with

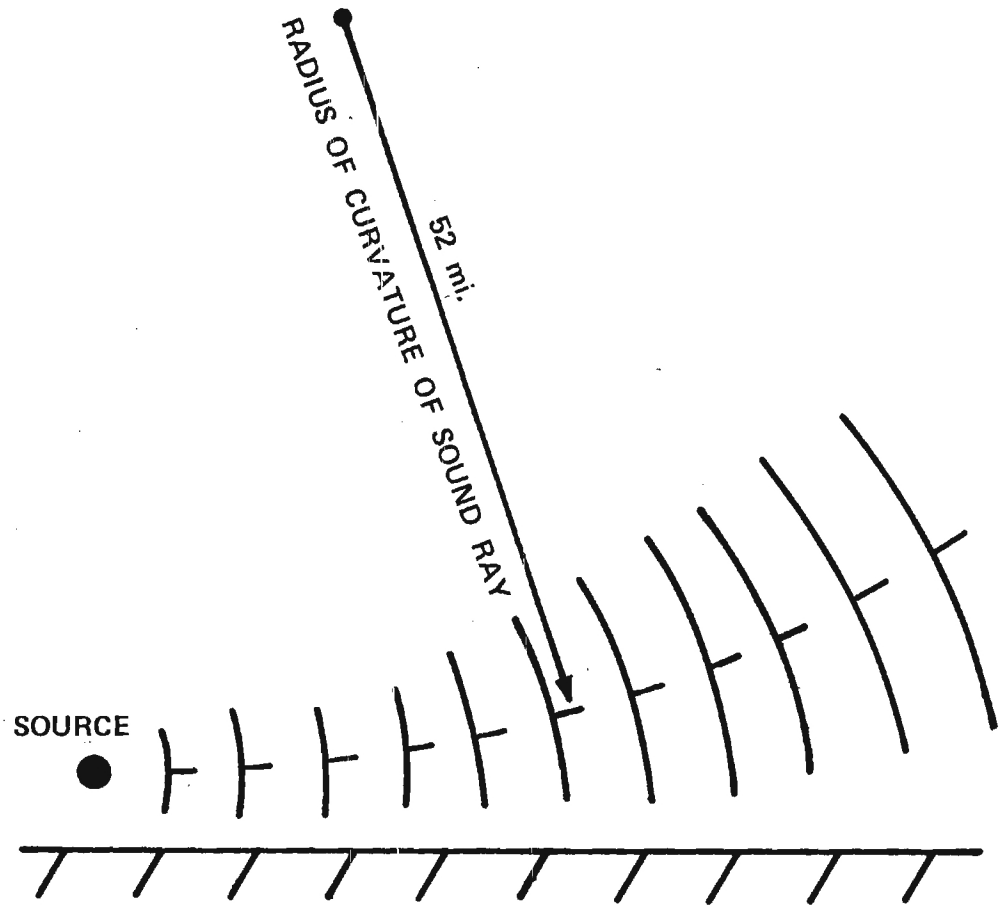

Figure III-8. Upward refraction of sound under standard atmospheric conditions. Standard tropospheric lapse rate of -5.4 °F per 1,000 feet.

increasing altitude. In the warmer stratospheric atmosphere the wave front will be refracted back down toward the Earth, skipping a certain zone between its points of refractive departure from the Earth's surface and its later refractive return to the surface as indicated in Figure III-9 as reproduced from Stephens and Bate.[7]

Atmospheric non-homogenieties such as dust and precipitation also affect sound propagation. Normally only higher frequency sounds experience any appreciable attenuation and lower frequencies may sometimes experience propagation enchancement by dust particles, presumably because the particles will tend to reduce thermal gradients.[8] Heavy fog consisting of 5400 droplets per cubic centimeter of 6.6×10^{-4}cm radius has produced attenuations of approximately 7 dB per 1000 feet of frequencies of 500 Hz and below, according to measurements.[8]

Wind gradients may appreciably affect the propagation of sound. As Figure III-10 illustrates, the windward directed acoustic wave front will be bent upward and the leeward front bent downward when the wind speed increases with altitude. As a consequence of this wind gradient the range and clarity of upwind sources are considerably greater than for downwind sources.

Energy absorption by a sound-propagating medium takes place by several distinct mechanisms. If $\psi = \psi_o e^{-\alpha x} \cos(\omega t - kx)$ describes a plane wave traveling in the x direction in a medium of viscosity η, α is known as the amplitude absorption coefficient and may be written (following complicated analysis) as[9]

$$\alpha = \frac{2\pi^2 f^2}{\gamma P_o c} \left[\frac{4\eta}{3} + (\gamma - 1) \frac{K}{C_p} \right] \qquad (8)$$

where f is the frequency of the sound, γ is the ratio of specific heat at constant pressure to the specific heat at constant volume, and P_o is the mean equilibrium pressure. This expression, known as the classical absorption formula, holds very

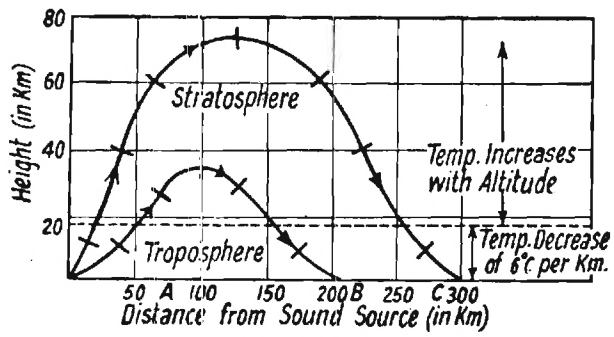

Figure III-9. Acoustic skip zone caused by ray refraction in standard atmospheric thermal gradients.

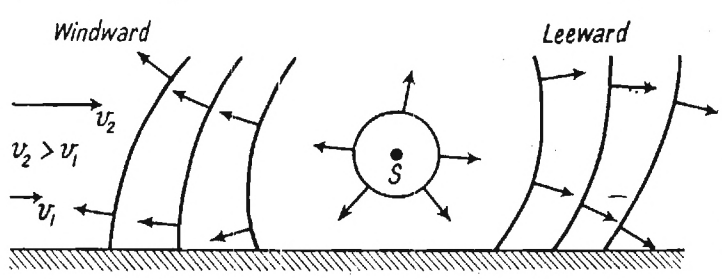

Figure III-10. Wind shear causing downward deflection of leeward directed sound rays. An upward deflection of windward directed rays. Acoustic detection range is increased in leeward direction.

well for monatomic gases over very wide pressure and temperatures ranges. It is somewhat less satisfactory for diatomic and other polyatomic gases in that these gases have absorptions much greater than predicted by the formula for certain frequency regions. The discrepancies result from molecular absorption in rotational and vibrational modes of energy storage thus reducing the energy available for translational wave propagation.

The classical absorption formula includes loss contributions from viscosity, conduction, diffusion and radiation (α_v, α_c, α_D, α_R).[8]

$$\alpha_v = \frac{8}{3} \frac{\pi^2 \eta f^2}{\rho_o c^3} \quad \text{nepers/cm} \tag{9}$$

$$\alpha_c = \frac{2\pi^2 f^2 (\gamma-1) K}{\rho_o c^3 C_p} \tag{10}$$

$$\alpha_D = \frac{(\gamma-1)\,\omega^2 .51\, D_{12}}{2\gamma c^3}$$

(.51 is a molecular constant for air) (D_{12} = mutual diffusion coefficient of N_2 and O_2 in cm^2/sec.) (11)

$$\alpha_R = \frac{(\gamma-1)\,10^{-3}}{2c\,C_v}$$

(10^{-3} is radiation coefficient of air in cal $sec^{-1} gm^{-1}\, {}^oC^{-1}$) (12)

η = viscosity of air, poise

f = frequency

$\omega = 2\pi f$

ρ_o = density

c = speed of sound

$\gamma = C_p/C_v$

K = thermal conductivity

C_p = specific heat at constant pressure

C_v = specific heat at constant volume

1 NEPER/cm = 264,500 dB/1000 ft.

Some values of α_v, α_c, α_D, α_R according to temperature are given in Table III-I.[8]

Molecular absorption is an important attenuation effect in diatomic or polyatomic gases at higher frequencies. As a compressional wave arrives at a certain small volume or group of molecules of a sound-propagating gas, compression (phasewise lagging the pressure) will occur. The compression and rarefaction, however, are not quite adiabatic. Some of the acoustic energy is taken up by internal molecular mechanisms and retained as heat with relaxation times longer than the acoustic wave period, thus preventing its contribution to translational energy which would maintain the propagated wave.

One important case of molecular absorption is the vibrational mode of acoustic energy absorption by oxygen molecules. Oxygen's vibrational absorption is

Table III-I. Classical Attenuation Formulas (dB/1000 ft.)

^{o}C	$\alpha_v + \alpha_c$	α_D	α_r
-50	$.033\ f_{kc}^2/P_{atm}$	$.0037\ f_{kc}^2$	.0051
0	$.036\ f_{kc}^2/P_{atm}$	$.0038\ f_{kc}^2$	.0046
25	$.037\ f_{kc}^2/P_{atm}$	$.0039\ f_{kc}^2$	.0044
50	$.038\ f_{kc}^2/P_{atm}$	$.0040\ f_{kc}^2$	.0042
100	$.039\ f_{kc}^2/P_{atm}$	$.0041\ f_{kc}^2$	.0039

enhanced by the presence of atmospheric water vapor. The molecular absorption of oxygen α_{mol} may be calculated as follows:[10]

$$\alpha_{mol} = \alpha_{max} \frac{2\,(h/h_m)^2}{1 + (h/h_m)^4} \quad \text{(dB/1000 ft.)} \tag{13}$$

where $\alpha_{max} = .009\ f$,

$h_m = \frac{f}{1010}$ is the absolute humidity which would produce maximum attenuation of frequency f

h = absolute humidity in gms/m^3

The velocity of sound in air depends on the humidity. An expression relating the velocity of sound in humid air, v_h, to the velocity v_d in dry air is [4]

$$v_h = v_d \left[1 - \frac{e}{p} \left(\frac{\gamma_w}{\gamma_a} - \frac{5}{8} \right) \right]^{-1/2} \tag{14}$$

where p = barametric pressure

e = pressure of water vapor

γ_w = specific heat ratio of water vapor

γ_a = specific heat ratio of air

3. <u>Overflight Geometry, Kinematics and Doppler Effect</u>. Consider a single acoustic sensor located at an x, y, z coordinate system origin as in Figure III-11. Suppose an aircraft flying at constant velocity $v = v_x i + v_y j + v_z k$ at altitude h (x) follows a ground path described by $x\sin\alpha - y\cos\alpha = -\rho_o$ inclined at angle α to the x axis and passing at a distance ρ_o from the origin. Then the radial velocity of the aircraft with respect to the coordinate origin will be given by $\dot{R} = \frac{\rho\dot{\rho} + h\dot{h}}{R}$ where $\rho = (x^2 + y^2)^{1/2}$.

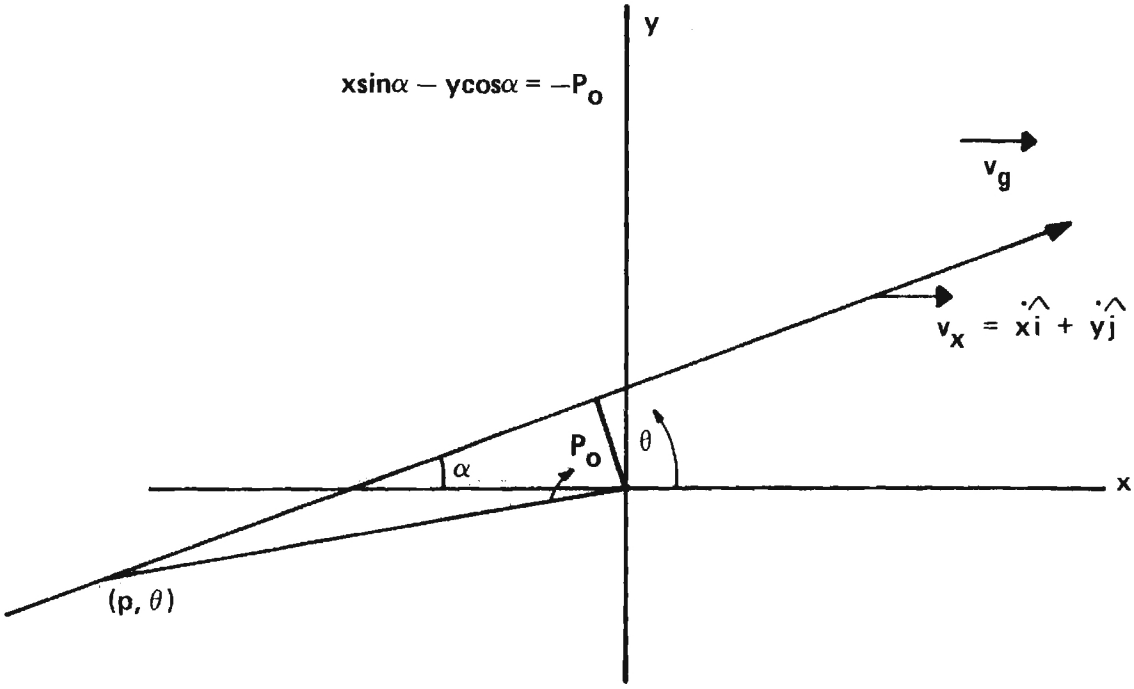

$$\dot{R} = \frac{(x_d + \dot{x}t)\,\dot{x} + (y_d + \dot{y}t)\,\dot{y} + h\dot{h}}{(x^2 + y^2 + h^2)^{1/2}}$$

$$f_o = f_s \frac{C}{C + \dot{R}} \qquad \text{DOPPLER SHIFT}$$

Figure III-11. Low level overflight geometry. h = aircraft altitude. Microphone is located at coordinate origin.

The analysis is as follows:

$$\rho = (x^2 + y^2)^{1/2},\ x = x_d + \dot{x}t,\ y = y_d + \dot{y}t \tag{15}$$

where x_d, y_d = the x and y coordinates of the point on the x, y plane over which the aircraft was passing when its first detectable sound was emitted. t is the real time after the instant at which the first detectable sound was emitted.

$$\dot{\rho} = \frac{1}{2}\ \frac{2x\dot{x} + 2y\dot{y}}{(x^2 + y^2)^{1/2}} = \frac{x\dot{x} + y\dot{y}}{\rho} \tag{16}$$

$$\dot{x} = v_g \cos\alpha,\ \dot{y} = v_g \sin$$

where v_g = constant aircraft ground speed, $v = (v_g^2 + v_z^2)^{1/2}$, $v_z = \dot{h}$ = constant descent rate of the aircraft. Thus

$$\dot{\rho} = \frac{(x_d + \dot{x}t)\dot{x} + (y_d + \dot{y}t)\dot{y}}{\rho} \tag{17}$$

and $\quad R = (\rho^2 + h^2)^{1/2}$

whence $\quad \dot{R} = \dfrac{\rho\dot{\rho} + h\dot{h}}{R} = \dfrac{(x_d + \dot{x}t)\dot{x} + (y_2 + \dot{y}t)\dot{y} + h\dot{h}}{R} \quad (18)$

where $R = (x^2 + y^2 + z^2)^{1/2}$. Since R is the radial distance between the source and the sensor, $\dot{R} = \frac{dR}{dt}$ is the radial velocity of Doppler significance.

Now consider the simple case of an aircraft flying at 100 kts constant speed and 1000 feet constant altitude and passing directly over the sensor as shown in Figure III-12. From Figure III-11 we find,

$$R = (x^2 + h^2)^{1/2} \tag{19}$$

$$\dot{R} = \frac{x\,\dot{x}}{(x^2 + h^2)^{1/2}} \tag{20}$$

At the assumed initial detection range of -2 mi. = -10,560 ft.,

$R = 10{,}607$ ft.

$\dot{R} = -168.05$ ft./sec.

The sound emitted by the aircraft as it approaches the sensor at the coordinate origin at speed R is Doppler shifted and is measured at the orgin as f

$$f = \frac{c\,f_o}{c + \dot{R}} \tag{21}$$

where f_o is its unshifted frequency and c is the speed of sound with respect to the

OVERFLIGHT KINEMATICS

$\dot{h}$ = DESCENT RATE (NEGATIVE)

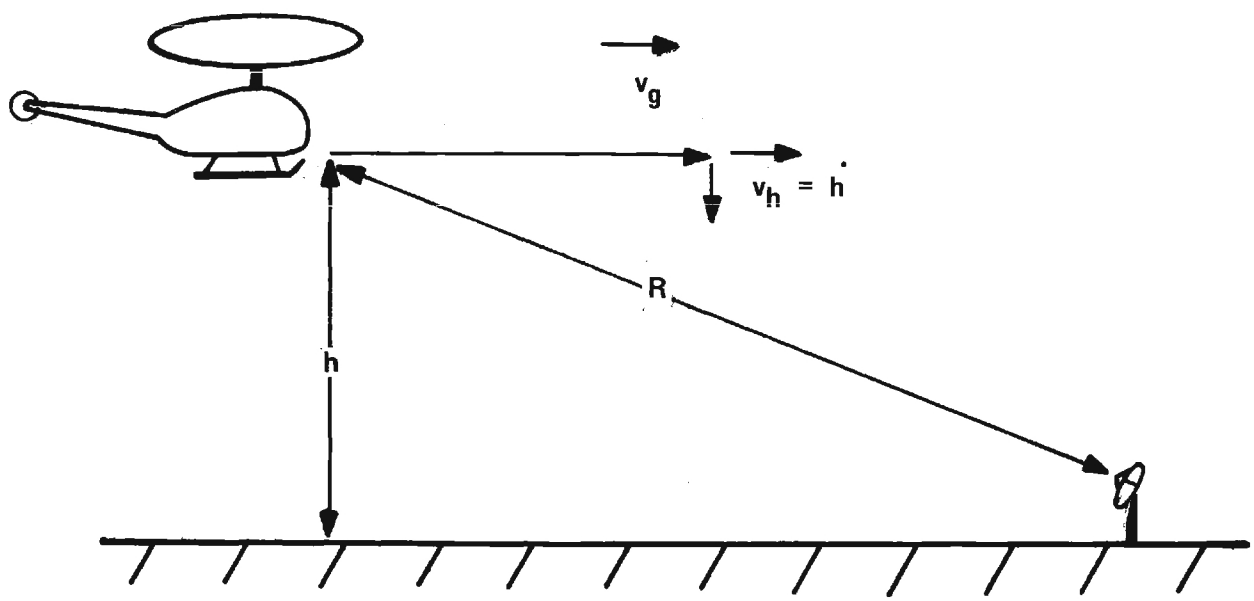

Figure III-12. Aircraft flying directly over acoustic sensor. Example in text supposes $\dot{h}$ = o.

air (wind speed is assumed here to be zero). Assuming f_o to be 1000 Hz and c = 1088 ft./sec.,

$$f = \frac{1088 \times 1000}{1088 \times \dot{R}}$$

$$f\ (x = -2\ \text{mi}) = \frac{1088 \times 1000}{1088 - 168.05} = 1182.67\ \text{Hz}$$

$$f\ (x = 0) = 1000\ \text{Hz}$$

Figure III-13 is a plot of f vs x (t) for the aircraft flyover case under consideration.

Consider now the simple case of an airborne acoustic source approaching a microphone which is stationary with respect to the coordinate axes, in the presense of a steady wind of speed w blowing in the positive x direction as shown in Figure III-14. Let the source produce a sound of frequency f_s, measured at the source. The wave length λ' of this sound wave in the air will be given by the ratio of the speed with which the wave is advancing in front of the source to the frequency f_s, i.e.,

$$\lambda' = \frac{c + w - v_s}{f_s} \tag{22}$$

The frequency f_o of this same wave as sensed by the microphone will be given by the ratio of the speed with which the wave passes the microphone to its

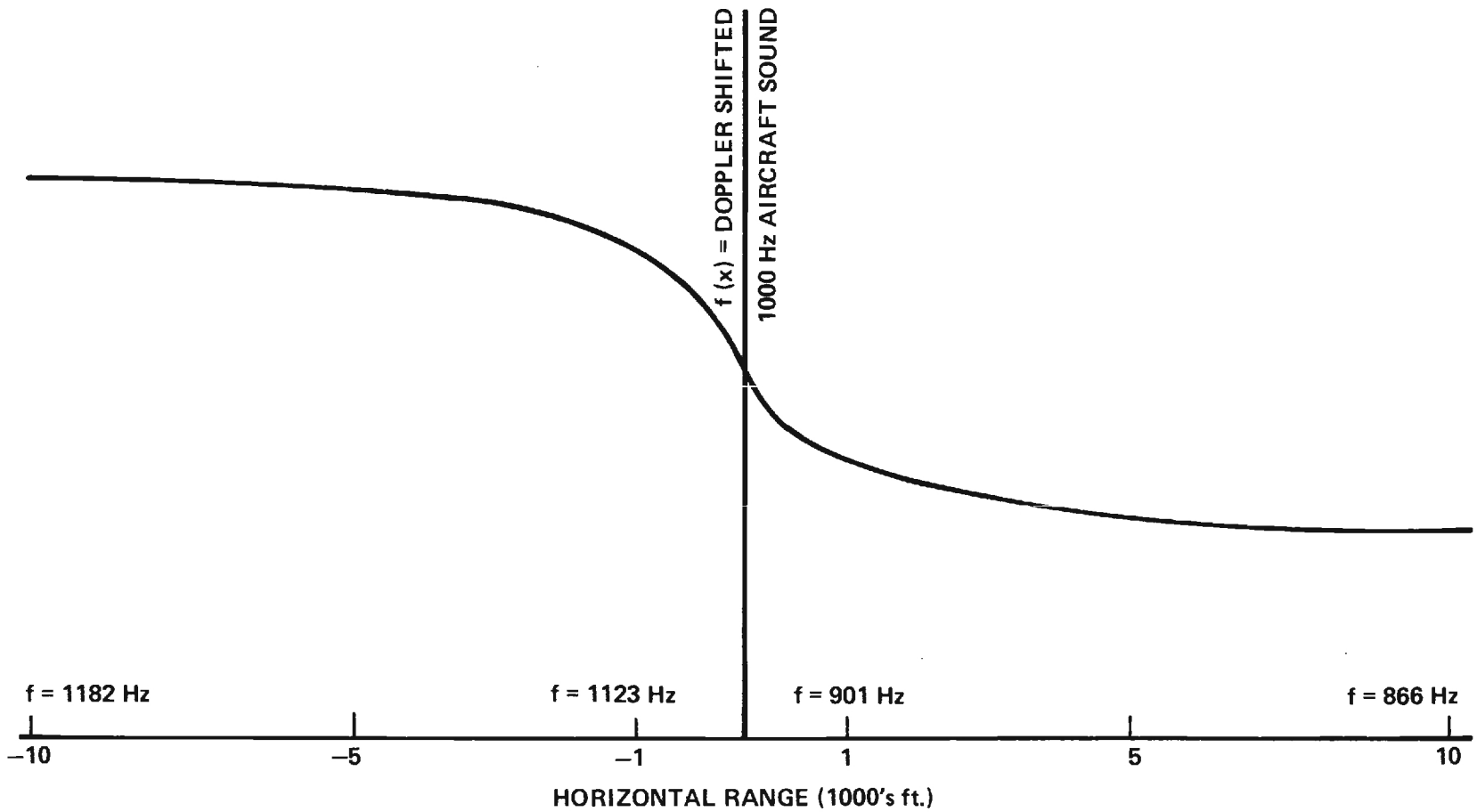

Figure III-13. Doppler shifted frequency f(x) as a function of horizontal range x in 1000's offt. The acoustic source is flying directly over the sensor at a speed of 100 kts (168.8 ft/sec) and at an altitude of 1000 ft.

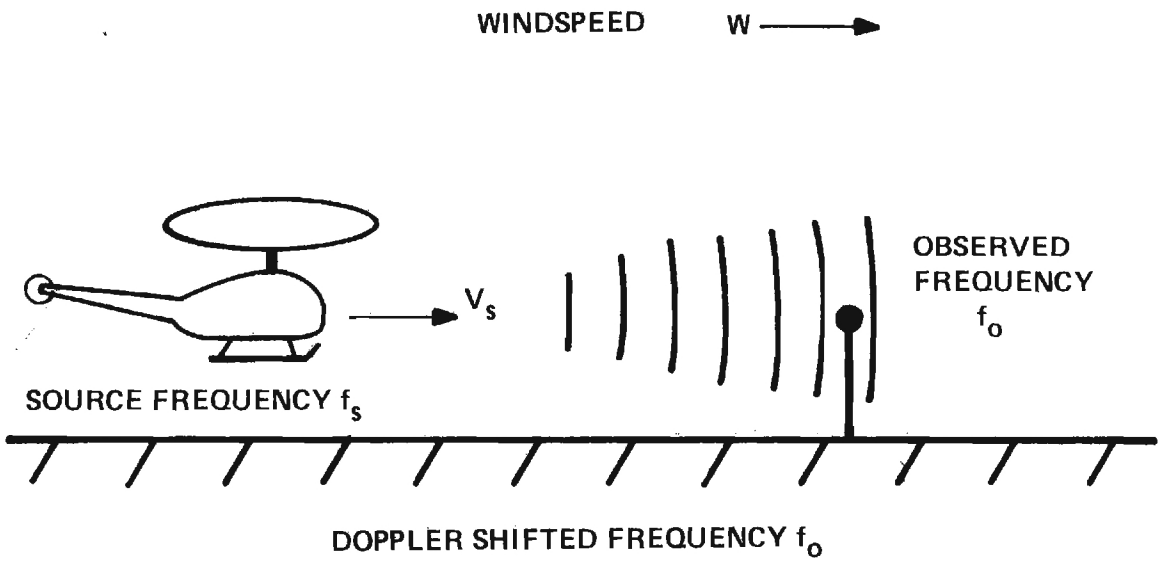

$$f_o = \frac{C + W}{C + W - V_s} f_s$$

Figure III-14. Doppler Kinematics. The Aircraft is Approaching the Sensor at Ground Speed Vs.

wavelength λ' in the medium, i.e.,

$$f_o = \frac{c + w}{\lambda'} \tag{23}$$

$$f_o = f_s \frac{c + w}{c + w - v_s} \tag{24}$$

It must be noted here that all the velocities, w and f_s, must be defined in the direction of propagation of the sound wave considered.

A more general method of obtaining the frequency of the observed sound wave is to first write an expression giving the observed wave in terms of the same time variable with which the wave is described at the source. That is, if the sound wave at the source is described as $\psi_s = A_s \sin 2\pi f_s t$, then the same sound wave when it reaches the observer can be described as $\psi_o = A_o \sin 2\pi f_s (t-T(t))$ where T(t) is the time delay between the time of a particular phase emission and the time of receipt of that same phase at the observer, expressed in terms of the same variable t used to describe the original wave function ψ_s. This means that at t = o both ψ_s and ψ_o have the same phase. Moveover, since the frequency of a wave is given by the time rate of change of its phase, $f = \frac{d\phi}{dt}$, the frequency f_o observed at the origin will be given by

$$2\pi f_o = \frac{d}{dt}\left[2\pi f_s(t - T(t))\right]$$

E. Acoustical Detection Range.

The maximum range of acoustic detection is determined by the signal to noise ratio S/N at the detector. The signal sound pressure level S_{spl} at the detector is determined by the intensity of the source, atmospheric conditions,

atmospheric attenuation, and source-to-sensor range. The noise sound pressure level N_{spl} at the sensor is the sound pressure level of the ambient background noise in the neighborhood of the sensor. These quantities may be related by the following equation:

$$\left(\frac{S_{spl}}{N_{spl}}\right)^2 = \frac{S_{spl}^{\ 2}(R_1)\,R_1^{\ 2}}{N_{spl}^{\ 2}\,R^2}\,10^{-\frac{\alpha}{10}(R - R_1)} \tag{25}$$

where S_{spl} = signal sound pressure level

N_{spl} = noise sound pressure level

R_1 = range at which a reference sound pressure level $S_{spl}(R_1)$ is known

R = range between source and sensor

α = atmospheric sound attenuation constant

Sound pressure levels in the equation are squared terms because the sound intensity (i.e., power per unit area normal to the propagation direction) is proportional to the square of the sound pressure level. The S/N ratio will actually be specified in terms of signal power and noise power, i.e.

$$S/N = \frac{\text{signal power}}{\text{noise power}} = \left(\frac{S_{spl}}{N_{spl}}\right)^2 = 5 \text{ dB minimum} \tag{26}$$

for detection. Figure III-15 illustrates the use of the acoustic range equation. To reduce this acoustic range equation to decibel form, we take the common logarithms

SENSOR RANGE R (ft.)

SPL = Sound Pressure Level

$S_{SPL}(R_1)$ = Signal SPL at R_1

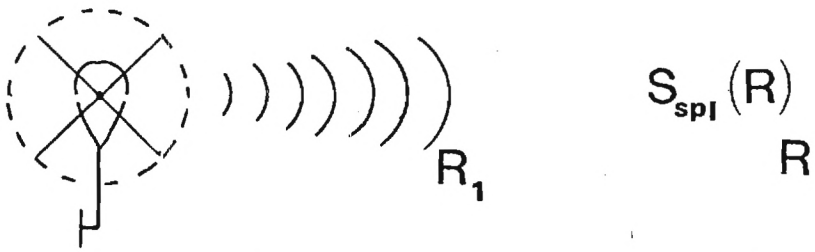

N_{spl} = Ambient Noise SPL

α = Sound Power Attenuation Constant in db/ft

$$\left(\frac{S_{spl}}{N_{spl}}\right)^2 = \frac{S_{spl}^2(R_1)\,R_1^2}{N_{spl}^2\,R^2}\,10^{-\frac{\alpha}{10}(R-R_1)}$$

Sound power equation

S/N at Microphone, Assume Min 5 db for Detection

Figure III-15. Acoustic Range Equation. R_1 is range at which a signal sound pressure level $S_{spl}(R_1)$ is known (200 ft.). The left side of the equation is the S/N ratio (acoustic source signal intensity/ambient background noise in detection band) at the sensor located at distance R from the source.

of both sides and multiply by 10,

$$5 \text{ dB} = 20 \text{ Log } \frac{S_{spl}}{N_{spl}} = 20 \text{ Log } S_{spl}(R_1) + 20 \text{ Log } R_1$$

$$- 20 \text{ Log } N_{spl} - 20 \text{ Log } R - \alpha(R - R_1)$$

i.e., $$R + \frac{20}{\alpha} \text{ Log } R = \frac{1}{\alpha} \left\{ 20 \text{ Log } S_{spl}(R_1) + 20 \text{ Log } R_1 \right.$$

$$\left. - 20 \text{ Log } N_{spl} - 5 \right\} + R_1$$

As an example of detection range for a detector having a minimum S/N for detection of 5 dB, with ambient background noise of 50 dB, a source producing 90 dB sound pressure level at 200 ft., and with $\alpha = 0$ for 10 - 20 Hz:

$$20 \text{ Log } R = 20 \text{ Log } S_{spl}(R_1) + 20 \text{ Log } R_1 - 20 \text{ Log } N_{spl} - 5$$

$$20 \text{ Log } R = 90 + 46 - 50 - 5 = 81 \quad (27)$$

$$R = 11{,}110 \text{ ft.} \qquad (N_{spl} = 50 \text{ dB})$$

$$R = 35{,}480 \text{ ft} \qquad (N_{spl} = 40 \text{ dB})$$

In the case of finite α the range is somewhat reduced. For 63 Hz α = .0001 dB/ft., approximately.[11] Then with N_{spl} = 50 d B

$$R + 200{,}000 \text{ Log } R = 10{,}000\,(90 + 46 - 50 - 5) + 200$$

$$R = 9000 \text{ ft.}$$

F. Acoustic Sensor Arrays.

For maximum effectiveness in establishing position and velocity of airborne acoustic sources, microphones should be deployed in perimeter segment arrays as shown in Figure III-16. Each array element (or certain array elements) moreover, may consist of a two or three element subarray which is capable of giving independent direction information based on relative phases of received acoustic waves. Figure III-17 illustrates the principle of multielement subarray direction finding.

The perimeter array shown in Figure III-16 consisting of the subarray elements shown in Figure III-17 is herein thought of as the optimum acoustic sensor deployment configuration for the considered application. It affords source direction information of an instantaneous nature provided by the subarray phase information and an independent determination of flight path given by sound intensity time histories at the major array elements.

G. Concepts of Acoustic Data Handling.

Probably the most efficient method of acoustic airborne instrusion detection and source identification would be the use of on site (i.e. located at the acoustic sensor) acoustic signal processing. This would require a micro processor capable of performing a Fast Fourier Transform (FFT) on a stored digital time series of acoustic sound pressure level measurements. If the frequency domain spectral intensity function thus produced were to resemble that of an aircraft, the unit would automatically transmit information on the direction and type of aircraft to a central security station.

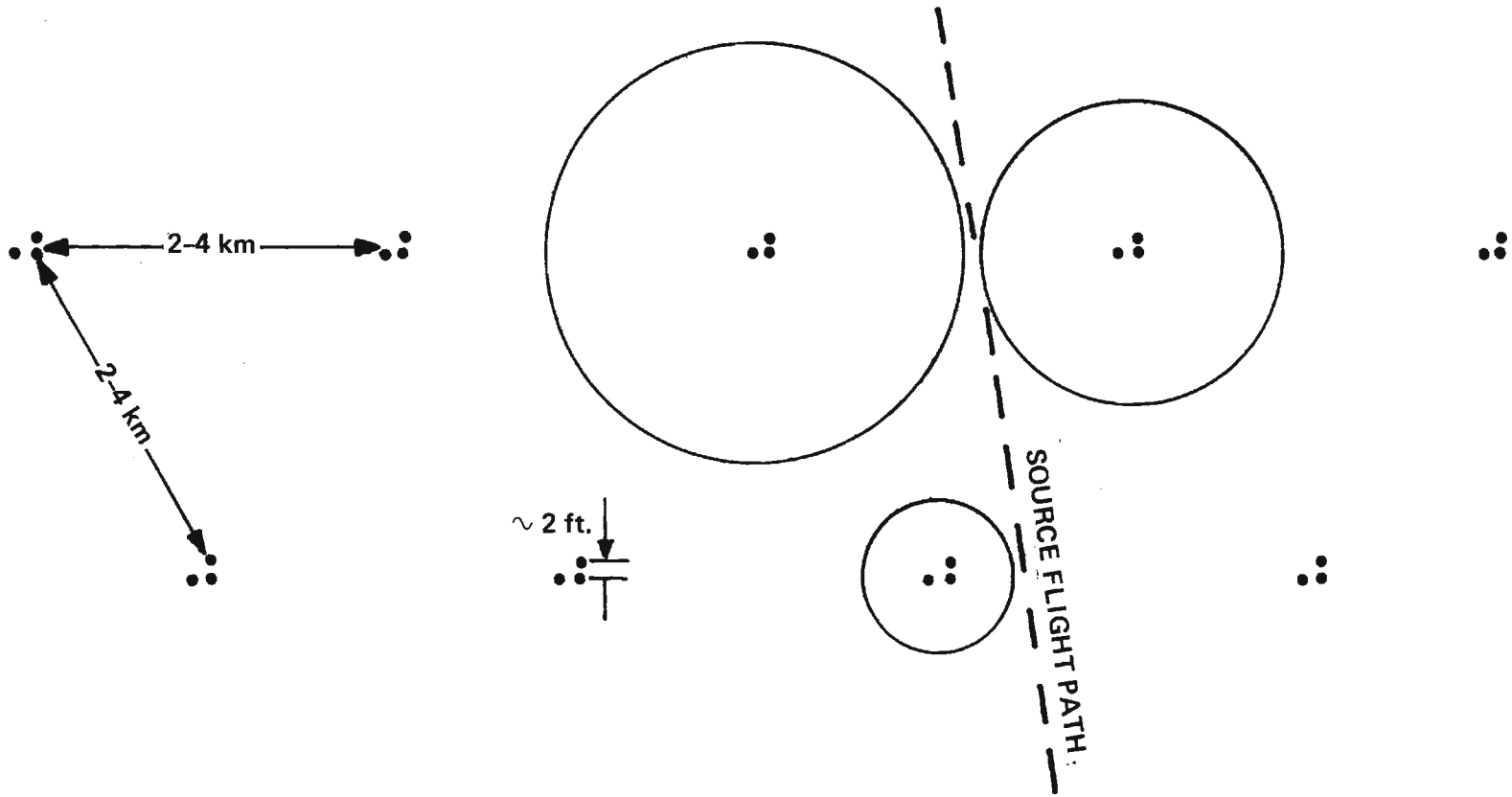

Figure III-16. Perimeter segment array. Sound levels and sensor activation times imply path of acoustic source, assuming constant source strength and straight level flight. The array elements shown here actually consist of three microphones each, set at the corners of right triangles, and spaced about 2 ft. apart.

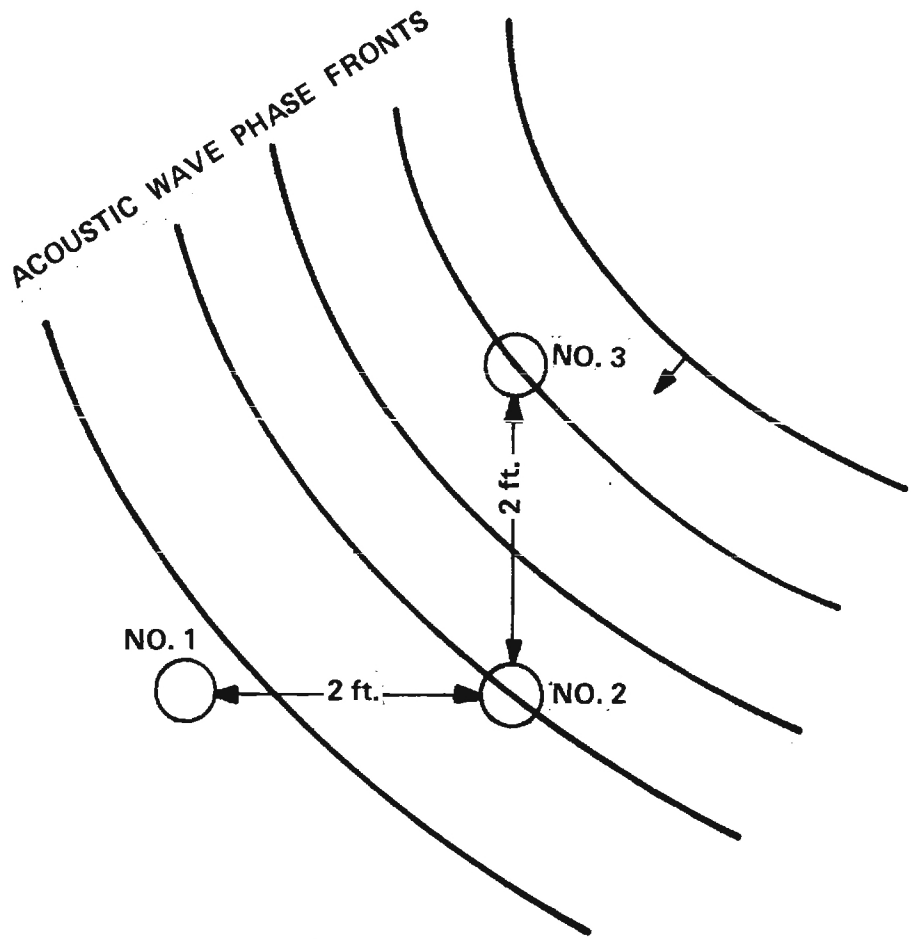

Figure III-17. Element of main array may actually be subarray consisting of 2 or 3 elements (microphones). The arrival times of acoustic wave phase fronts at the various microphones imply source direction (i.e., instanteous propagation direction) in both azimuth and elevation.

An alternative to on-site data processing is the concept of central data processing of acoustical signals transmitted directly from the remotely deployed microphone to the central security station. This will require a central data processor of sufficient capacity to perform FFT's on the received acoustic signals (for target identification) and to maintain track of individual subarray source direction information.

Another possibility makes use of comb filters [12] to detect sets of acoustic spectral lines. This approach has the advantage of economy, however, it's limited to narrow bandwidth and, therefore, cannot cover the full range of Doppler shift for most aircraft. It can be made to distinguish one type of helicopter from another on the basis of the ratio of frequencies of main rotor harmonics to frequencies of the tail rotor harmonics.

SECTION III

REFERENCES

1. Gasaway, D. C., "Characteristics of Noise Associated with the Operation of Military Aircraft", Aerospace Med. April 1964 pp. 327 - 336.

2. Lowson, M. V., Ollerhead, J. B., "A Theoretical Study of Helicopter Rotor Noise", J. Sound Vib Vol. 9, 1969, pp.197 - 222.

3. Leverton, J. W., Taylor, F. W., "Helicopter Blade Slap", J. Sound Vib. Vol 4 (1966) pp. 345 - 357.

4. "Handbook of Chemistry and Physics, College Edition,", 50th Edition, Chemical Ruber Company (1969).

5. Weber, R. L., White, M. W., Manning, K. V. "College Physics", McGraw-Hill, 1952.

6. Seto, W. W. "Schaum's Outline of Theory and Problems of Acoustics", McGraw-Hill, 1971.

7. Stepehens, R. W. B., Bate, A. E., "Acoustics and Vibrational Physics", Edward Arnold (Publisher), LTD., London (1966).

8. Crom, C. L., Oldham, W. J. B., Humphries, E. M., "Final R & D Report on Border Crossing Surveillance", Report No. G3753.1701. 01A, E-Systems, Inc., Greenville, Texas.

9. Encyclopedia Britanica, "Sound", 1959.

10. Evans, "Atmospheric Absorbtion of Sound: Theoretical Predictions", JASA, 51, #5, Part 2, (1972).

11. Lince, D. L. "A technique for Measuring the External Noise of a Moving Helicopter", U. S. Army Human Engineering Laboratory, Aberdeen Proving Ground, Maryland, AD 773687, (1973).

12. Hemdal, J. F., "An Investigation of Automatic Detection Identification of Acoustic and Seismic Sources", Final Technical Report Contract DAAD05-71-C-0024, July, 1971.

(This Page Intentionally Blank)

SECTION IV

OPTICAL SENSORS

The primary role of optical sensing in the DoE mission is that of target identification by long range or short range closed circuit TV (CCTV) once an airborne perimeter penetration has been indicated by one or more of the initial acquisition sensors. In practice, a CCTV (or several CCTV's possibly located at select terrain-specific vantage points) might be kept scanning and continuously monitored for ground intrusions. Following an airborne intrusion detection the CCTV system would slew over to the penetrated sector. The human operator would manually scan the airspace of interest using radar and acoustic data for cuing and aiming purposes.

In clear air and daylight, this capability may permit an early effective visual identification of the alarm source by security personnel, thereby affording increased response time. This same detection procedure could be followed at night using a low light level system. The low light level system may also be able to produce monitor images that would enable target identification under moonlight or starlight illumination.

For purposes of this report, it has been supposed that the potential of using the CCTV (the principle optical sensor) as a primary airborne detection system is minimal. Therefore, the optical sensor will receive only a cursory treatment. Moreover, the effectiveness of optical sensors in the aircraft detection role can be assessed only by experience.

Several types of passive infrared sensors have been considered for airborne intrusion detection; however, all information collected to date indicates that optical sensors are limited in performance for this application.

SECTION V

EVALUATION AND RATING OF GENERIC SENSORS

A. Tabular Rating and Evaluation Matrix

Presented on the following page is Table V-I, the tabular rating and evaluation matrix for the generic sensors under consideration. This matrix is divided into three major sections of interest. These are "Generic System Technical Characteristics", "Real World Considerations", and "Potential Applications". The Technical Characteristics are intended to give a baseline understanding of each sensor as it potentially relates to the airborne intrusion detection problem. "Real World Considerations" relates the factors which must be taken into account if a detailed evaluation is to be meaningful. Finally, the "Potential Application" relates how each sensor is currently seen to fit into the detection/warning scheme.

Each entry of the matrix includes an identifying set of numbers (e.g. coverage for Monostatic Radar is entry 1,1). These will be used in the following section to provide any pertinent clarifying information required for each entry.

This matrix is, of course, summary oriented and limited to generic sensor types and "standard" conditions. As has been stated throughout this report, detailed evaluation of site dependent conditions and sensor characteristics including potential complicating factors will be required in order to generate a full understanding of anticipated system performance.

B. Detailed Expansion of Elements in Matrix

Presented below are detailed expansions of the individual elements of the tabular rating and evaluation matrix. These are referenced by the element

Table V-I

TABULAR RATING & EVALUATION MATRIX

GENERIC SYSTEM TECHNICAL CHARACTERISTICS						REAL WORLD CONSIDERATIONS					Potential
Sensors Generic Type	Coverage	Range	Target Handling Capability	Discrimination	Tracking Capability	Environmentally Degrading Factors	Vulnerability to Intentional Compromise	Cost Factors	Maintainability	Automation	Application
Monostatic Radar	1,1 Azimuth 360° Elevation 90°	1,2 Horiz. Limit Nom. 20 km	1,3 Multiple Targets	1,4 Fixed wing/ Helo Potential- Helo Types	1,5 Instant. Position and Velocity	1,6 Weather, Terrain Air/Ground Traf. Vegetation, Structures	1,7 Chaff, Jam. Vandalism, Power Loss	1,8 $\$10^5$-$10^6$ /unit	1,9 MTBF 300 hrs.	1,10 Good Candidate for Automation	1,11 Initial Acquisition, Tracking, Discrimination
Bi-Static Radar	2,1 Fixed-Sector Fence, Setable Elevation	2,2 N/A	2,3 Multiple Targets Potential	2,4 Potential Fixed Wing/ Helo	2,5 Limited Position and Velocity	2,6 Weather, Terrain Air/Ground Traf. Vegetation, Structures	2,7 Chaff, Jam. Vandalism, Power Loss, Comm. Interupt	2,8 $50K /unit	2,9 MTBF 1000 hrs.	2,10 Good Candidate for Automation	2,11 Tripwire Sensor, Additional Potential
Acoustic	3,1 Azimuth 360° Elevation 90°	3,2 Amb. Limit, Opt. 10km	3,3 Multiple Targets Potential	3,4 Fixed Wing/ Helo Between Helo Types	3,5 Limited w/ Array Deployment	3,6 Weather, Terrain Air/Ground Traf. Vegetation, Structures, Wildlife	3,7 Jamming, Vandalism, Power Loss, Comm. Interupt	3,8 $1,000-$25,000 /unit	3,9 MTBF 1-12 mo.	3,10 Good Candidate for Automation	3,11 Initial Acquisition, Discrimination, Gross Tracking
Optical (Low light level telephoto lens)	4,1 Azimuth 360° Elevation 90°	4,2 Amb., Horiz. Limit	4,3 Single Target	4,4 Universal Discrimination	4,5 Limited: Precise Angle, Approx. Range	4,6 Weather, Terrain Air/Ground Traf. Vegetation, Structures, Wildlife	4,7 Vandalism, Power Loss	4,8 $2,000-$100,000 /unit	4,9 MTBF 1 yr.	4,10 Limited Automation	4,11 Terminal Phase Identification

identifying numbers found in each entry and are organized by columns such that for a particular column, the expansion of the elements for all four sensor types will be presented together for ease of comparison.

Coverage

1,1 In general, angular coverage by a monostatic radar is limited only by limits established on the scanning mechanisms. Thus, it is fairly common to achieve 360° azimuthal coverage and full elevation coverage to 90°.

2,1 As was discussed in Section II-B, coverage by a bistatic radar is dependent on the choice of beamwidths and the overlap region associated with the actual deployment configuration. It is usually thought of as a fixed sector fence coverage.

3,1 Acoustical sensor coverage is basically hemispherical although weather and terrain conditions may assymetrically degrade directional sensitivity (e.g. Figure III-10). Care should be taken in the deployment of acoustic sensors to afford maximal detectability in the direction of greatest tactical interest (viz. away from the sensitive area, toward the anticipated intrusion approach direction). Buildings, vegetation, hills, etc., may seriously attenuate acoustic signals. If acoustic sensors are applied as a complement to radar, they will probably be deployed in ravines, along rivers, in valleys and other low-lying areas not covered by radar, where their coverage and range requirements would be limited.

4,1 Under normal daylight clear air conditions CCTV will have potential hemispherical coverage. Careful placement of TV cameras may be required to avoid vision blockage by trees, buildings, towers or hills.

Range

1,2 Section II-B discussed the range to the horizon as being related to antenna height by

$$R = 3.56 \sqrt{h}.$$

The nominal case referred to is for a radar located on a 30 meter tower.

2,2 Because of the sector type deployment normally associated with bistatic radar, range is not a useful measure of sensor characteristics (see Section II-B).

3,2 Acoustical detection range is limited basically by the S/N ratio at the sensor as described in Section III, subsection E. If placed in a low-lying area its range may be further reduced by its geographical confines. Under normal conditions of background noise levels between 30-40 dB, maximum detection ranges for low flying helicopters will be up to about 5 miles. Parabolic reflectors may be able to enhance sensitivity in one preferred direction per sensor, at the expense of directional coverage.

4,2 Under fair weather daylight conditions, the optical sensors (i.e CCTV) are basically horizon limited. Fog, dust or precipitation may severely degrade ranges of all optical sensors.

Target Handling Capability

1,3 A monostatic radar can be capable of handling a very high traffic load (multiple targets) dependent on sensor characteristics and processing capabilities.

2,3 Dependent on the requirements placed on the system, a bistatic radar may be utilized to handle multiple targets. The information available may be limited as discussed in Section II-A.

3,3 Attempts have been made to develop multiple target (i.e multiple acoustic source) counting capabilities for acoustic sensors. The capability of

discriminating between one target and multiple equal-signal-level targets seems to be readily achievable, however, as the number of targets increase beyond two, the difficulty in counting them increases very rapidly. What little information has been found describing efforts toward multiple target capabilities of acoustic sensors has indicated little progress in the discrimination area.

4,3 Optical sensors (e.g. CCTV) are normally limited to perception through a narrow solid angle. Therefore, they are thought of as having only single target capabilities unless two targets happen to be occupying the same solid angle of sensor view.

Discrimination

1,4 Discrimination between fixed wing and helicopter aircraft types is possible via doppler information (Section II-D). Potential exists for discrimination between helicopter types via fine-grain detailed processing of this data.

2,4 Potential may exist for a bistatic radar to discriminate between fixed wing and helicopter aircraft types via doppler information. However, further evaluation is required primarily due to the complexity of the doppler information obtained (see Section II-A).

3,4 Discrimination capabilities of acoustic sensors depends on their associated acoustic data processing capabilities. With state of the art data processing (esp. FFT capable microprocessors) practically complete discrimination between any fixed wing aircraft and any helicopter should be expected. Moreover, discrimination among many helicopter types can be readily achieved.

4,4 CCTV under clear daylight conditions should be considered to have practically universal target discrimination capabilities, dependent to some extent on operator skill, and target to background contrast or vegetation interference.

Tracking Capability

1,5 Tracking capability can be very good for a monostatic radar with actual accuracies dependent on the specific radar characteristics. Complete three-dimensional information is generally available on an instantaneous basis where simultaneous elevation and azimuthal scan is employed.

2,5 Limitations in the bistatic tracking capability are primarily due to the complex geometry involved (see Section II-A). Various ambiguities exist in the bistatic geometry that simple systems cannot resolve.

3,5 A single acoustic sensor array element consisting of three separate microphones may have a capability of angle tracking (see Figure III-16). When deployed in the perimeter segment array shown in Figure III-15, the sensors' signal intensities and activation times provide information implying the path of a straight, level-flight, constant-speed overflight.

4,5 Optical sensors (CCTV) are able to track in angle (azimuth and elevation) quite precisely, however, range determination would depend largely on operator skill.

Environmental Degrading Factors

1,6 Environmental degrading factors on a family of sensors can vary from minor to severe dependent upon actual conditions experienced (see Section II-E). These must be taken into account in order to gain confidence in the usefulness of system performance analysis.

2,6 The discussion of Section II-E applies equally to the bistatic radar case as it does to the monostatic radar.

3,6 Any environment conditions producing high levels of background noise between 10 and 500 Hz may seriously reduce acoustic detection range. Heavy

precipitation with thunder, high winds, nocturnal insects or birds, may all degrade sensor performance to some extent. Thirty (30) mph winds may produce noise levels of 50 dB which, according to the acoustic range equation of Section III subsection E, may reduce helicopter detection ranges to less than 2 miles. Care should be exercised to avoid acoustic sensor deployment around areas of excessive ground or air traffic.

4,6 Adverse weather may extremely limit the usefulnes of CCTV under severe conditions. Heavy fog or precipitation may effectively blind optical sensors. Obviously, surrounding buildings, hills, trees and various types of structures may also block CCTV view.

Vulnerability to Intentional Compromise

1,7 There is no sensor that cannot be compromised if the penetrator force is willing to expend the effort. Thus, the safest policy toward protecting sensors against compromise is to develop safeguards to detect compromise attempts. The detection of compromise or attempted compromise should be treated as if the sensor being affected had made a detection of the threat target.

2,7 Those comments made for the monostatic radar apply equally to the bistatic radar. Unique vulnerability may exist if this sensor is located separate from a main facility thus requiring some form of communication link.

3,7 Acoustical sensors would probably be much more vulnerable to vandalism in their remote deployment positions than would centrally located monostatic radars. Jamming would be a possibility, however, the known fact of jamming attempts would be interpreted as equivalent to an alarm situation. The remote sensor power source, whether wires from a central location or solar energy units would be vulnerable to vandalism in their envisioned unprotected remote locations.

Obviously, too, the communication link (whether wire or radio) between a remote sensor and the central security station is a source of system compromise.

4,7 As envisioned, CCTVs would be centrally located near the central security station where they would probably be safe from vandalism. But since they must be elevated in an open area to optimize their fields of vision, they could be damaged by weapons fire originating outside the secure area.

Cost Factors

1,8 Cost per unit for a monostatic radar will, of course, depend on complexity and the degree of automation required. The figures indicated are intended as an approximation of the cost which might occur.

2,8 The cost quoted is an approximation based on the relative cost of the basic components required.

3,8 Some field-deployable acoustic sensor units giving limited information on acoustic sources (comb filter units) could be marketed in quantity for around $1,000 each. Units using FFT microprocessors, three microphones, direction finding circuitry, solar power, and radio transmitters might cost several times as much. More cost information can be generated as system concepts crystalize.

4,8 CCTVs for the considered uses would probably start around $2,000 including a servo system for slewing the cameras around on command. It is understood that at least one unit already in use with powerful telephoto capabilities cost about $100,000. Radar controlled camera aiming is also possible. The cost of slaving an optical system to a radar will be dependent on numerous factors.

Maintainability

1,9 Mean time between failure (MTBF) of ~300 hours is well within the state-of-the-art.

2,9 MTBF of ~1000 hours is based on the assumption that system complexity is less than for a monostatic radar.

3,9 No firm MTBF figures or results of life tests of acoustic sensor units are available at this time, however, the best opinion available estimates typical acoustic sensor MTBF about 1-12 months.

4,9 Since many CCTV monitors are available and have been in use for years, considerable efforts have been invested in their reliability upgrading. MTBF's for outdoor CCTV units are around 1 year.

Automation

1,10 Levels of automation up to and including complete automation are possible. Considerable automated target detection, tracking and discrimination can be achieved before a human is required to make a final evaluation of the threat.

2,10 The automation potential for a bistatic radar is equivalent to that for a monostatic radar.

3,10 Practically complete automation including target direction finding, target type identification, position, altitude, speed and direction are achievable. The acoustic unit can also turn on its radio transmitter after processing all the data and report automatically to central security. Precise position and altitude data will have to be acquired by processing at the central station since that information requires data from more than one sensor.

4,10 A CCTV could be slaved to a radar sensor in such a manner that the target of interest can be located to the accuracy of the radar's resolution. Security personnel could then attempt to identify the alarm source on the CCTV

monitors. The range at which automatic optical acquisition would be practical may be limited to short distances.

Potential Application

1,11 Monostatic radar is seen currently as the primary sensor for the airborne intrusion detection problem. This is due to its coverage and range capabilities under environmental conditions that may degrade other sensors. Initial acquisition, tracking and discrimination can be handled by a single radar sensor with limitations or coverage anomalies being solved by supplemental use of other sensor types.

2,11 Bistatic radar has varied potential applicability in this problem dependent on requirements placed on it. However, the major application seen at this time is as a tripwire sensor to cover fixed sectors for detection of targets crossing towards a defended area.

3,11 The acoustic sensor would be best applied as a complement to monostatic radar to fill the gaps in coverage such as low-lying areas, valleys, ravines or the shadow zones formed by mountains where the radar cannot achieve low level coverage. In this role, the acoustic system would be an initial acquisition sensor. It can also serve to discriminate among target types. Information from the perimeter sector array elements can also be used for target tracking, and radar acquisition cuing.

4,11 The basic role of CCTV would be to investigate the perimeter sector following initial penetration detection (with the intention of identifying the alarm source). For example, when the monostatic radar indicates a target at a certain range and azimuth the CCTV would be slewed to that azimuth and set to an

appropriate magnification to allow security personnel to observe the airborne target generating the alarm on the CCTV monitor.

(This Page Intentionally Blank)

SECTION VI

INTRODUCTION TO EXISTING AIR SURVEILLANCE FACILITIES

The design of an air penetration and warning system at a nuclear site must necessarily include dedicated air surveillance sub-systems designed, controlled and operated by the Department of Energy (DoE) or their assigned contractors. The final form that the dedicated DoE system will take can be influenced by other air penetration detection systems that may be in the area but not necessarily controlled by the Department of Energy if data from these non DoE controlled systems can be shared. One existing non DoE system of this type is the National Air Route Surveillence Radar System operated by the Federal Aviation Administration (FAA).

Georgia Tech analysts were tasked to study this national resource (FAA Network) and determine how the U. S. FAA system might be used as a component of an early warning penetration system at selected DoE sites. The remainder of this section is devoted to a review of the FAA resources, an operating description of the equipment and organization found within the system, and a first look analysis of which of these resource may be applicable for various DoE sites that may in the future require an airborne penetration and warning system.

A. The U. S. Air Traffic System

The FAA has the legal responsibility to control air space above the United States. All aircraft on an instrument fight plan (IFR) or in controlled air space must be under positive control of an FAA controller. Several levels of control are exercised on aircraft flying within the United States. Total control is exercised

over IFR flights. Little or no control is exercised over aircraft flying under visual flight rules (VFR), if the VFR flight does not originate or land at a controlled airfield. VFR flights leaving a controlled airfield may discontinue all communications with the airfield controller after leaving the airfield control zone (usually extending a radius of five to six miles around the field). Thus, there are cases where a pilot is not legally required to communicate with the FAA or follow specific airways. It is the pilot operating under visual flight rules in this manner that represents the greatest potential threat to air space security over a nuclear site. The topic of airspace control will be discussed in later sections. Other degrees of surveillance control of airspace over the U. S. is exercised by the FAA. Airspace surveillance outside the U. S. is the responsibility of the military.

The U. S. Air Force Air Defense Command (ADC) and the Canadian Air Defense Command comprise the North American Air Defense Command (NORAD). NORAD is responsible for the air defense of the U. S. and Canada. An air defense intercept zone (ADIZ) has been established around the United States and Canada. Aircraft entering the air space of either nation from outside the country must be positively identified at the time of entry into the ADIZ. Unidentified aircraft entering into the ADIZ and meeting a threat speed threshold criteria are subject to intercept by NORAD interceptor forces. Thus, the NORAD mission is to provide detection and intercept capability against aircraft penetrating the ADIZ, and the FAA's mission is surveillance and control of the airspace above the continental U. S.

B. The Aircraft Detection Network in the U. S.

During the early 1950's when the manned bomber threat was greater than the threat from ICBM systems, NORAD operated a very dense radar network dedicated to the defense of the U. S. against manned bomber attacks. During the intervening twenty years, this network has been reduced to a handful of dedicated NORAD radar sites. Many of the former NORAD sites have been deactivated and disassembled or turned over to the FAA. These remaining consolidated or joint use radar sites may feed information to both the FAA's regional air route traffic control center (ARTCC) and the regional NORAD air defense command center. While not optimum for defense purposes, the sharing of sites represents the most economic approach to air surveillance.

Analysis conducted by Georgia Tech shows that the radar resources most applicable to the DoE air surveillance mission are controlled by the FAA. Thus, the discussion that follows concerning radar resources that may be applicable for the DoE air surveillance mission will not consider NORAD resources in their present form.

C. FAA Resources Considered for Airborne Penetration Surveillance

There are two radar systems operated by the FAA that may be of use in detecting an intruder entering airspace above a nuclear site. The airport surveillance radar system (ASR) generates radar coverage of airspace within the terminal control zone area of an airport. The other source of radar surveillance data is the long range air route surveillance radar system (ARSR).

The terminal radar system consist of a medium range radar usually located on an airfield used by commerical traffic. The terminal radar system detects moving

airborne targets within the airspace around a terminal area. The resultant radar data is displayed to the air traffic controllers responsible for vectoring air traffic within the controlled airspace around the terminal. In most cases, the ASR data is not transmitted beyond the terminal user level.

The long range ARSR Network detects moving airborne targets within the Victor airways and the open airspace over the United States. Radar data developed by the ARSR Network feeds the regional air route traffic control centers (ARTCC).

The two systems are complementary. For example, a departing IFR flight from a terminal area with an ASR installation would be under positive radar control of the terminal controllers until leaving the terminal control zone. After leaving the terminal control zone boundary, the flight would be handed off from the terminal controller to a controller at a regional air route traffic control (ARTCC) facility. The FAA controller at the ARTCC would use radar data supplied from the long range air surveillance network to provide further enroute vectoring and air safety advisory information until the flight reaches the destination terminal area where the flight would again be "handed off" to a terminal area radar controller.

Georgia Tech analysts have considered how the two radar systems operated by the FAA may be of value to DoE as an adjunct to any dedicated air penetration surveillance system installed at a nuclear site. Before the results of this analysis are presented, an overview of the technical organization of the ARSR and ARTCC system will be discussed.

D. Information Flow within the Long Range Air Surveillance and Terminal Systems

A total of five to ten long range air surveillance radars may feed a single ARTCC. The equipment operating at the remote radar sites sends radar data to the ARTCC via both telephone lines and a wideband microwave link. Figure VI-1 shows how the ARTCC radar network is organized in the southwest region of the United States. The ARTCC is the primary hub for the radar networks. Several of the radars in the system feed several centers either side of the primary ARTCC. Thus, selected data that is displayed at the primary ARTCC may also be available at the neighboring ARTCC's.

Both wideband microwave and narrow band telephone line data links are used to transmit the radar and transponder reply data back to the ARTCC. The microwave links are in place as a redundant back up to the narrow band telephone line transmission system. The microwave links were used prior to narrow band installation as the primary channel for transmission of radar data to the centers. However, the desirability of the digital format and the narrow band inexpensive telephone links has made the wideband system somewhat obsolete for the day to day activity of controlling aircraft.

Raw radar data is not transmitted to the center. Before transmission, raw radar data is processed in numerous ways at the radar site. Figure VI-2 is a simplified block diagram of the equipment groups and the data flow typical to each radar site found in the FAA long range air surveillance radar system. Referring to Figure VI-2, it can be seen that there are actually two active systems that develop track information on the aircraft. There is a primary search radar transmitter and receiver group shown in block 1 and an air traffic control beacon transceiver shown

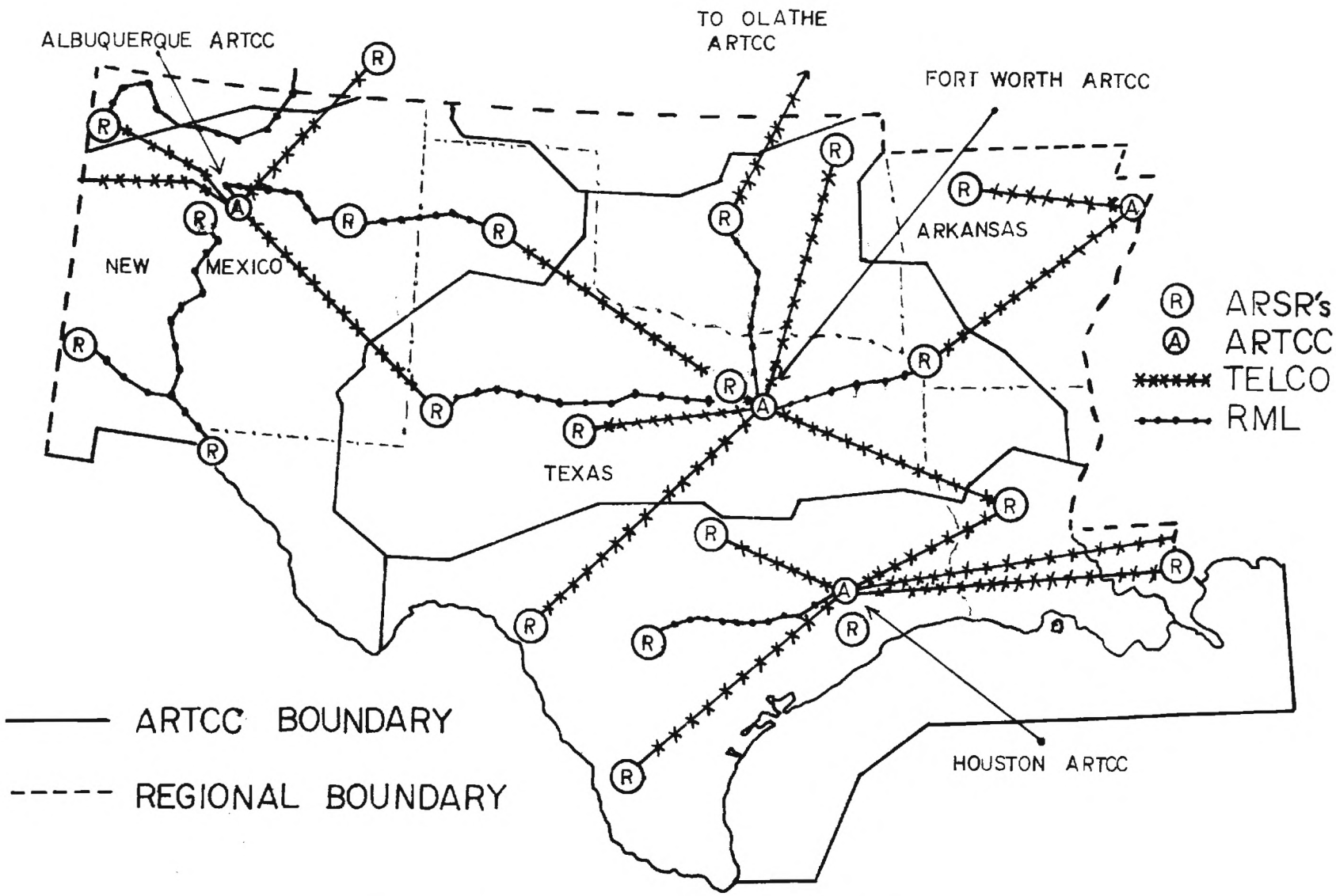

Figure VI-1. Diagram Showing the Long Range Air Route Surveillance Network in the Southwest Region of the United States.

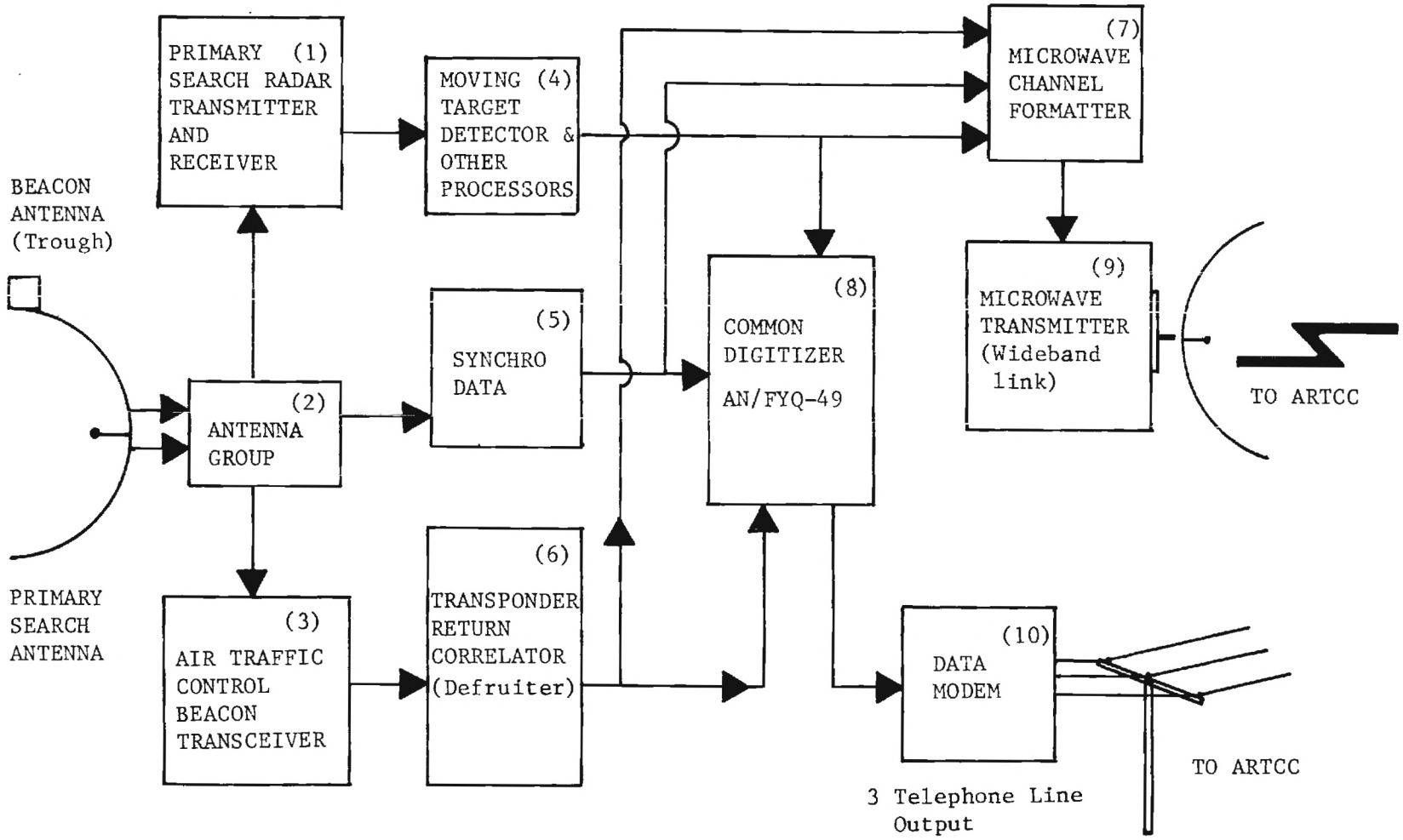

Figure VI-2. Detection and Processing Equipment Associated with an FAA Long Range Radar Site.

in block 3. The primary search radar receiver requires no active cooperation from the target aircraft. The air traffic control beacon transceiver unit shown in block 3 requires that an active air traffic control transponder be aboard the aircraft being tracked.

The primary search radar transmitter generates a four million watt, microsecond length pulse. This pulse of energy is transmitted from the primary search antenna into the airspace within the azimuthal volume illuminated by the antenna. The energy is propagated into space and when it strikes an aircraft a small portion is reflected back to the radar. This energy is captured by the primary search antenna and feed back to the primary search radar receiver. Following initial detection, the signal is processed by the moving target indicator (MTI) shown in block 4 (and other processors). Targets with velocities above a pre-set threshold are passed by the MTI while fixed targets (ground clutter) are suppressed. The video is then transferred to both the common digitizer shown in block 8 and the microwave channel formatter shown in block 7 for transmission to the center. The azimuthal antenna pointing angle is resolved by digital and analog shaft position sensors represented by blocks 2 and 5. The azimuthal angle at which the antenna points (referenced to magnetic north) is converted to analog information and/or digital information for transmission back to the center. The antenna azimuthal data is fed to the common digitizer for format structuring and also to the microwave channel formatter.

The common digitizer shown in block 8 receives the processed analog radar data, converts it from the analog to a digital format and organizes the various digital words into a rigid format for transmission to the ARTCC. A slightly different process is followed in the transmission of analog data by the microwave

channel formatter. The analog information is used to modulate a frequency modulated (FM) or pulse code modulated (PCM) wideband microwave channel. Thus, two redundant channels of information regarding targets detected by radar are sent to the center.

The air traffic control beacon transceiver (interrogator) system is also used to locate and identify aircraft equipped with an air traffic control transponder. A pair of closely spaced interrogation pulses are generated by the ground station air traffic control beacon transmitter (co-located with the radar). The generated pulse is propagated by the beacon antenna. Depending on system type, the beacon antenna might be a large trough type radiator co-mounted on the search antenna with a narrow azimuthal beamwidth, or the beacon radiator may simply be a second feed attached to the existing primary search antenna feed point. The interrogation pulse is transmitted on a frequency of 1030 MHz. The pulse pair (framing pulse) is propagated into space in a narrow beamwidth in the azimuthal plane in order to limit the number of replys from aircraft not on beacon antenna Boresite Axis. When the transmitted ground station interrogation pulse is received by the aircraft's on board transponder system and after a fixed delay, the aircraft transponder replies to the ground based interrogator signal. This reply is transmitted on 1090 MHz. It is received by the ground station beacon interrogator antenna and routed to the air traffic control beacon receiver. The reply code from the aircraft is decoded in the beacon transceiver group. Filtering and timing reconstruction is achieved in the transponder return correlator group sometimes known as the "defruiter" shown as block 6. The received and decoded transponder signal is transferred from the return correlator and goes to both the common digitizer and the microwave channel formatter for eventual transmission back to

the center. As in the case of the primary search radar signal, the return from the air traffic control beacon transceiver is digitized by the common digitizer and assigned a slot in the common digitizer message for transmission back to the center.

In actual practice, the transponder and radar associated signals are multiplexed by the common digitizer for transmission back to the center. The digital information from the common digitizer is transferred to the data modem for transmission. The data modem converts the serial data stream to a parallel data format. The conversion process takes the serial data from the common digitizer and breaks it up into three parallel with 2,400 baud rate channels. These three channels of data are transmitted to the center via special compensated telephone lines. This transmission method results in less than real-time data being transmitted to the center.

The microwave channel formatter in similar fashion assigns the decoded transponder signal a slot in the frequency or pulse code modulated microwave carrier. The microwave formatter inserts the FM or PCM modulated analog search radar and beacon video data in parallel format on the wideband microwave carrier signal. The wide bandwidth of the microwave channel allows real-time parallel transmission of the microwave data to the ARTCC.

The data flow at the ARTCC is shown in Figure VI-3. The narrow band data reaches the ARTCC via the 32,400 baud compensated telephone lines. The incoming audio frequency shift keyed (AFSK) data is converted back to a digital format by the data modem and the resulting digital output is transferred to the data receiver group. Three parallel channels exist up to this point of data flow. The three channel parallel input data is converted to a serial stream in the data

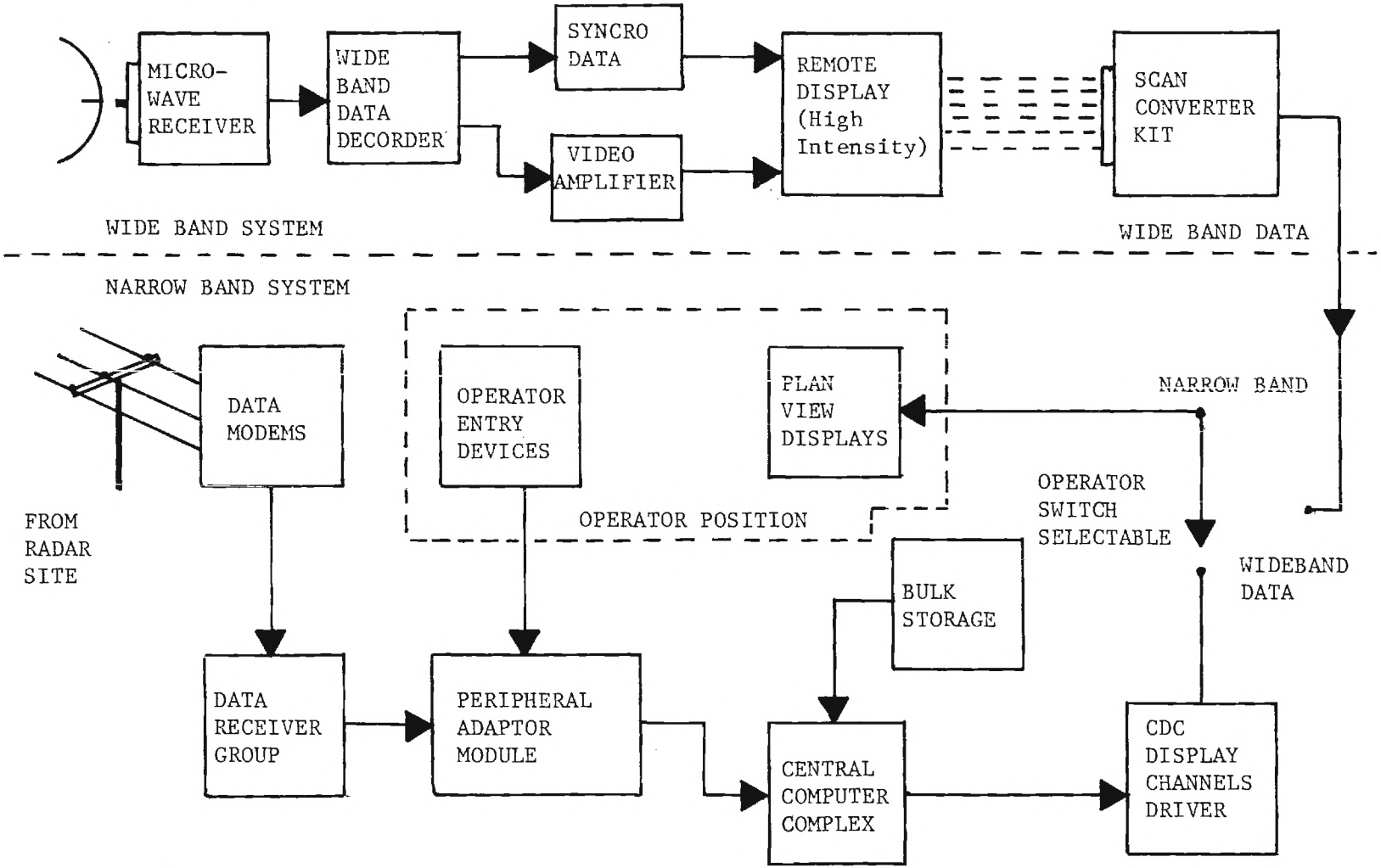

Figure VI-3. Major Data Flow Points within the ARTCC.

receiver group. From the data receiver group it is passed to the peripheral adaptor module (PAM). There are as many data modems, data receiver groups and PAM's as there are radar sites. The output from all of the PAM's in turn feed the ARTCC central computer.

Within the central computer coordinate transformation, flight plan correlation and flight plan computations are carried out as well as general station keeping chores. The output from the computer is used to drive a second smaller computer which in turn drives up to 50 plan view displays (PVD). Each display is manned by a team of FAA air traffic controllers. The FAA controller has access to aircraft position data, and other flight information that can be recalled from the primary ARTCC computer through an operator controlled data entry device (operator keyboard). The data entry device (the keyboard in this case) allows the operator to interface directly with the computer to recall the various parameters that can be displayed.

The target aircraft can be located in a coordinate system referenced to any navigation aid or airport in the region. Altitude information is displayed directly on the PVD if the target is equipped with a transponder and mode 'A' encoder. When a flight plan is on file, the flight plan data can be recalled and displayed on the radar console computer readout device which is an auxiliary display separate from the PVD. Thusfar, only the narrow band capability of the system has been discussed in relation to the information displayed on the PVD.

The analog radar video is transmitted via the broadband microwave link and is received at the ARTCC by the wideband receiver group. Target data is reconstructed from the detected microwave link base band signal by the broadband data decoder. The azimuthal antenna pointing information is stripped off the

broadband carrier and sent to a synchro driver unit. The broadband video representing the analog radar and beacon returns is stripped off the carrier and sent to a small high resolution plan position indicator (PPI). A scan converter scans the face of the PPI and converts the information (displayed in theta/rho coordinates) to a raster scan television type format. Thus, the operator has a switch selectable choice of displaying either narrow band digitized data on the PVD or the broadband data that has been converted to a raster scan television format. The electron gun in the PVD can be driven in both the selectable refresh or raster scan mode.

No flight plan data is displayed on the PVD when it is operated in the broadband mode. Only switch entry (a cumbersome technique compared to the broadband system) transponder code information is available on aircraft being tracked in the broadband mode. The transponder code is displayed on the PVD in the wideband mode as vertical "slashes" off-set in space (time) from the "skin return" location. The actual discrete code that the aircraft is "squawking" is not displayed on the PVD operating in the wideband mode. Thus, it is understandable why the wideband system has been surpassed by the narrow band digital display system for all air traffic control applications except when the narrow band is down for maintenance or a system failure has occurred.

E. The ASR System

The discussion of the ARSR enroute air surveillance system was presented in the previous section as the ARSR and related systems represent a source of air surveillance data to the DoE mission. A second data source is from the Airport Surveillance Radar (ASR) normally located at major airports. The purpose and operational charactertistics of the ARSR have been presented. Given this

established frame-work the ASR characteristics can be presented in summary form with major differences in the two systems highlighted.

The ARSR radar is designed to provide longe range coverage (greater than 200 miles) on relatively high altitude targets. By contrast, the ASR radar was designed to offer full coverage within the terminal control area (TCA). Given this short range requirement, the pulse repetition frequencey (PRF) of the ASR is higher than that of the ARSR. Most ASR radars operate with a PRF that produces a maximum unambiguous detection range of 60 nmi. The higher PRF produces more hits per scan providing a slightly better detection capability for the ASR (vs ARSR) if other comparative factors are equal. The ASR operates at S-band (2.5-3GH_z) frequencies at lower output power levels than the L-band (1.5-2 GH_z) megawatt power output ARSR. By design the ASR provides better low altitude coverage than the ARSR system.

The ARSR and ASR systems are very similar when compared from a modular approach. Figure VI-4 is presented to show the detection and processing equipment associated with the ASR system. The primary difference between the block diagram of the ARSR and ASR is absence of the common digitizer and microwave data communication links normally associated with the ARSR installation. The common digitizer and/or microwave link is not used to transmit data from the ASR to the air traffic control tower under normal circumstances. There is a lack of need for this data transmission equipment because the radar installation is usually co-located near the area where the radar data will be displayed. A multi-conductor cable containing control and video grade circuits are usually run between the radar site and display area located on the airfield.

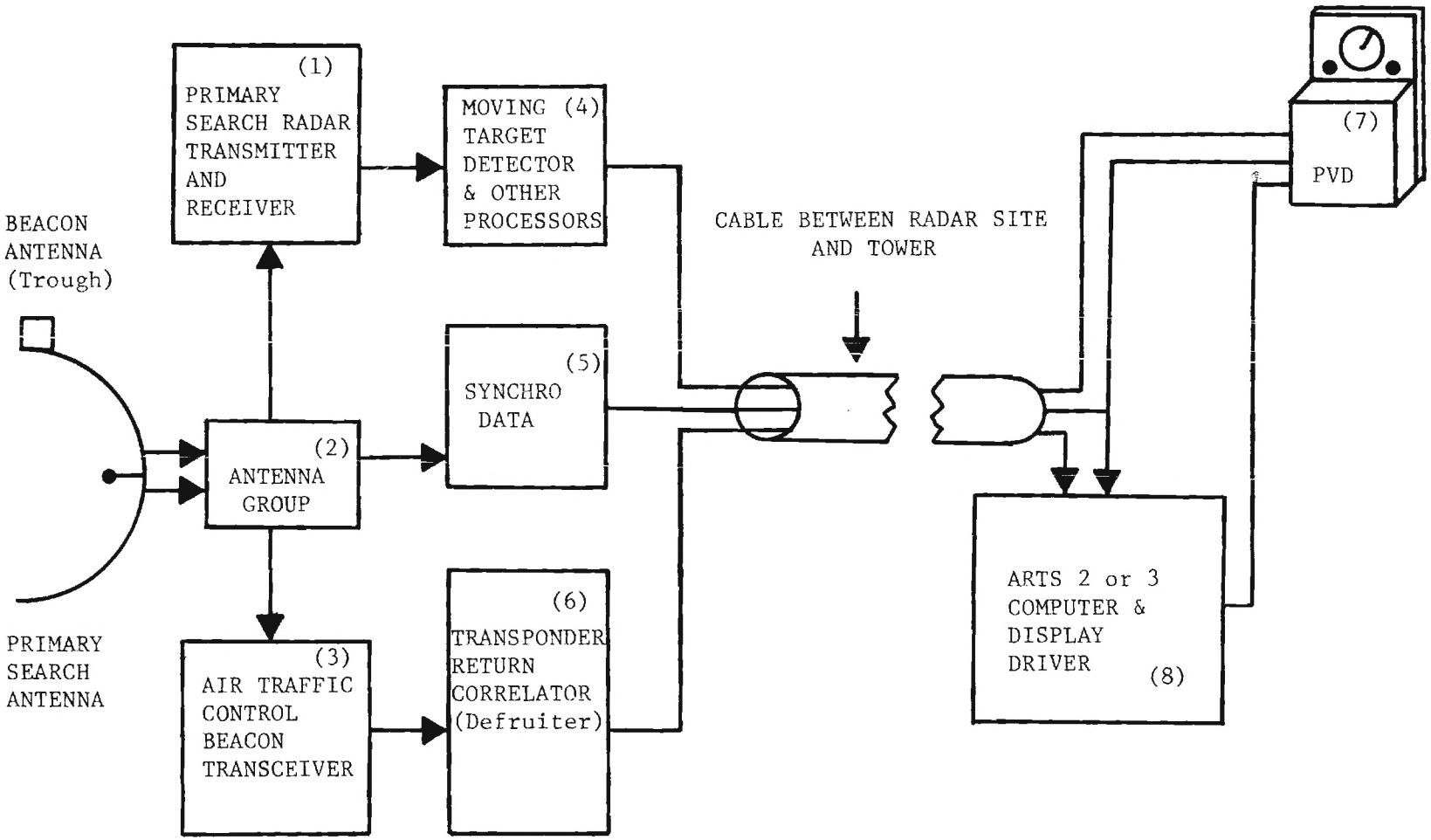

Figure VI-4. Detection and Processing Equipment Associated with the ASR Terminal Radar Installation.

When the radar video arrives at the display area it is displayed on the PVD in theta/rho coordinate format. The ASR radar video is not processed and displayed synthetically because terminal control area operators perfer to work with full dynamic range video.

The beacon video is processed and displayed synthetically. The beacon receiver video is transmitted via cable direct to the automated radar terminal system (ARTS) computer which is located in the same vicinity with the PVD's. The coded beacon returns (transponder replys) are matched to flight plan information in the ARTS computer. A data block of alpha-numeric flight plan information is generated and sent to the PVD. The data timing is reconstructed by the ARTS computer in such a manner that the synthetic alpha-numeric beacon data is slightly off-set from the radar "skin return" displayed on the PVD in theta/rho coordinates.

F. Data Pick-Off Points within the FAA System

The foregoing discussion of the FAA's ARSR and ASR radar systems was presented to give the reader a feel for the elements common to both systems and those elements unique to each system. If it should be determined that FAA facilities are useful inputs to a DoE airborne penetration detection and warning system then it is also important to understand wherein the FAA system the DoE air penetration and warning system might eventually interface. Numerous factors regarding the air penetration and warning system design must be determined before the extent of FAA facility utilization can be decided. However, given the prior discussion of the ASR and ARSR systems certain conclusions concerning the potential role that these FAA facilities might play can be reached.

1. In a case where an ARSR installation provides coverage over a DoE site, the radar and beacon video information can be recovered from the common digitizer at the radar site. DoE supplied equipment will be necessary only at the DoE facility to decode and display the data from the common digitizer.

2. If processed radar, beacon, and flight plan information on targets over DoE facilities are necessary it must be acquired at the ARTCC level.

3. If air surveillance coverage is provided over a nuclear site by an ASR radar installation the radar and beacon video must first be digitized by DoE equipment for transmission on telephone lines or as an alternative a DoE microwave link must be supplied between the radar site and the nearby DoE facility air penetration/detection warning system.

4. DoE officials would be required to make a formal request of the FAA to supply data from the ARSR, ASR or ARTCC systems.

G. Study of FAA Facilities with Possible Application to DoE Needs

Georgia Tech analyst have attempted to determine the value of FAA facilities to the DoE needs in the limited amount of time available for such a study. Table VI-I represents a first cut attempt to determine the DoE facilities that may have existing air surveillance radar coverage.

Table VI-I was developed to provide information concerning possible FAA radar coverage over the candidate 17 DoE facilities. An attempt was made to organize the table to allow the reader to quickly determine which DoE facilities presently have a nearby FAA radar with sufficiently low altitude coverage to be of use.

Table VI-I

Correlation of DoE Facility Location and Nearest FAA Radar Facility

DoE Facility of Interest			Nearest Airport		Value of Radar to DoE	Nearest FAA ARSR to DoE Facility					ARTCC Fed by Nearest ARSR
Name	Minimum Altitude Coverage	FAA Fac. Type	Name	Dist. Mi.	Narrative Evaluation of Coverage Offered	Name	Mi.	Azi.	Radar Type	Form	Name
1. Sandia Laboratories	100'	ASR	Abq. Int.	3	Excellent coverage by ASR at airport. ARSR provide coverage but not as extensive.	(West Mesa) Abq.	11	266°	FPS-60	RML TELCO	Albuquerque
2. Pantex Plant	100' 1000'	ASR ARSR	Amarilo	7	same as above	Amarillo, TX	57	171.3°	FPS-60	RML	Albuquerque
3. Monsanto Research	Unknown	Un-known	Cinn.	13	London ARSR should cover to 4000 ft. No info. available at this time.	London, Oh.	61	54.12°	ARSR-2	TELCO RML	Cleveland Indianapolis (RML)
4. Los Alamos Sci. Lab	800'	ARSR	Santa Fe	17	Alburquerque ARSR gives coverage. No info. obtained on Santa Fe radar facilities.	(West Mesa) Abq.	55	213.5°	FPS-60	RML TELCO	Albuquerque
5. Rocky Flats Plant	100'	ASR	Stapleton	10	ASR at Stapleton gives best coverage.	Denver, Co.	20	117.4°	ARSR-2	RML	Denver
6. Argonne Nat. Lab.	Unknown	Un-known	O'Hare	15	No info. available, ARSR and O'Hare. ASR should cover the site down to 200'	Chicago, ILL.	11	247°	ARSR-3 ARSR-2	RML TELCO	Chicago
7. Brookhaven Nat Lab	2000' 200'-500'	ARSR ASR	LaGuardia	5	ASR gives best coverage. ARSR too far away to be effective.	New York	11	119.6°	JSS ARSR-3	RML TELCO	New York
8. Oak Ridge Lab	19,000'	ARSR	No major airport		No coverage.	Joelton, Tenn.	176	277.5°	ARSR-2	TELCO	Atlanta
9. Hanford Works	4000'	ARSR	Tri-Cities	21	No. ASR info. available. ARSR will give some coverage when it is completed.	Condon	75	210°	ARSR-3	TELCO	Seattle

Table VI-I (Cont'd)

DoE Facility of Interest			Nearest Airport		Value of Radar to DoE	Nearest FAA ARSR to DoE Facility					ARTCC Fed by Nearest ARSR
10. Idaho Falls	Unknown	ARSR	Fanning	22	Ashton ARSR probably gives limited coverage. No information available.	Ashton	78	35.5°	ARSR	RML	Salt Lake City
11. Nevada Test	Unknown	N/A	No major airport		Nellis AFB said that they have gunnery radar in the area that could give excellent coverage.	Cedar City	74	83°	ARSR-2	RML	Salt Lake City
12. Paducah	8600'	ARSR	No major airport		No ASR information. Joelton ARSR gives very poor low altitude coverage.	Joelton	94	178°	ARSR-2	TELCO	Atlanta
13. Goodyear Atomic	Unknown	ARSR	No major airport		No information on London ARSR available. No ASR known in vicinity.	London, Oh	67	167.45°	ARSR-2	TELCO	Cleveland Indianapolis (RML)
14. Naval Reactors	700'	ASR	Allegheny	6	Oakdale ARSR blanked inside 8 mi. radius. Allegheny ASR gives only coverage.	Oakdale	7.5	254°	FPS-60	RML	Cleveland
15. Univ. of Calif.	2000'	ARSR	Livermore	2	Information on Oakland unavailable. Assume coverage exist above 2000 ft. ASR info. unavailalbe.	Oakland	30	253°	JSS, ARSR-2	TELCO RML	Oakland
16. Savannah River	500'	ARSR	Bush	24	Aiken ARSR only coverage. Site to be moved soon. New radar should improve coverage.	Aiken	24	348.8°	ARSR-3	TELCO	Atlanta
17. Knolls Atomic	5000'	ARSR	Schec-tady	4	No ASR at Schenectady. Cummington ARSR gives limited coverage.	Cummington	46	114.9°	Unknown	Un-known	New York

Table VI-I was designed to be read from left to right. In the far left hand column the name of the DoE facility of interest is listed. Sandia Laboratories is shown as the first entry. The minimum altitude covered by radar is shown in the second column. Table VI-I shows that Sandia Laboratories has radar coverage down to 100 feet. The third column shows which type of FAA facility offers this 100 foot coverage shown in the second column. In the example case, the 100 foot coverage is provided by an ASR radar. The fourth column shows the name of the nearest airport, while the fifth column shows the distance of the airport to the DoE facility of interest. In the example case, the Albuquerque International Airport is three miles from Sandia Laboratories. The airport name and distance is provided to the reader to help locate the ASR radar in cases where the ASR system provides primary coverage over the DoE facility of interest.

The third primary topic in Table VI-I is entitled "Value of Radar to DoE". This entry provides a short narrative that further amplifies the data found in columns 1 through 5. For example, the reader is apprised that excellent coverage of airspace over Sandia Laboratories exists from the ASR at Albuquerque Airport. The reader is also provided with information that the closest ARSR radar provides some coverage, but this coverage is not as extensive as the ASR system at the airport.

The next major entry is the "Nearest FAA ARSR Installation to the DoE Facility". The first information provided under this heading is the name of the nearest ARSR radar to the Albuquerque facility; in this case, the West Messa radar at Albuquerque. The distance from the radar to the Sandia facility is shown in the next column. The azimuth from the DoE facility to the radar site is shown in the nineth column of Table VI-I. The tenth column shows the type of radar at the site. This information will be of further value to analysts if specific radar sites are

modeled in a later phase of analysis. The "form" entry is included to document the form or type of communication links between the ARSR site and the nearest ARTCC. In the case of the West Messa site at Albuquerque both the remote microwave link and common digitizer (TELCO) data links are available. The final entry in the far right hand column gives the name of the ARTCC fed by the nearest ARSR to the DoE facility of interest.

The data in Table VI-I was developed as part of the overall assessment scheme used to rate the various FAA radar sites. The assessment technique was a multi-step process. Topographical maps were obtained for the area around each of the 17 candidate DoE sites. The Mean Sea Level (MSL) altitude of the DoE site and the nearest ARSR facility was noted. The highest intervening terrain along the azimuth of interest was determined (in this case 266 degrees) and a rough estimate of terrain blockage was made. Given terrain blockage data, a first cut attempt was made to define radar coverage. This technique was superceded when actual measured radar coverage data was provided by the FAA.

It should be emphasized that the information in Table VI-I was developed consistent with the time and funding available. If additional phases of airborne penetration detection and warning system analysis are pursued a much better estimate of radar coverage over a selected DoE facility can be developed using Georgia Tech radar simulation modeling techniques. Even though the information developed in Table VI-I is not absolute it does represent a good first order estimate.

H. Considerations Relating to National Airspace Restriction over Nuclear Sites

A second area of potential future FAA/DOE interface involves the possibility of developing restricted airspace over a DOE facility. Consideration of this action stems from the advantages gained from low density air traffic over a facility. At some sites current conditions may be such that minimal air traffic exits. Therefore, many of the objectives for considering airspace restrictions may already be met. For the remaining sites it may be advantageous to consider the benefits of minimizing air traffic through a mechanism such as airspace restruction. Thus, certain advantages of low density air traffic have been discussed which can be used in this consideration. They are as follows:

1. From a defense standpoint the most obvious reason for affecting low density air traffic is (by one concept) the resulting defense operational simplification. Any unauthorized aircraft detected in the restricted airspace may be cause for full alert status. This defense mode could afford maximum time for response in case of a real attack since the response would begin with initial detection and would not be delayed by processes of threat assessment.
2. Conceivably, with this simplified defense decision process some of the automatic target tracking and discriminating functions which might otherwise be needed as part of a target detection system could be eliminated as a cost reducing measure.
3. Another apparent benefit of lower air traffic restriction would be a lower false alarm rate: the fewer the aircraft in the area, the lower the expected false alarm rate. Principles of psychology and

human behavior seem to indicate that operational simplicity plus a low false alarm rate would lead to a more prompt defensive posture by security personnel, with longer effective attack warning times and commensurate reduction of the surprise element of an attack.

(This Page Intentionally Blank)

SECTION VII

CONCLUSIONS

The information contained in the foregoing sections has been used in conjunction with complementary Engineering Experiment Station expertise to further analyze the central problem of assuring advance warning of airborne intrusion of the sensitive areas of nuclear installations in the first phase, and secondly, of affording information indicating the intent and capability of detected airborne intruders. The salient conclusions reached via this report information are hereunder enumerated.

1. Omnidirectional airborne intrusion detection (detection probability greater than 99%) by any probable threat aircraft can be achieved out to any given detection radius by an appropriate combination of the sensors (monostatic radar, bistatic radar, acoustic, optical) evaluated in this report. The nature, complexity and cost of the detection system will be dependent on the environment, terrain and desired detection range requirement which will in turn be site dependent.

2. It may be possible to effectively and economically augment an implemented airborne intrusion detection system by use of an existing FAA radar for higher altitude (over 1,000 feet) coverage at some installations.

3. Conditions of restricted air space over the sensitive installations under protection, could lead to considerable detection system cost savings and reduce the false alarm rate.

4. Intrusion vehicle type discrimination can be done automatically by both monostatic radar and acoustic sensors.

5. Detailed design requirements and performance of any airborne intrusion detection system depend strongly on specific site factors, therefore, specific site analysis is required for realistic design, costing and evaluation of any such system.

SECTION VIII

RECOMMENDATIONS

The conclusions of Section VII together with knowledge of (a) the recent worldwide increase of political and criminal terrorism, with commensurate advances in technology available to terrorists; and (b) the potential consequences of nuclear potential in terrorists' hands, lead directly to the following recommendations:

1. That further study be devoted to the development of methodology of airborne intrusion detection system design for some selected site and for site vulnerability assessment.

2. That the developed methodology then be applied to a selected nulcear facility site with a view toward maximizing cost effectiveness of system design and establishing system cost.

3. That the feasibility and advisability of a field demonstration of the designed system be established.

4. That in order to accomplish recommendations one (1) through three (3) in a timely manner, an exploratory hardware sensor development phase be initiated.

5. That Sandia/DoE investigate the possibility and ramifications of imposing restricted airspace over certain nuclear facilities consistent with threat analysis.